**University of Alberta**

# Comprehensive Study of the Bioconversion of Coal Using Laboratory Core Flooding Experiments

by
**Anil Stephen**

A thesis submitted to the Faculty of Graduate Studies and Research in partial fulfillment of the requirements for the degree of

**Master of Science**

Department of Mechanical Engineering


Spring 2014
Edmonton, Alberta

To My Parents and Family

# Abstract

Core flooding experiments were performed to understand *in-situ* coal bioconversion process. Subbituminous coal particles packed inside a biaxial core holder was inoculated with microbial culture and was continuously flooded with mineral salts medium and nitrogen rich nutrient solution. Colonization and conversion of coal by microbes was evident from the presence of metabolites and gases in the effluent. The identification of signature metabolites of anaerobic bioconversion of hydrocarbons shows fermentative microbes are able to convert the complex coal over a period of time to simple molecules such as acetic acid, which is a substrate for methanogenesis. Presence of succinic acid in the effluent, suggests that the coal bioconversion process can be used for extraction of other value-added product apart from $CH_4$ generation. The results presented here indicate that the coal bioconversion by biostimulation at reservoir conditions is a scalable technology with great potential to reduce overall greenhouse gas emission.

**Keywords:** bioconversion, core flooding, coal, methane

# Acknowledgements

I would like to express my deep gratitude to my supervisor, Dr. Sushanta K. Mitra, for his tremendous support and guidance in the last two and a half years. I am greatly thankful to my co-supervisor, Dr. David S. Nobes, for his technical guidance, motivations throughout this research. Their insightful direction, gracious support and encouragement were integral to this thesis. I am greatly indebted to them for their support in improving my scientific and technical writing skills. It was a great privilege for me to work with them and I gratefully admit that I have learnt many things about scientific research from them.

I would also like to thank the members of my examining committee: Dr. Siddhartha Das and Dr. Hongbo Zeng for reviewing my thesis.

I am grateful to my colleagues and group members in Micro and Nano-scale Transport Laboratory (MNTL) for their untiring support and help. A special mention goes to Aleksey Baldygin for his constant support and timely help during the course of my research. I thank him for taking time out from his busy schedule, especially for building graphical user interface (GUI) used for this work. I would also like to extend my heartfelt gratitude to Dr. Prashant R. Waghmare, Naga Siva Kumar Gunda, and Dibyo Sarkar for their advice and overwhelming support whenever I needed. It has been indeed a great pleasure working with them.

Outside the laboratory a special mention must go to Dr. Karen Budwill at

Alberta Innovates Technology Futures (AITF) for her valuable inputs for my research work. I would also like to extend my gratitude to Twyla Malcolm, Stephanie Trottier and Wanyu Chen at AITF for their help in the preparation of MSM and inoculum for my experiment and useful discussion I had with them.

This work could not have been completed without support from a number of people: sincere gratitude to Prof. Julia Foght in the Department of Biological Sciences for permission to use her lab for effluent and gas analysis; Dr. Abigail Adebusuyi, Anh Dao and Annie Wong for their help in those analyses; Dr. Japan Trivedi in the Department of Civil and Environmental Engineering for providing core holder used for my research work. I would like to thank all technical support staffs in machine shop, IT group and electric shop in the Department of Mechanical Engineering for their help at numerous occasions.

I gratefully acknowledge the financial support from Carbon Management Canada (CMC), NSERC CFI and NSERC Discovery grants for my research work.

Most importantly, I would like to take this opportunity to thank my parents and my family for their never-ending love, support and prayer. I am extremely indebted to them for their sacrifices and supports in all aspects and for being wonderful people in my life. I would like to thank my M.Tech supervisor, Prof. Subhash C. Mishra for inspiring me to pursue higher studies.

Last, but not the least, I thank GOD Almighty for all the help.

# Contents

# List of Tables

# List of Figures

# Chapter 1

# Introduction

## 1.1 Motivation

Fossil fuels, including coal, oil and natural gas, are likely to remain as the worlds primary energy sources and these have been fuelling global economic development for centuries. These fossil fuels accounted for almost 87% of global energy consumption in 2012 [Global Carbon Project, 2013]. Fossil fuels are non-renewable sources of energy and their reserves are dwindling as the years pass. The combustion of fossil fuels is a major source of global emissions, which contribute to health and environmental hazards. Global emissions of $CO_2$ have continued to increase at an average rate of 2.7% over the past 10 years [Global Carbon Project, 2013]. According to recent figures, the total global emissions of $CO_2$ in 2013 might reach a record high of 36 billion tonnes, which is 61% above 1990 levels, the baseline year for the Kyoto Protocol [Global Carbon Project, 2013]. The atmospheric concentration of $CO_2$ increased by 42%, from 227 ppm in 1750 (the Pre-Industrial Era) to 393 ppm in 2012 [Global Carbon Project, 2013]. Since many countries have increased their dependence on coal, it has contributed 54% of the growth in the global $CO_2$ emissions in 2012, as compared to oil (18%) and natural gas (21%) [Global Carbon Project, 2013]. Natural gas, composed primarily of methane, is the cleanest fossil fuel, although it still produces $CO_2$ and other toxic gases when burned, but a very small amount when compared to other fossil fuels.

Coal is an abundant and widely distributed energy resource with reserves in more than 70 countries [Center for Climate and Energy Solutions, U.S.A, 2013]. Coal continues to be widely used as a major energy source for electricity generation and other industrial purposes due to rising energy demand, its high energy content and the low cost per unit of energy produced. High energy demand arises in developing countries and even developed countries, surging their appetite toward coal. According to the International Energy Agency's prediction, by 2017, coal will replace oil as the major energy source worldwide. Coal supplies 26.6% of energy produced worldwide; however it contributes significantly to the total greenhouse gas (GHG) emissions, which accounts for 43.1% of global $CO_2$ emissions [Center for Climate and Energy Solutions, U.S.A, 2013]. Coal-fired power plants are the major contributors to the total GHG emissions [International Energy Agency, 2012]. Coal mining can have significant physical impacts on the environment. To access the coal deposits, large areas of land must be evacuated, which may cause physical disturbances to eco- systems. To meet higher energy demand, to enable the use of coal in the future and to reduce environmental impacts, low-carbon footprint technologies will be playing an important role across the globe. One such promising low-carbon technology is the *in-situ* bioconversion of coal to methane as a source of coal bed methane (CBM), rather than the direct combustion of coal resulting in a large generation of $CO_2$.

Unconventional gas resources, such as coalbed methane (CBM) have an important role in the present growing world and they are acquiring significant attention in gas-consuming and producing countries. Commercial production of CBM is established in several countries, such as the United States, Australia, China, Indonesia and Canada [International Energy Agency, 2012]. CBM is playing an expanding role in the global energy resource mix as an unconventional energy resource and cleaner fuel than the combustion of coal or oil. Currently, the CBM industry aims to tap already-accumulated methane that has been produced/deposited in the coal bed over the centuries. Higher utiliza-

tion of this CBM, without stimulating its production will eventually result in its rapid decline to the point that it may even vanish. For enhanced methane generation in the coal bed, one such promising technology is the *in-situ* bioconversion of coal in the presence of a microbial consortium. Stimulating biogenic methane production can extend the life of these CBM reservoirs, reverse decline curves etc.

The main motivation for the present research work is to further investigate the bioconversion of coal into *in-situ* methane; thus, substantial coal reserves can be made available as low-carbon energy resources. By enhancing *in-situ* biogenic methane generation, biogenic methane would emerge as a potential clean fuel to meet high energy demands. As an example, if 1% of the remaining coal in the Powder River Basin could be converted to methane by supplying inexpensive nutrients to stimulate endemic microorganisms, that could be more than enough to meet the current annual natural gas demand of the United States [Pfeiffer et al., 2010]. If methane is available as a free gas in the coal bed (i.e., if generation exceeds solubility in water), it can be produced without the costly dewatering process and hence, environmental damage can be avoided. If biogenic methane replaces a 150MW coal-fired power plant, it could result in the reduction of 1 M tonnes/year of GHG emissions, or the equivalent of the removal of 0.2 M cars from the road (www.davidsuzuki.org).

## 1.2 Objective

To date, published studies on coal bioconversion are few and no works have been reported on the laboratory-scale experimental study that mimics field conditions.

The objective of this research work is the laboratory bioconversion of coal into gaseous products by stimulating microbes involved in coal conversion. A step toward achieving this goal is to perform laboratory core flooding experiments that mimic field conditions.

This experiment attempts to:

- Characterize the methane generation potential of coal at reservoir conditions in response to the addition of nutrients and microbial culture.
- Investigate gases and key metabolic by-products formed during the coal methanogenesis.
- Understand the pathways of coal methanogenesis.
- Investigate the microbial interaction with coal and subsequent permeability changes of the coal pack.
- Investigate the factors that affect the coal methanogenesis.

## 1.3 Structure of the Thesis

The guidelines from the Faculty of Graduate Studies and Research (FGSR) at the University of Alberta have been followed in preparing this thesis and the content of this thesis is subdivided into the following five chapters:

This first chapter presents the motivation and objectives of the present study.

In Chapter 2, a thorough review of existing work on coal bioconversion has been presented. This chapter sets the foundation for the remaining chapters of the thesis in which we discuss the core flooding experiment and laboratory scale bioconversion process. The present chapter also highlights the scope of the present work.

Chapter 3 presents a detailed study of the designed core flooding experiment setup for the bioconversion of coal. A detailed description of the experimental setup, the procedure for the execution of the experiment, coal packing, water degasification, microbial culture and MSM (growth medium for microorganisms) preparation, effluent collection, gas desorption from effluent, gas analysis and metabolic profiling are provided in this chapter.

Chapter 4 provides the results and discussion of the current core flooding experiment for coal bioconversion, including the characterization of the coal pack, the permeability changes of the coal during the experiment, the effect of effluent pH changes on the coal methanogenesis, $CH_4$ and $CO_2$ production rate, factors that affect the methanogenesis, metabolites analysis and key metabolic by-products.

Finally, Chapter 5 summarizes the key findings of this research. Future works based on the outcome of this research have also been recommended.

# Chapter 2

# Literature Review

## 2.1 Introduction

The previous chapter described the significance of coal bioconversion to potential gaseous fuels, such as methane, to meet the rapidly-growing energy demand without significantly contributing to environmental emissions. The objectives of the present research work were also discussed. In this chapter, different literature studies related to the works that tried to understand the coal biodegradation into the final fuel products, such as methane, are discussed. The literature review was focused on the understanding of the following important aspects of coal bioconversion: different mechanisms of methane generation, feasibility of coal bioconversion in the coal bed, understanding of coal bioconversion pathways, predominance of each pathway in different coal reservoirs, methanogenic end reactions, rate-limiting steps in the methanogenesis, types of microbes involved in the coal bioconversion, effect of nutrients addition in coal methanogenesis, laboratory bottle experiments for the understanding of factors that control methanogenesis, key metabolic by-products and significance of the coreflooding experiment for the field scale simulation.

The idea that microbial consortia can metabolize coal has existed since the beginning of 20th century [Potter, 1908]. Later, this idea of microbial metabolism of coal was laid back for several decades. Recent studies indicated the presence of microbes (fungi and bacteria) in the unconsolidated sediment

and rock types [Penner et al., 2010; Harris et al., 2008; Green et al., 2008; Wawrik et al., 2012; Unal et al., 2012; Rice and Claypool, 1981; Papendick et al., 2011], oil reservoirs [Kotelnikova, 2002] and marine and fresh water sediments [Whiticar et al., 1986]. Some researchers found that microbes can metabolize and solubilize coal [Faison, 1991; Catcheside and Ralph, 1999]. Recently, methanogenic coal biodegradation was the focus of scientific research. Endemic methanogenic bacteria can naturally augment the production of biogenic methane [Strapo et al., 2007; Faiz and Hendry, 2006; Smith and Pallasser, 1996].

## 2.2 Mechanisms of Methane Generation

The methane generation in a coal seam is controlled by a thermal or biological mechanism [Clayton, 1998; Harris et al., 2008]. The first mechanism includes the thermocatalytic breakdown of the organic matter at an elevated temperature and pressure [Clayton, 1998; Harris et al., 2008]. Thermogenic methane generation is predominant only if the coal reaches the threshold thermal maturity [Scott, 2002]. The methane generation in coals increases as the vitrinite reflectance ($\%R_0$) of the coals increases, which in turn depends on the coal maturity [Clayton, 1998; Scott, 2002]. The thermogenesis of coal to gases begins when the coal rank reaches a vitrinite reflectance of approximately 0.6 [Clayton, 1998] and continues as the coal maturation progresses. For significant thermogenic methane generation, a high vitrinite reflectance ($>0.8\%$) of the coal is required and hence, this is generally associated with higher-maturity coals such as bituminous and anthracite, which usually occur at sub-bottom depths [Scott, 2002].

The second mechanism, biogenic methane is a consequence of microbial activity on coal [Jones et al., 2008]. Infiltration of meteoric water can transport microbes and nutrients into coal aquifers, resulting in the production of biogenic methane generation [Green et al., 2008; Pashin, 2007]. Biogenic methane generation appears to be predominant in lower-maturity coals, which

usually occur at shallower coal seams [Rice and Claypool, 1981; Clayton, 1998]. Although much of the methane in coal bed gas is thermogenic, a significant portion of coal bed methane is a result of microbial action [Smith and Pallasser, 1996]. Biogenic methane constitutes about 20% of the total natural gas reserves worldwide [Rice and Claypool, 1981]. Another study shows that secondary biogenic methane accounts for 15-30% of the total gas deposit of coal seams [Scott et al., 1994]. The biogenic methane starts to generate during the peatification process (i.e., early stages of coal formation) and continues throughout the coalification process. The new drilling and fracturing technologies (i.e., horizontal, multi-lateral drilling) that have allowed access to the deeper coal seams ($>$ 1000 m deep) and recovery of methane.

Researchers investigated the origins of methane deposit at several methane-producing coal basins and identified that the predominance of the thermogenic or biogenic origin of methane varies from one basin to another. Some reservoirs primarily support either the thermogenic or biogenic origin of methane, but others support both mechanisms. Hence, it is important to identify the geochemical origin and history of $CH_4$ in coal seams before commencing the field trial for coal bioconversion. One such widely-using method used to identify the origin of methane in coal basins is the carbon and hydrogen stable isotope analysis of $CH_4$, $CO_2$ and formation water [Scott et al., 1994; Strapo et al., 2007; Flores et al., 2008]. This technique is useful in distinguishing the biogenic and thermogenic origins of methane.

The methane deposits in some coal seams have been proven to have primarily biogenic origins (e.g., Alberta basin [Cheung et al., 2010], Black Warrior Basin [Pashin, 2007], Illinois basin [Schlegel et al., 2011; Strapo et al., 2007; Strapo et al., 2008], Colorado Basin [Scott et al., 1994], Powder River Basin [Green et al., 2008; Rice et al., 2008; Flores et al., 2008; Rice, 1993], San-Juan Basin [Scott et al., 1994; Zhou et al., 2005], New Mexico Basin [Scott et al., 1994], Surat Basin [Papendick et al., 2011], Bowen Basin [Kinnon et al., 2010;

Smith and Pallasser, 1996], Sydney Basin [Faiz and Hendry, 2006] and Upper Silesian Basin [Kotarba, 2001; Weniger et al., 2012]. The methane content in some coal basins is a mixture of both secondary biogenic and thermogenic gases (e.g., San-Juan Basin in the United States [Rice, 1993; Scott et al., 1994; Zhou et al., 2005] and The Bowen, Sydney [Smith et al., 1985] and Surat [Papendick et al., 2011] Basins in Australia). The relative proportion of biogenic or thermogenic methane in most of the basins is related to the depth of the coal seam and the maturity of the coal. The microbial origin of methane primarily occurs in low-maturity coals, or at shallower depths in higher-maturity coals [Scott et al., 1994].

## 2.3 Coal Bioconversion Pathways

A prior knowledge of methanogenic pathways provides insight into the process of coal biodegradation. Coal is characterized by a lignin-derived macromolecular structure with various functional groups, such as hydroxyl, methoxy, carboxylic and methyl groups and these functional groups are more susceptible to microbial attack [Strapo et al., 2008; Strapoc et al., 2011; Jones et al., 2010]. Coal bioconversion happens through multiple discrete stages of breakdown of organic matter, where metabolic products of some microbes serve as substrate for other microorganisms [Strapoc et al., 2011; Flores et al., 2008]. Metabolically-diverse groups of microbes (fermenters, acetogens and methanogens) with a range of metabolic strategies are required to be involved for the bioconversion of coal [McInerney and Bryant, 1981; Strapoc et al., 2011]. Coal fragmentation into soluble biodegradable intermediates may require hydrolytic enzymes located on the microbial surface [Jones et al., 2008; Strapo et al., 2008; Strapoc et al., 2011; Papendick et al., 2011]. Figure 2.1 shows the model for microbial methanogenesis of organic constituents of coal into methane. Fermentative anaerobes hydrolyse and break down complex organic polymers (i.e., oligomers and monomers) into organic acids (e.g., fatty acids, succinate), alcohols (i.e., ethanol, methanol), aromatic compounds, $H_2$

and $CO_2$ [Strapoc et al., 2011; Flores et al., 2008; Thauer et al., 1977]. Secondary fermentation of these organic acids, alcohols and some aromatic and amino acids into acetate, formate, butyrate, $H_2$ and $CO_2$, is achieved by syntrophs [Faiz and Hendry, 2006; Strapoc et al., 2011; Flores et al., 2008]. These simple intermediate molecules can be effectively utilized by the methanogens as a substrate for $CH_4$ production through the following pathways:

**$CO_2$ reduction pathways**: $CO_2$ can be reduced to $CH_4$ depending on the availability of $H_2$ as an electron source by hydrogenotrophic methanogens [Thauer et al., 1977; Whiticar et al., 1986].

$$CO_2 + 4H_2 \rightarrow CH_4 + 2H_2O \qquad \triangle G^0 : -131kJ/mol \tag{2.1}$$

**Acetoclastic reaction (methyl fermentation)**: Acetoclastic methanogens utilize acetate and transfer the methyl group to produce $CH_4$ [Smith and Mah, 1980; Thauer et al., 1977; Strapoc et al., 2011; Whiticar et al., 1986].

$$CH_3COOH \rightarrow CH_4 + CO_2 \qquad \triangle G^0 : -31kJ/mol \tag{2.2}$$

where, $\triangle G^0$ is the Gibbs free energy function which is the measure of energy exchange associated with reactions.

In addition to these, methanogens can also convert substrates such as alcohols and formate into $CH_4$ (Eq. 2.3 and 2.4) [Thauer et al., 1977; Green et al., 2008]. However, $CO_2$ and acetate are the important substrates for methanogenesis.

$$4CH_3OH \rightarrow 3CH_4 + HCO_3^- + H_2O + H^+ \qquad \triangle G^0 : -105kJ/mol \tag{2.3}$$

$$HCOO^- + H^+ + 3H_2 \rightarrow CH_4 + 2H_2O \qquad \triangle G^0 : -134.3kJ/mol \tag{2.4}$$

The $H_2$ isotope analysis indicated that generation of $CH_4$ depends upon the availability of $H_2$ for both acetate fermentation and $CO_2$ reduction processes. For the $CO_2$ reduction process, methanogens utilize $H_2$, which is supplied by formation water. For the acetate fermentation process, 3/4 of the required $H_2$ comes directly from the acetate and the remaining 1/4 comes either directly

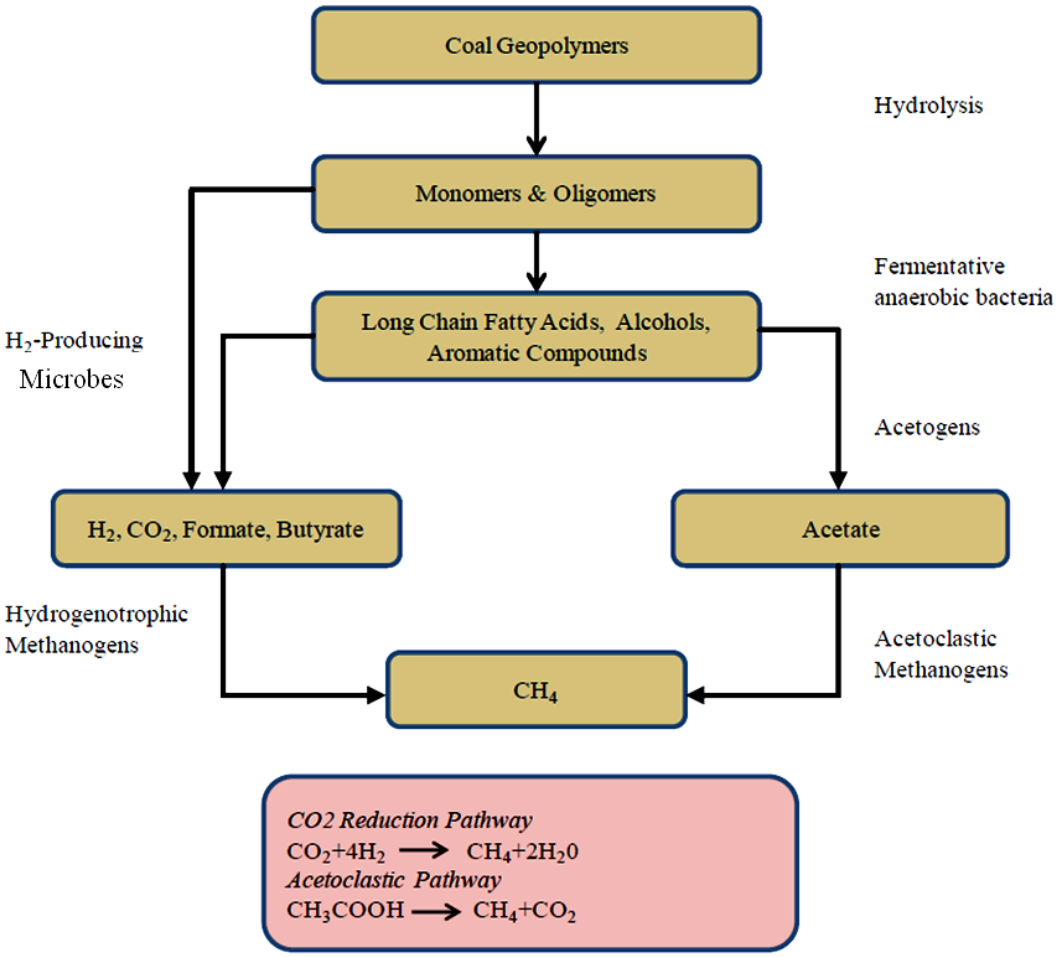


Figure 2.1: Model showing microbial methanogenenic pathways of coal bioconversion. Modified from Flores et al. (2008).

from the formation water or from the fractionalization of the $H_2$ [Whiticar et al., 1986]. Although, $H_2$ is supplied by formation water, the sole source of $H_2$ may be the fermentation of the organic coal substance [Papendick et al., 2011]. The overall enhanced biomethane generation depends on the availability of $H_2$ flux and hence, $H_2$ is considered to be a limiting methanogenic substrate.

All methanogens must rely on syntrophic relationships with fermenters, which degrade complex organic compounds into simple usable substrates such as acetate and formate for methanogens. The initial break down and solubilization of coal macromolecules, which consist of aromatic and poly-cyclic rings having hydroxyl groups, carboxyl groups, or methoxyl groups, into usable substrates, may be a rate-limiting step in coal bioconversion [Fakoussa and Hofrichter, 1999]. Hence, the successful conversion of coal to methane depends on both methanogens and fermentative bacteria. Another hypothesis suggests that methanogenesis would be a rate-limiting step in the coal biodegradation process if the availability of optimized concentration of trace elements (cobalt, Nickel, iron, Zinc etc.) for the growth of methanogens and enzymatic activities are limited [Unal et al., 2012]. In the absence of alternate electron acceptors, $H_2$ may oxidize via $CO_2$ reduction into $CH_4$ and $CH_3COOH$, which are catalyzed by methanogens (Eq. 2.1) and homoacetogens (Eq.2.5), respectively. Hence, the intense competition between methanogens and homoacetogens would exist in environments where free $H_2$ is available, and it would eventually affect the net $CH_4$ generation [Harris et al., 2008]. The required methanogenesis pathways are different from basin to basin and depend on the physiochemical properties of the environment and the methanogenic population that governs these pathways [Strapoc et al., 2011]. Methanogenic pathways in coal bioconversion are not well understood and have been subject to ongoing research.

$$2CO_2 + 4H_2 \rightarrow CH_3COOH + 2H_2O \tag{2.5}$$

Two primary methanogenesis pathways, $CO_2$ reduction and acetoclastic reaction (acetate fermentation), can be distinguished by the carbon and hy-

drogen stable isotope analysis [Scott et al., 1994; Strapo et al., 2007; Clayton, 1998; Formolo et al., 2008; Cheung et al., 2010]. Isotope analysis indicated that the main mechanism of biogenic methane content in Australian Basins such as the Bowen, Sydney [Smith et al., 1985] and Surat [Papendick et al., 2011] basins is $CO_2$ reduction, while in the Powder River Basin [Green et al., 2008; Rice et al., 2008; Flores et al., 2008; Rice, 1993] and the Horseshoe Canyon and Mannville Formations in Alberta the main mechanism is acetate fermentation [Cheung et al., 2010]. Stable isotope analysis of coalbed methane from several reservoirs indicates that methane generation occurs mostly due to microbial activities [Faiz and Hendry, 2006; Flores et al., 2008].

## 2.4 Microbial Communities for Coal Bioconversion

Coal biodegradation and methanogenesis require a diverse community of bacterial and archaeal species for fermentation and syntrophic reactions. Bacterial species, namely Proteobacteria, Firmicutes (e.g., *Clostridia* sp.), Bacteroides and Actinomycete, etc., can break down (ferment) complex organic molecules into simple substrates [Wawrik et al., 2012; Strapoc et al., 2011]. These species are capable of utilizing several carbon substrates. Sulfate-reducing bacteria (e.g. *Desulfobulbus* sp.) are also an important species, known for the syntrophic relationship with several methanogenic archaea [Wawrik et al., 2012; Strapoc et al., 2011]. $H_2$-producing acetogenic bacteria are capable of producing acetate and $H_2$ from fatty acids [Thauer et al., 1977]. The presence of a diverse community of methanogenic archea, mainly comprising of Methanomicrobiales and Methanosarcinales, are detected in various coal beds [Strapoc et al., 2011; Penner et al., 2010; Harris et al., 2008; Green et al., 2008; Wawrik et al., 2012]. The lineage of Methanosarcinales contains metabolically diverse methanogens (*Methanosaeta*, *Methanosarcina*, etc.), which are capable of utilizing acetate, $H_2/CO_2$ and methyl compounds as substrates [Wawrik et al., 2012]. Methanosarcinales are known for the utilization of acetate and methyl compounds (methanol, methyl amines etc.) [Wawrik et al., 2012]. These are

the most efficient methanogens for the acetate catabolism. Methanomicrobiales (e.g. *Methanocorpusculum*) are known for the utilization of $H_2/CO_2$ and formate, but not acetate [Wawrik et al., 2012]. $H_2$-utilizing methanogens (e.g., *Acidovorax* and *Hydrogenophaga*) utilizing available $H_2$ for the conversion of formate and $CO_2$ into $CH_4$ and therefore, they are important members for methanogenesis [Penner et al., 2010; Strapoc et al., 2011]. Hence, active methanogenic pathways in each coal bed may be related to the presence of predominant methanogens utilizing substrates such as $H_2/CO_2$ or acetate.

Two general approaches are widely used for the stimulation of biogenic methane: nutritrient supplementation to the endemic population (biostimulation) and an additional microbial consortium of bacteria and methanogens (bioaugmentation) [Jones et al., 2010]. Although, endemic microbial populations in coal are capable of converting bioavailable coal to methane, the bioaugmented microorganism can generate methane more rapidly and in higher concentrations than biostimulated microorganisms [Jones et al., 2008, 2010].

## 2.5 Key Metabolites in the Biodegradation of Coal

Elucidating the biological pathways of methane formation required the detection and identification of metabolites formed during the coal biodegradation. Several studies have reported on the detection and identification of *in-situ* metabolomics in coal formation water to describe the biogenic pathways associated with methanogenesis in the coal bed [Wawrik et al., 2012; Orem et al., 2007, 2010]. Key metabolic substances, such as longer-chain alkanes, cyclic aliphatic compounds, ether and saturated fatty acids (hexadecanoic acid, octadecanoic acid), are detected in formation water [Orem et al., 2007; Wawrik et al., 2012]. Water-soluble methanogenic substrates, such as acetate and formate, are detected in the effluent produced by anaerobic biodegradation [Orem et al., 2010]. Several aromatic compounds, such as polycyclic aromatic hydrocarbons (PAHs) and its derivatives, benzene derivatives (benzoic acid),

phenols, aromatic amines and phthalates, are detected in the formation water [Orem et al., 2007; Wawrik et al., 2012]. Metabolites profiling and analysis on the coal bed water elucidated the presence of aromatic, n-alkane, cyclic alkane, aliphatic, fatty acid and naphthalene metabolism during the coal biodegradation process [Wawrik et al., 2012]. A detailed analysis of the effluent formed during the coal biodegradation is required to be carried out for the understanding of coal biodegradation pathways.

## 2.6 Bottle Experiments for Coal Methanogenesis

The extent of methanogenesis and methane generation also depends on the availability of methanogenic substrates, an electron acceptor, donor and a nutrient-rich medium. Multiple researchers have performed laboratory incubation studies with coal as a sole carbon source, as well as with the addition of $H_2/CO_2$ [Harris et al., 2008; Green et al., 2008], formate [Harris et al., 2008] and acetate [Green et al., 2008]. Introducing $H_2$ and formate (an electron source) has been found to increase the methane production in the laboratory incubations [Harris et al., 2008]. Since formate and $H_2/CO_2$ are methanogenic substrates, their availability can shorten the time lag prior to the start of methane production [Harris et al., 2008]. Hence, the fermentation of coal macromolecules into a simple substrate is an important step in the biodegradation of coal. Microbial consumption of $H_2/CO_2$ may lead to acetate accumulation, which can adversely affect methane production [Harris et al., 2008]. Harris et al. (2008) observed that the $CO_2$ - reduction pathway is predominant over the acetate fermentation pathway in the laboratory incubations of coal samples from the Fort Union Formation in the Powder River Basin. Contrary to that, Green et al. (2008) reported the predominance of acetate fermentation pathways in the incubation study of coal samples collected from different sites in the same basin. These studies indicates that methanogenic pathways may differ within the same basin. The addition of hydrogen and carbon sources other than coal, such as $H_2/CO_2$, formate and acetate may cause an overesti-

mation of the microbial degradation capability of coal.

Rate of methanogenesis is controlled by several other factors. Green et al. (2008) observed temperature-dependent methane generation. Reduction in the particle size of incubated coals apparently enhances methanogenesis by increasing surface area, dissolution rate and susceptibility to microbial attack [Green et al., 2008; Papendick et al., 2011]. Hence, the coal dissolution rate is suggested to be a rate-limiting parameter for overall conversion to methane [Green et al., 2008; Papendick et al., 2011; Jones et al., 2008]. The pH of the medium in contact with the microbial consortium has an effect on the biomethane production from coal. Microbes favour a pH value between 6.0 and 7.0 for methanogenesis [Taconi et al., 2008; Green et al., 2008]. A lower pH, via the accumulation of intermediate organic acids, may inhibit methanogenesis [Strapoc et al., 2011]. Formation water (i.e., the growth medium) with lower salinity may provide more favorable conditions for the microbial consortia [Papendick et al., 2011]. A microbial incubation study on coals of varying maturity shows that methanogenic rates are comparatively higher in coals of lower maturity [Strapoc et al., 2011; Clayton, 1998; Jones et al., 2008].

Biogenic methane generation is controlled by several other factors, such as the presence of microbes supporting methanogenesis, bioavailability of coal macromolecules, environmental conditions that influence methanogenesis, etc. [Jones et al., 2008]. Some of the enrichment studies on coal samples and coal bed formation fluid demonstrated the presence of not only methanogens, but also the complete microbial consortium required for the bioconversion of coal into methane, in the presence of appropriate environmental and nutrient supplements [Penner et al., 2010; Harris et al., 2008; Green et al., 2008; Wawrik et al., 2012; Unal et al., 2012]. The population and distribution of these microbes vary within a coal seam, as well as from basin to basin [Papendick et al., 2011]. Dissolution (i.e., mass transfer) of coal substrates into an aqueous microbial solution before biodegradation occurs governs the bioavailability

and hence, the generation of methane [Green et al., 2008; Papendick et al., 2011]. An increase in methane generation proportional to an increase in the exposed coal surface area indicates methanogenesis is mass-transfer (dissolution) limited [Green et al., 2008]. The same hypothesis is applicable in the field, where the quantity of methane is proportional to the surface area of the cleat system in coal seam. Biogenic methane generation may also be limited by the metabolic rate of the microbial consortia, where only a fraction of organic coal polymer is biodegradable [Papendick et al., 2011; Jones et al., 2010].

Most of the studies reported so far on coal bioconversion were limited to laboratory bottle experiments [Penner et al., 2010; Harris et al., 2008; Ulrich and Bower, 2008; Jones et al., 2008, 2010; Wawrik et al., 2012; Toledo et al., 2010; Gallagher et al., 2013]. These bottle experiments were performed at low headspace pressure, ranging from 106-137 kPa [Ulrich and Bower, 2008; Wawrik et al., 2012; Harris et al., 2008]. Higher loading of the medium, nutrient and inoculum compared to the mass of coal were considered for the bottle experiments, which indicated higher coal surface contact with these components [Ulrich and Bower, 2008; Wawrik et al., 2012; Harris et al., 2008; Jones et al., 2008, 2010; Gallagher et al., 2013]. The same amount of coal surface contact with the nutrients and inoculated media is not feasible in reservoir conditions. Hence, results from these bottle studies cannot be readily extrapolated for the field study.

## 2.7 Coreflooding Experiments

Coal is actually a porous medium with pore space varying from a few nanometers to even large fractures, which are in mm size [Gamson et al., 1993]. Existing literature indicates that reservoir engineers, who deal with a different kind of porous media (natural reservoirs), have studied oil and gas exploration using laboratory core flooding experiments [Hadia et al., 2008b, 2012; Mazumder and Wolf, 2008; Mazumder et al., 2008; Shen et al., 2009; Santosh et al., 2007;

Hadia et al., 2007; Nobakht et al., 2007; Lin et al., 2008; Hadia et al., 2008a]. In such cases, the reservoir is mimicked by packing sand particles [Santosh et al., 2007; Hadia et al., 2007; Shen et al., 2009; Nobakht et al., 2007], or by using an actual sample from the reservoir [Hadia et al., 2008b, 2012; Mazumder and Wolf, 2008; Mazumder et al., 2008]. Such a technique provides an effective means to understand and quantify the oil/gas recovery process due to a flooding fluid. In this work, we have adopted a similar laboratory core flooding experiment where the coal seam is represented by crushed coal samples of a finite size, thereby applying the established core flooding techniques used in case of porous media study for the coal bioconversion process. To date, no work has been reported in the open literature on core flooding experiments for the bioconversion of coal that mimics field conditions. Studying the process of methane generation using core flooding systems provides results that can be used for modelling actual coal seams in the future.

## 2.8 Scope of the Present Work

As demonstrated, coal is amenable to microbial degradation and it has the potential to convert into clean energy fuel such as methane. Conversion of 1% of these abundant reserves can produce a huge amount of gas that would be enough to remove many coal-fired power plants. Many works have been done to understand the methane production potential of various coal reservoirs, to investigate methanogenic pathways and to identify methanogenic by-products and various factors that control methanogenesis. All of these works have been based on the laboratory bottle experiments and the analysis of gas and formation water samples collected from the coal bed. Published studies on coal bioconversion are few. No work has been reported in the literature for coal bioconversion in the laboratory scale that mimics field conditions. Not many works have focussed on the detailed analysis of the effluent for the detection of various metabolic by-products formed during methanogenesis. The potential for the microbial activity to generate a highly valuable fuel source such as

methane requires additional studies in a controlled laboratory environment, in order to investigate its feasibility at the reservoir condition before commencing field trials. This work characterizes the methane generation potential of coal at the reservoir condition in response to the addition of nutrients and a microbial consortium, which contains fermenters, acetogens and methanogens. Emphasis is laid on the understanding of the methanogenesis process. These core flooding experimental results may be critical to any effort to stimulate methanogenesis in large-scale field studies.

In the present study, a core flooding experiment setup was designed and built, experimental methodology was developed and experiment was conducted to investigate the bio-conversion of coal into gaseous products. The process of methane generation in coal is sensitive to system conditions. Since the methanogens are strictly anaerobic bacteria, special care is required to maintain the anaerobic condition throughout the experiments [Budwill, 1996; Jones et al., 2008; Penner et al., 2010; Wawrik et al., 2012; Green et al., 2008]. Handling of effluent, which consists of dissolved gases, separation and analysis of those gases, involves a sophisticated and complex process. The procedure for the execution of experiment, sample preparation and gas analysis are described in detail for the experimental investigation of *in-situ* methane production. This study represents a scaling up of the process while simulating reservoir conditions. The identification of key metabolites formed during methanogenesis and the understanding of methanogenic pathways involved are of considerable interest to the scientific community. In the present study, crushed subbituminous coal was packed in a biaxial-type core holder. The coal pack was inoculated with an anaerobic, microbial enrichment culture. The core holder was continuously flooded with a nutrient-rich mineral salts medium (MSM) to feed the microbes. The gases generated by methanogenesis were analysed and effluents were also analysed to identify the key metabolites involved in the overall bioconversion process.

# Chapter 3

# Laboratory Core Flooding Experiment – Setup, Procedure and Methodology

## 3.1 Introduction

Reservoir simulation forms an important part of the planning and design of future field trial of any reservoir process. Reservoir engineers use core flooding experiment for the laboratory scale simulation of the reservoir process. Core flooding experimental setup was designed to mimic the actual reservoir conditions in terms of pressures. The operating pressure chosen for the experiment was replicating the reservoir conditions (see Appendix A.3). The developed system can run at low flow rate of 0.001 ml/min upto 204 ml/min. This chapter presents the laboratory core flooding experiment for the coal bioconversion process on crushed subbituminous coal packed inside the core holder. It also describes the designed core flooding experiment setup used for the coal bioconversion, materials and methods used in the experiment, the experimental methodology followed by procedures for the various processes and analysis conducted during the experiment.

## 3.2 Experimental Setup

A schematic of the core flooding experimental setup, used for the bioconversion of coal, is shown in Figure 3.1 and an image of the experimental setup is shown

in Figure 3.2. The setup and the selection of experimental physical parameters were designed to simulate *in-situ*, anaerobic reservoir conditions of elevated pressure, but ambient temperature ( $22^{O}$C) was used for incubation. Water and $N_2$ gas were injected for calculating packed coal porosity and absolute permeability, after which an inoculum suspension and mineral salts medium (MSM), containing tryptone were injected. The experimental setup can be divided into three sections: upstream, core block, and downstream, described below. Since the process of microbial methane generation can typically take months to complete [Harris et al., 2008; Jones et al., 2008; Ulrich and Bower, 2008; Gallagher et al., 2013], custom software was developed to monitor the experiment along with the use of a data acquisition unit (DAQ) and serial communication. Core flooding data (e.g., pressure changes) were processed in real time for online display and monitoring by using an in-house built graphical user interface (GUI), which also allowed overall control of the experiment.

### 3.2.1 Upstream

The upstream section, shown in Figure 3.1, is responsible for driving fluids into the core block. It comprises of a commercial single cylinder syringe pump, PUMP-1, (500D, Teledyne Isco, Inc.), upstream (U) piston accumulators (PA), U-PA-1 and U-PA-2 and inline pressure sensor, C-PT-1. A 15-micrometer filter, U-MF-1, (SS-2TF-15, Swagelok Co.) was used to filter fluids and to protect the PUMP-1 from contamination in case of any accidental backflow during the experiment. To determine the porosity and the permeability of the core, PUMP-1 was used to flow degassed water from CARBOY-1, directly into the core holder. In addition, during MSM-tryptone flooding, PUMP-1 was also used to pressurize U-PA-1 and U-PA-2. The direct injection of fluids into the core holder was done through valves U-3V-1 and U-3V-4. The inoculum was transferred aseptically inside U-PA-2, under anaerobic conditions. It was injected into the core holder through valves U-2V-3 and U-CV-1 by pressurizing U-PA-2, using degassed water through valves U-3V-1 and U-3V-4. The U-PA-1 was sterilized using ethanol (95% Vol.). The U-PA-2 was also sterilized

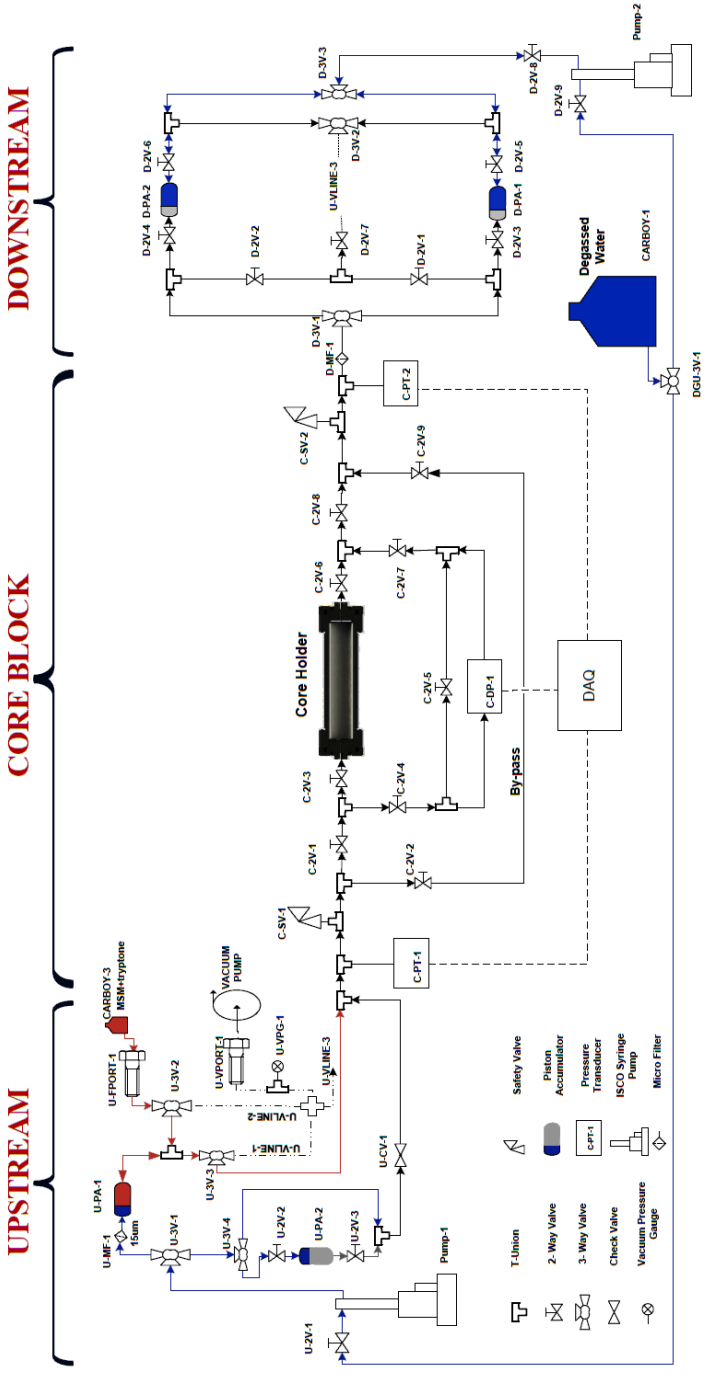


Figure 3.1: Schematic of the core flooding system used for the bioconversion of coal into methane, with three key sections - upstream, core block, and downstream.

using autoclave-steam sterilizer (3850M-B/L, Tuttnauer). The MSM-tryptone solution (described later) was filled into the sterilized and evacuated U-PA-1 through valve U-3V-2 and injected into the core through valve U-3V-3 by pressurizing it with water injection through valve U-3V-1. The check valve, U-CV-1, was incorporated into the system to avoid backflow of solutions to U-PA-2. U-PA-2 was disconnected after inoculum injection. The system was maintained anaerobically by closing valves U-3V-4 and U-2V-3.

### 3.2.2 Core Block

The core block consists of the core holder, inline pressure transducers, differential pressure transducers and safety valves. The biaxial core holder was oriented horizontally during the core flooding experiment. A porous disc with 40 micrometer mesh size was installed into both end plugs of the core holder to obtain the optimum flow redistribution in the radial direction of the coal pack. The real-time pressure monitoring at the upstream and the downstream sides of the core holder were achieved by using pressure transducers, C-PT-1 and C-PT-2 (FP2000 series, Honeywell International Inc.), respectively. The real time differential pressure across the core holder was measured by the differential pressure transducer, C-DP-1 (DP15, Validyne Engineering Corp.). The demodulator (CD15, Validyne Engineering Corp.) was used to convert the signal from C-DP-1 to the DAQ unit. Safety valves, C-SV-1 and C-SV-2, were installed into the flow lines on both upstream and downstream sides of the core holder to protect the system from any accidental pressure surge.

### 3.2.3 Downstream

The downstream side of the system was responsible for effluent collection, which consisted of a commercial single cylinder syringe pump, PUMP-2, (100DM, Teledyne Isco, Inc.), downstream piston accumulators, D-PA-1 and D-PA-2 (each with capacity of 125 $cm^3$) and filter with 15 micrometer mesh size, D-MF-1, (SS-2TF-15, Swagelok Co.). PUMP-2 was used to maintain a back pressure in the system, by holding the pressure at the back side of the D-PA-

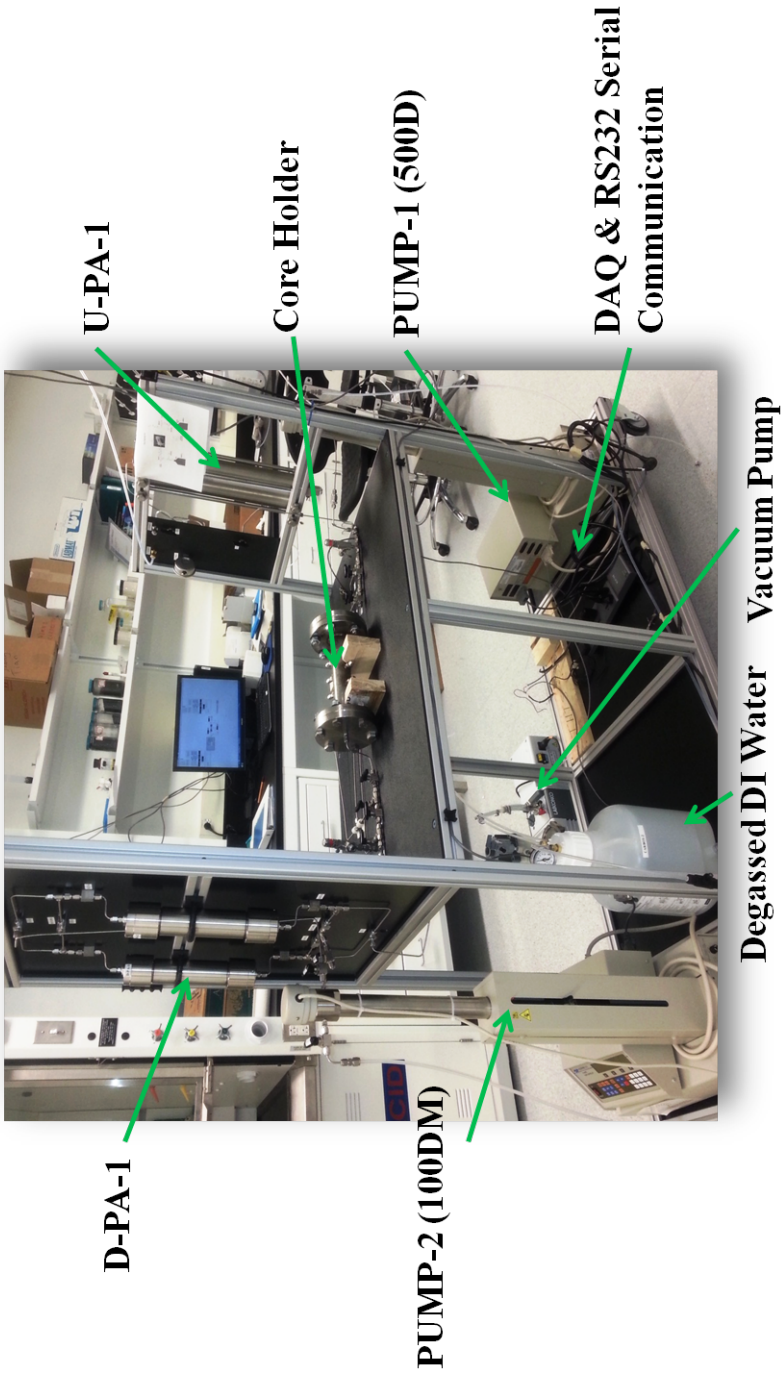


Figure 3.2: An image of the experiment setup used for the core flooding experiment.

1 or D-PA-2. The effluent from the core block could be diverted to any of the empty PAs at the downstream side through the three way valve D-3V-1. During the process of effluent collection inside a PA, PUMP-2 was operated in the constant pressure mode. At the same time, PUMP-1 was operated in constant flow mode to maintain constant volume flow rate through the system. Once a PA was filled with effluent, it was disconnected from the system and the effluent removed for analyses. Meanwhile, the effluent was collected continuously into another empty PA, thus allowing the core system to be continuously operated. The filter D-MF-1 was installed to filter out coal particles from the effluent and to protect the PAs from any contamination. Pressure recorded at the upstream side by PUMP-1 corresponded to the pressure set at the downstream side by PUMP-2 along with the pressure losses across the PAs, the coal pack and flow lines. The D-PA-1 and D-PA-2 were sterilized using autoclave-steam sterilizer (3850M-B/L, Tuttnauer).

### 3.2.4 Evacuation

It was necessary to maintain the system in an anaerobic condition for methanogenesis to occur. Thus, special care was taken to maintain the system anaerobically. An industrial vacuum pump (Model 117, Labconco Co.) was used to evacuate the entire system up to the vacuum level 6.5 kPa(a) (28 in. Hg). The upstream and downstream sides of the system were evacuated by connecting the vacuum pump to the vacuum port, U-VPORT-1, and to valves, D-2V-7 and D-3V-2. The vacuum gauge, U-VPG-1, was used to measure the vacuum level. Vacuum line, U-VLINE-1, was used to evacuate the core holder and the flow lines include bypass lines up to D-PA-1 and D-PA-2. The same can be performed by connecting vacuum line to valve, D-2V-7. The U-PA-1 was evacuated by connecting it to vacuum line U-VLINE-2. The flow line between PUMP$-1$, U-PA-1 and U-PA-2 was evacuated by connecting the vacuum line to the valve U-2V-1. The flow line between CARBOY-1 and PUMP$-1$ was evacuated by connecting vacuum line to valve U-3V-4. At the downstream side, flow lines between CARBOY-1 and PUMP$-2$ were evacuated by con-

necting vacuum pump to valve D-3V-2. D-PA-2 and D-PA-2 were evacuated by connecting the vacuum pump to valves, D-2V-7 and D-3V-2. The core holder or upstream side PAs were evacuated for an hour. Each flow lines or downstream side PAs were evacuated for 15 minutes. A leak test was performed while evacuating the entire system by monitoring vacuum pressure and using soap solution as a leak detector.

### 3.2.5 System Monitoring and Control

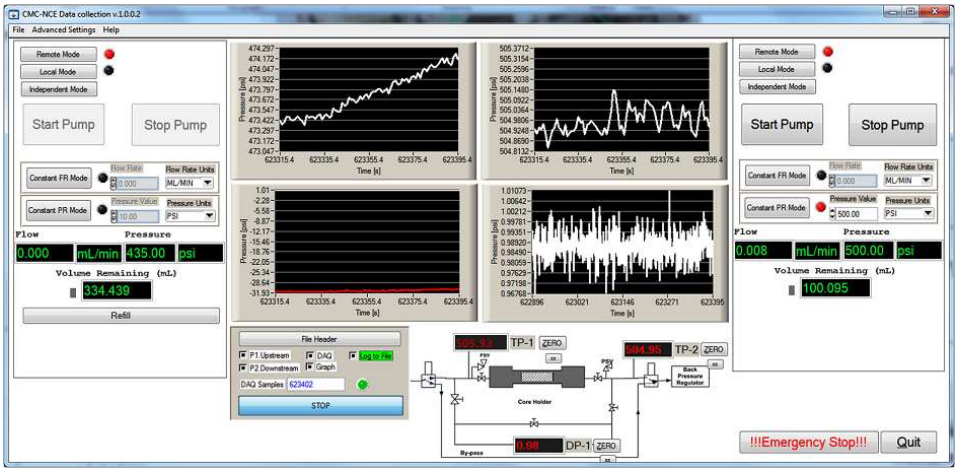


Figure 3.3: A computer screen-shot of the GUI interface used for system monitoring, experiment configuration and control.

Process of in-situ methane generation typically takes months to complete during each successful experimental run ( [Harris et al., 2008; Jones et al., 2008; Ulrich and Bower, 2008; Gallagher et al., 2013]). Manual collection of data during the extended period of the experiment from the system and future analysis can be difficult. For the real-time monitoring of the experiment, a GUI was developed using custom software (LabWindwos/CVI, National Instruments Corp.). A DAQ system (NI USB-6009, National Instruments Corp.) was used to collect data from pressure sensors. A PCI Express serial card (MPEX2S952, StarTech.com Ltd.) was installed in a computer for communication with the syringe pumps through RS-232 serial protocol. The developed GUI interface is shown in Figure 3.3. The left and the right sides of the control panel were responsible for communication with the syringe pumps, while the central panel

was developed for the loading configuration, saving data, monitoring pressure and other parameters using transient response plot of the parameter of interest. The display in the control panel was responsible for quantitative feedback of the system parameters.

## 3.3 Materials and Methods

### 3.3.1 Coal Preparation and Packing

Coal samples of subbituminous rank were collected from a mine face at Highvale mine located south of Lake Wabamun, Alberta, Canada. Coal blocks and chips were crushed into smaller pieces using a mortar and pestle. The required mesh size was obtained by grinding these smaller pieces in a bench-top planetary ball mill (PM 100, Retsch GmbH) and by sieving using a Ro-Tap sieve shaker (RX-29, W.S. Tyler Industrial Group). Standard test sieves (Fisher Scientific Co.) with ASTM E-11 specifications were used for grain separation based on different mesh sizes. Two groups of the crushed coal with mesh sizes 60-70 (250-210 $\mu$m) and 70-100 (210-150 $\mu$m) were used to pack the core holder. The coal pack was then treated as a heterogeneous porous medium. The mesh sizes chosen for the experiment and total mass of the coal for each mesh size are tabulated in Table table:mesh size. The average size of the packed coal particles, inside the core holder, based on the total weight of the crushed coal sample was 200 $\mu$m. In order to obtain a compact packing of the coal, the vibration table (VP-181, FMC Technologies, Inc.) with a vibrator controller (Syntron Power Pulse AC, FMC Technologies, Inc.) was used. The core holder was held vertically and kept under continuous vibrations while the crushed coal particles were being slowly poured into the core holder. The 60-70 mesh size coal particles (125.9 gm) were used first to fill 12.5 cm of the void space inside the core holder and thereafter 70-100 mesh size (174.5 gm) were used to fill the rest of the core holder, as shown in Figure 3.4. Often studies on the effects of reservoir heterogeneities (reservoir with layers of different permeability) employ such dual size sand grains [Chaudhari et al., 2011]. Also, in

Table 3.1: Mesh size, particle size and mass of each group of the crushed coal packed inside the core holder

| Mesh size | Particle size ($\mu$m) | Coal mass (gm) |
|---|---|---|
| 60-70 | 250-210 | 125.9 |
| 70-100 | 210-150 | 174.5 |

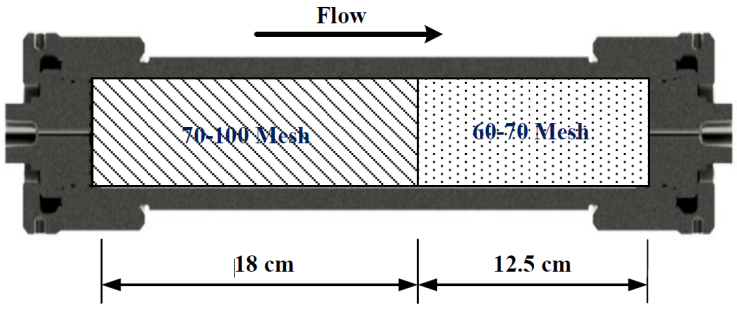


Figure 3.4: Coal mesh size distribution inside the core holder.

an actual reservoir, methane flows from low permeability zones (due to higher overburden pressure as depth increases) to higher permeability zones. Therefore, an attempt has been made to simulate different permeability zones by establishing a lower permeability coal pack at the inlet side and a higher permeability coal pack at the outlet side of the core holder. The packing density (ratio of the mass of the coal packed to the volume of the core holder) was calculated to be 864.64 kg/m$^3$ (53.97 lb/ft$^3$).

### 3.3.2 Water Degasification

In order to achieve accuracy in the values for produced gas and to maintain the system under anaerobic conditions, the water used in the system was degasified prior to the flooding step. Degassed water was used at the upstream and downstream sides of the system for pressurizing the PAs. Also, it was used during the initial experiments for porous media characterization to calculate porosity and permeability values.

Figure 3.5 shows the schematic of the water degasification unit. Dissolved oxygen and other gases were removed from water using a commercial mem-

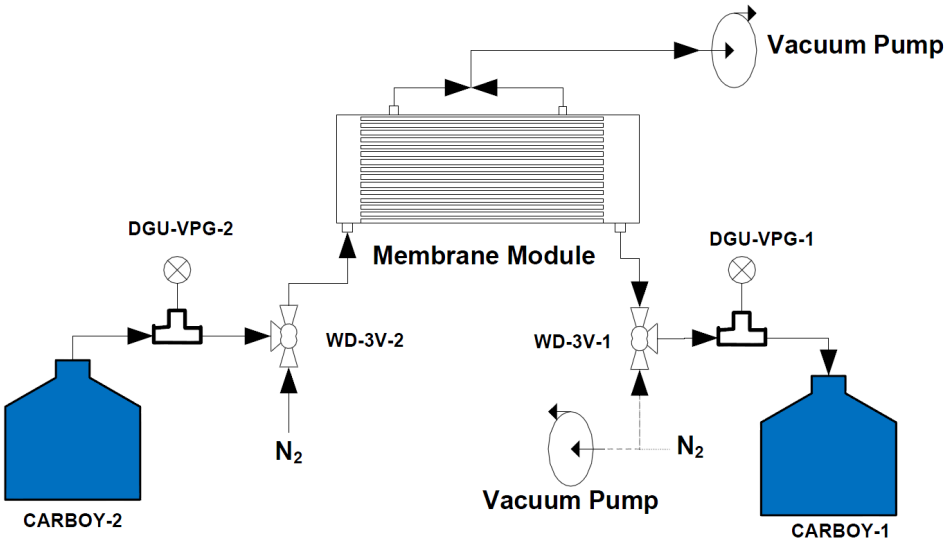


Figure 3.5: Schematic of the water degasification unit.

brane module (PDMSXA 1.0, PermSelect). This membrane module consists of several hydrophobic silicone hollow fibres which act as a membrane. The dissolved gases present in the water permeate the hollow fibres by diffusion. Water targeted to be degassed from the CARBOY-2 was passed through the hollow fiber while vacuum was maintained outside the fiber using an industrial vacuum pump (Model 117, Labconco Co.). Degassed water from the outlet side of the module was stored inside a CARBOY-1, where a vacuum was applied prior to storing. As a result, further dissolution of oxygen from air was prevented. After the water degasification, the carboy was maintained at 20.6 kPa(g) using $N_2$ to prevent the dissolving of $O_2$ into the water.

### 3.3.3 MSM-Tryptone and Microbial Culture Preparation

A mineral salts medium, MSM, (WR-86) [Fedorak and Hrudey, 1984] with the nutrient tryptone at 5 gm/L (MSM-tryptone), was continuously supplied to the coal pack as a growth medium for methanogenesis during the core flooding experiment. It is to be noted that the coal sample was not sterilized at any point and thus was expected to harbour indigenous microbes. However, the coal was exposed to air during processing and packing, which may

have rendered strict anaerobes (particularly methanogens) unviable. Hence, an appropriate coal-derived microbial inoculum was required to determine whether microbes would survive and be active during the core flood. QSAF, a methanogenic culture, enriched from coal cuttings sampled from a coal seam in Alberta [Budwill et al., 2011], was used as the inoculum. To prepare a sufficient culture volume, QSAF, was sub-cultured into replicate serum bottles containing MSM-tryptone [Penner et al., 2010], which has the following composition: Bacto™ Tryptone (Becton, Dickinson and Co.) (5 gm/L MSM), ground coal (Highvale Mine, Alberta), and resazurin as a redox indicator, incubated in the dark at 30$^{O}$C for 5 weeks. Methane production in the inoculum bottles was monitored during incubation period and constituted 30-40% of the headspace volume of the culture bottles at the time of inoculation. To prepare the inoculum for introduction into the core system, equal volumes of MSM-tryptone and the inoculum (total 165 ml) were transferred to a clean, sterile U-PA-2.

Subsurface environments are often deficient in nutrients required for microbial growth. Therefore, microbial metabolism of organic compounds, and hence, the rates of *in-situ* methanogenesis, can potentially be improved by the addition of nutrients [Jones et al., 2008; Harris et al., 2008; Penner et al., 2010; Jones et al., 2010]. The addition of yeast extract, milk, vitamins [Jin et al., 2009], carboxylate compounds, phosphate, ammonia [Pfeiffer et al., 2010], tryptone, and Brain-Heart Infusion [Penner et al., 2010] to coal cultures have been reported. A substantial increase of methane was reported with the addition of tryptone to coal in a mineral salts medium than nutrient-only (4- fold increase) or coal-only (55- fold increase) cultures [Penner et al., 2010]. Additions of organic nutrients, such as tryptone supplements, assist in more rapid biodegradation of the metabolic intermediates [Penner et al., 2010]. Hence, tryptone is an appropriate nutrient amendment for this laboratory trial, but being expensive, its use (continuous or discontinuous injection) for field trials needs to be further evaluated.

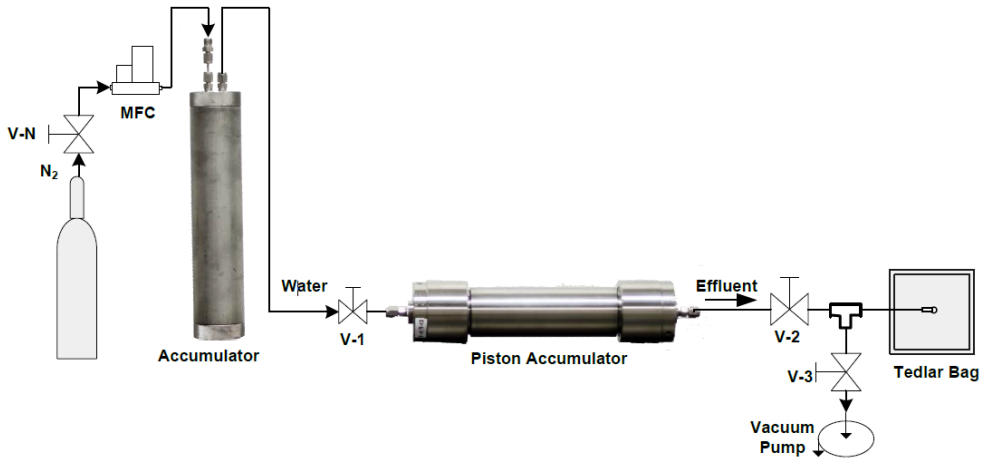


Figure 3.6: Separation of gas from the effluent by pressure reduction method. Pressurized water is used to push the effluent into the Tedlar bag.

### 3.3.4 Desorption of Gases from the Effluent

The pressure reduction method was used to separate the dissolved gases from the effluent, which were collected during the core flooding experiment. Figure 3.6 shows the schematic of the hydraulic system developed for separating the gases from the effluent. Initially, the Tedlar bag (Model 22049, Restek Corp.) and connections between the Tedlar bag and valve, V-2, on the effluent side of the PA were evacuated using an industrial vacuum pump (Model 117, Labconco Corp.). Once the evacuation process completed, all valves were closed. Nitrogen cylinder with preset pressure at 380 kPa(g) was connected to the accumulator, to pressurize the water inside the accumulator. A mass flow controller (MFC) (Model 32907-57, Cole-Parmer) was installed between the nitrogen supply and the accumulator to control the nitrogen flow.

For each sample, the pressure inside the PA was initially released by opening the valve, V-2 allowing a portion of the effluent to flow into the Tedlar bag. The residual unpressurized effluent was recovered into the Tedlar bag by setting the desired nitrogen flow rate at the MFC and opening the valve V-1. As the effluent transfer from the PA to the Tedlar bag progressed, the nitrogen flow rate was decreased and pressure was increased to the preset nitrogen

supply pressure. The zero reading in the MFC indicated that the effluent was completely transferred from the PA to the Tedlar bag. The volume of the Tedlar bag was chosen accordingly to allow the required gas expansion corresponding to the pre-estimated gas production and pressure of the effluent inside the PA. A rapid pressure reduction inside the PA resulted in gas desorption from the effluent. The desorbed gases from the effluent were observed as bubbles on the top of the effluent.

## 3.4 Core Flooding Operation and Sampling

The crushed coal was packed inside the core holder and compact packing of the coal was ensured by comparing packing density with published data [Speight, 2013]. The entire experimental setup including the core holder was evacuated and leak tested. Permeability of the coal pack was estimated using nitrogen as working fluid. Permeability and porosity were also calculated based on the amount of water injected into the core holder.

The next step was the flooding of the water-saturated coal pack with MSM-tryptone solution. Three pore volumes of the solution were injected into the coal pack to fully saturate it followed by inoculation with 1.25 pore volumes of microbial culture. The entire system was then incubated for two weeks at room temperature ($22^{o}$C). Such long incubation period allows the microbial culture to become established with the core conditions. During that time, the core holder was isolated from the rest of the experimental set-up by closing valves C-2V-3 and C-2V-6. After the incubation period, the coal pack was continuously flooded with the MSM-tryptone solution at 0.006 ml/min (0.000305 SCF/day) to feed the microbes.

The effluent was collected in the downstream side of the PAs. Each effluent sample was limited to the volume of downstream pump and was approximately 100 ml and represented three-fourths of a pore volume (PV). Eight effluent samples were collected before the core flooding experiment was stopped on

the $90^{th}$ day of a continuous flooding cycle. Each sample was then analysed for gas production and composition (after separation from the liquid phase) as well as for the presence of metabolites. A total of 760 ml or 5.75 PV of MSM-tryptone flowed through the core system. Methane production continued until the last day of the experiment. The continuous methane generation in this dynamic system, where nutrients are continuously supplied and waste materials are (intuitively) continuously removed, suggests that the experiment, in principle, could have been carried out for a longer period of time. However, the experimental trends, reported here, may not deviate much beyond a certain time period. Hence, the time span of 90 days was considered as a judicious and manageable experimental cycle.

## 3.5 Analytical Methods

### 3.5.1 Gas Analysis

Gas was collected in a Tedlar bag (Model 22049, Restek Corp.) and its volume was measured using a syringe. The gas was transferred from the Tedlar bag into an evacuated sealed vial having a PTFE septum screw cap. Subsamples of (0.1 ml) were transferred from this vial to the gas chromatograph (GC) using a 0.5 ml disposable syringe. Alternatively, 0.1 ml of gas was injected directly from the Tedlar bag into the GC. For each method, three replicate subsamples were injected into the GC to obtain the mean peak area and to ensure precise gas measurements. Gas volume percentages were comparable for both methods, with 0.5-0.6% and 1.8% deviation for $CH_4$ and $CO_2$, respectively. For the detailed explanation of the gas measurement, see Appendix A.6.

Gases were analysed for the presence of $CH_4$ and $CO_2$ using two different gas chromatographs (GC). $CH_4$ was measured using a 5700A model GC (Hewlett-Packard Co.) equipped with a flame ionization detector. $CO_2$ was measured using a 5890 series II model GC (Hewlett-Packard Co.) equipped with a thermal conductivity detector. The measurement standards for both

$CH_4$ and $CO_2$ were adopted from the procedure described by Budwill et al. [Budwill, 1996]

For methane analysis, $N_2$ was the carrier gas maintained at a flow rate of 46.1 ml/min and $H_2$ and air flow rates were set at 30.7 ml/min and 260 ml/min, respectively. The detector temperature was 200$^{O}$C and the injector was at room temperature. The volume percentage of methane in 0.1-ml samples was calculated from the peak area, which was obtained using a 3390A integrator (Hewlett-Packard Co.). For $CO_2$ analysis, helium was the carrier gas. The peak area was obtained using a 3396 series III integrator (Agilent Technologies).

### 3.5.2 Metabolite Profiling

At certain specified intervals during core flooding, 5 ml sub-samples were collected from the effluents and acidified to pH $< 2$ using concentrated HCl to stop microbial activity and protonate the acidic intermediates. Three 5 ml sample replicates of the core flooding fluids as well as an MSM-tryptone control were also processed. An extraction standard, 4-fluoro-1-naphthoic acid, was added before the extraction of acidic metabolites using 5 ml ethyl acetate in each replicate. Extracts were derivatized by reaction with N,O-Bis (trimethylsilyl) trifluoroacetamide (Sigma-Aldrich Corp. LLC) at 70$^{O}$C. Gas chromatography-mass spectrometry (GC-MS) analysis was performed using a 6890N GC (Agilent Technologies) with an inert mass selective detector (5973, Agilent) fitted with a capillary column (HP-5MS, Agilent) of 30 m length, 0.25 mm ID and 0.25 $\mu$m film thickness. Helium was used as the carrier gas. Metabolites were identified based on the comparison of the respective retention times and characteristic ion fragmentation of the authentic standards. The concentration of metabolites in each sample was normalized to the concentration of the surrogate extraction standard, 4-fluoro-1-naphthoic acid for statistical analysis.

Statistical relationships of metabolites in effluents at different times versus uninoculated MSM-tryptone control were determined using statistical packages in a comprehensive web server, MetaboAnalyst 2.0 [Xia et al., 2012]. Hierarchical clustering was performed using hclust and presented as a dendrogram visualized through a conventional heat map. Euclidean distances and Ward's linkages [J. H. Ward, 1963] were used in the hierarchical clustering analysis to measure similarity among samples.

## 3.6 Summary

The core flooding experiment setup was designed for the coal bioconversion process that mimics reservoir conditions. Since the methanogens are strictly anaerobic, entire system was maintained at anaerobic conditions. Experimental data was processed in real time using purpose build graphical user interface (GUI) which also allowed overall control of the experiment. Crushed subbituminous coal sample was packed inside the biaxial type core holder. Reservoir heterogeneity was achieved by packing coal particles of different size, which formed two layers of different permeability. Degassed water was used in the experiment to maintain the system under anaerobic conditions. The combination of MSM and tryptone was used as a growth medium for methanogenesis during the core flooding experiment. The pressure reduction method was used to desorb the gases from the effluent. Gases separated from the effluent were analysed for the presence of $CH_4$ and $CO_2$ using GC. Metabolite profiling was performed in the effluent samples at distinct times for the detection of metabolic compounds. Having presented the core flooding experiment, in the next chapter, we look at the results and discussion of the coal bioconversion process.

# Chapter 4

# Coal Bioconversion-Results and Discussion

## 4.1 Introduction

This chapter presents the comprehensive study of the coal bioconversion process. The changes in the physical properties of the coal pack during the core flooding are the measures of coal bioconversion under the experimental conditions. Rate of metabolic reactions and thus methane generation was controlled by several factors. Microbial distribution and their growth in the coal pack, availability of mineral source and nutrient for microbial growth are some factors control the rate of methanogenesis. Laboratory scale simulation of coal methanogenesis and quantification of potential gas fuels are important step for the design of strategies for the field trial. Identification of predominant pathways is important for the optimization of coal methanogenesis. Coal bioconversion occurs through series of metabolic reactions. The metabolism of organic compounds involved in the coal bioconversion process and methanogenic pathways can be elucidated by detecting metabolites in the core flooding effluent sample. In the following pages, results obtained from the present work has been presented.

## 4.2 Characterization of the Coal Pack

### 4.2.1 Porosity of the Coal Pack

The porosity, $\epsilon$, of the packed coal bed was estimated by two different approaches. For the first approach, degassed water was directly pumped into the evacuated coal pack using PUMP−1 (see Figure 1). PUMP−1 was operated in a constant flow rate mode, pressure and flow rate of which were recorded using GUI. Once, the downstream side pressure reached atmospheric pressure, the pump was stopped and the volume of water injected into the coal pack was recorded ($RV$). Using dead volumes ($DV$) calculations bases on the void volumes in tubes and fittings and the bulk volume ($BV$) of the core holder, the porosity was calculated using the following formula:

$$\epsilon(\%) = \left[\frac{RV - DV}{BV}\right] \times 100 = \frac{PV}{BV} \times 100 \tag{4.1}$$

where, $PV$ is the pore volume.

For the second approach, porosity was estimated from the known density of the bulk coal and the calculated packing density. The packing density is the ratio of amount of coal packed and bulk (empty) volume of the core holder. The porosity of the coal pack was calculated as:

$$(1 - \epsilon)\rho_{\text{bulk coal}} = \rho_{\text{packed coal}} \tag{4.2}$$

where, $\rho$ is the density, kg/m$^3$. Parameters for the porosity calculations using saturation experiment and density approach and obtained porosity values are listed in Table 4.1.

### 4.2.2 Permeability of the Coal Pack

The permeability of the coal pack was found using two working fluids - liquid (water) and gas (nitrogen). The gas permeability was calculated prior to the porosity estimation (water saturation). The core holder was connected

Table 4.1: Parameters for the estimation of porosity using the saturation experiment and density balancing methods

| **Porosity from saturation experiment** | | **Porosity from density balance** | |
|---|---|---|---|
| Core length (cm) | 30.5 | Total mass of packed coal (g) | 300.4 |
| Core diameter (cm) | 3.81 | Volume of core column (ml) | 347.5 |
| Bulk volume (ml) | 347.5 | Packing density of coal (kg/m$^3$) | 864.64 |
| Dead volume (ml) | 6.22 | Density of Sub-bituminous | |
| Pore volume (ml) | 131.95 | coal* (kg/m$^3$) | 1422 |
| Porosity (%) | 38 | Porosity(%) | 39.2 |

* [Parkash, 1985]

to the nitrogen supply (NI 4.8OF, Praxair, Inc.), and the MFC (T-32907-69, Cole-Parmer) was used to control and to record the flow rate. Two pressure transducers (FP2000 series, Honeywell International Inc.) were used to measure the pressure drop across the core holder by monitoring the pressure at the upstream and at the downstream sides of the core holder. The downstream side of the core holder was opened to the atmosphere. To calculate the permeability, the experimental parameters, such as a gas volume flow rate, $Q_g$ (m$^3$/s), and the differential pressure were recorded using the MFC and pressure transducers. The gas volume flow rate was varied in a range from 25 cm$^3$/min up to 675 cm$^3$/min. The dynamic viscosity of nitrogen, $\mu_g$, at experimental conditions was equal to $17.594\times10^{-6}$ Pa·s. Since nitrogen is compressible, Darcy's equation was modified to account the compressibility effect. The gas permeability of the coal pack was calculated as [Scheidegger, 1974]:

$$K_g = \frac{Q_g}{A}\mu_g L\frac{2P_2}{P_1^2 - P_2^2} \tag{4.3}$$

where, $K_g$ is the gas permeability, Darcy; $A$ is the cross sectional area of the core holder, m$^2$; $L$ is the core length, m; and $P_1$ and $P_2$ are inlet and outlet pressures, respectively, Pa.

The mean absolute pressure $P_m$ was also calculated using experimental

data as:

$$P_m = \frac{P_1 + P_2}{2} \tag{4.4}$$

Using obtained data from the experiment, Figure 4.1 has been plotted for different permeabilities correspond to the reciprocal of mean pressure. According to the Klinkenberg equation [Klinkenbeg, 1941], when the pressure approaches to infinity, gas can be considered as a continuous medium and gas permeability becomes equivalent to the liquid permeability [Klinkenbeg, 1941]. In other words, the absolute permeability of the coal pack equals to the permeability measured by water. In order to estimate water permeability from the gas permeability, the empirical equation derived by Klinkenberg [Klinkenbeg, 1941] was used. This equation relates the gas and liquid permeability values to the mean absolute pressure:

$$K_g = K_l \left(1 + \frac{b}{P_m}\right) \tag{4.5}$$

where, $K_g$ is the gas permeability, mD; $K_l$ is the liquid permeability, mD; $b$ is the Klinkenberg factor, Pa; and $P_m$ is the mean absolute pressure, Pa.

From Figure 4.1, the absolute permeability was approximated by extrapolating measured $N_2$ permeabilities to the value at $(\frac{1}{P_m}) = 0$. Figure 4.1 shows the exponential variation of $N_2$ permeabilities with respect to the reciprocal of mean pressures, where $K_{N_2} = 13.8 \times \exp^{\left(38.1 \times \frac{1}{P_m}\right)}$. By setting the $(\frac{1}{P_m}) = 0$, the absolute permeability was calculated to be 13.8 mD.

In addition, results obtained from the nitrogen injection were compared with an empirical solution. To compare results with empirical solution, permeability was calculated from known porosity, particle sphericity, $\phi$, and grain size, $d$, in $\mu$m, using the Kozeny - Carman equation [Carman, 1939]:

$$K_e = \frac{\phi^2 d^2 \epsilon^3}{180(1-\epsilon)^2} \tag{4.6}$$

The sphericity was specified to be 0.65 based on the shape of coal particles used for packing [Krumbein and Sloss, 1963]. Since the permeability varies

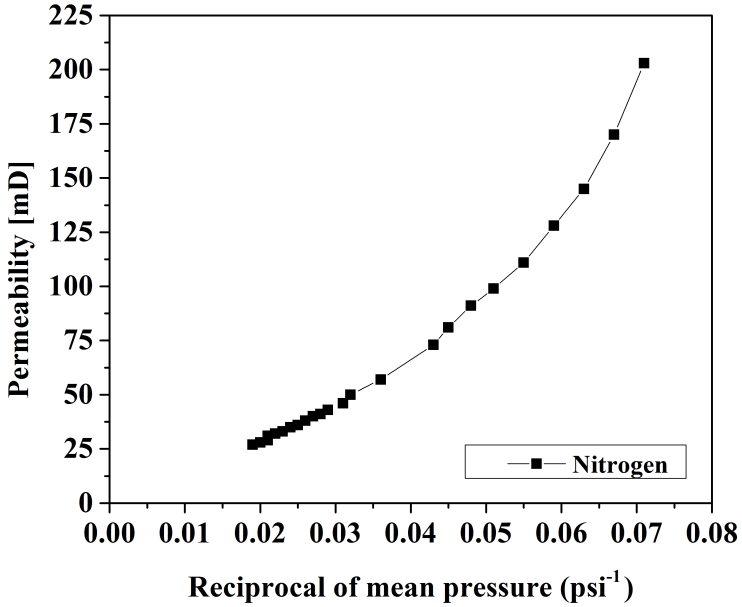


Figure 4.1: Klinkenberg effect due to nitrogen flow through the core holder. Plot shows the variation of the nitrogen permeability for different values of reciprocal of mean pressure.

with the grain size, the weight averaged grain size was considered, which is 200 $\mu$m for the permeability calculation. The verification of measured permeability with the empirical correlation provides a level of confidence that the core pack is dense. In case of the loose pack, the packing process could be modified without wasting the dry coal particles.

Once, the permeability values based on experiment and correlation are verified, the absolute permeability values with water were obtained by flooding degassed water into the core holder at different volume flow rates. The water volume flow rate, $Q_w$ (cm$^3$/min), was varied in a range from 0.5 cm$^3$/min to 4.0 cm$^3$/min. The dynamic viscosity of water, $\mu_w$, at experimental conditions was equal to $1.002\times10^{-3}$ Pa·s. The pressure drop, $\Delta P$ (Pa), was recorded. Permeabilities were calculated using Darcy's equation:

$$K_l = \frac{Q_w}{A}\mu_w\frac{L}{\Delta P} \tag{4.7}$$

Figure 4.2 shows the permeability values obtained for different flow rates

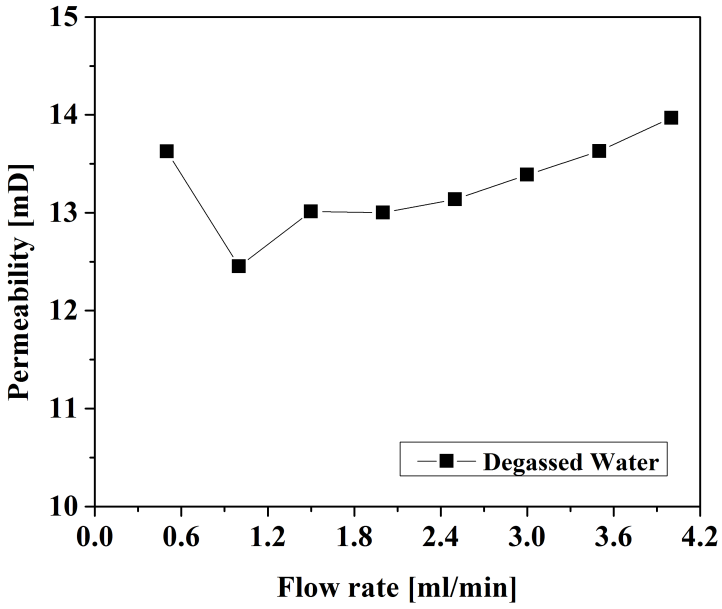


Figure 4.2: Variation of permeability for different volume flow rates of water

of water injected. The obtained permeability values using water varied across the different flow rates with an average value of 13.28 mD.

The absolute permeability of the coal pack, estimated from these three different methods, such as the Klinkenberg effect, the water injection and the Kozeny-Carman equation, were 13.8, 13.28, 13.4 mD, respectively. These values yield an average permeability of the coal pack to be 13.5 mD.

## 4.3 Generation of $CH_4$ and $CO_2$

Experimental parameters, such as operating (back) pressure and flow rate for MSM-tryptone supply, chosen for each sample are provided in Table 4.2. The operating pressure was set at the downstream side of the system at 3447 kPa(g) (500 psi). The pressure was reduced to 1724 kPa(g) (250 psig) for the $4^{th}$ and $5^{th}$ samples to investigate the effect of pressure on methanogenesis. For the final sample, the pressure was further reduced to 69 kPa(g) (10 psig) to desorb as much gas from the coal, which was produced during the experiment and adsorbed in the coal matrix. The time averaged differential pressure across

Table 4.2: List of parameters corresponding to eight effluent samples analyzed during core flooding experiments.

| Sample No. | Time (days) | Back pressure (kPa(g)) | Average differential pressure (kPa) | Flow rate (ml/min) | Cumulative feed injected (PV) |
|---|---|---|---|---|---|
| 1 | 10 | 3447 | 2.027 | 0.006 | 0.640 |
| 2 | 24 | 3447 | 2.000 | 0.005 | 1.370 |
| 3 | 34 | 3447 | 3.757 | 0.007 | 2.107 |
| 4 | 45 | 1724 | 3.716 | 0.006 | 2.804 |
| 5 | 58 | 1724 | 3.723 | 0.006 | 3.507 |
| 6 | 69 | 3447 | 4.192 | 0.006 | 4.257 |
| 7 | 80 | 3447 | 4.660 | 0.006 | 5.000 |
| 8 | 90 | 69 | 5.136 | 0.006 | 5.757 |

the core was recorded (Table 4.2) and found to increase gradually throughout the experiment. The flow rate chosen for the experiment was 0.006 ml/min. Flow rates of 0.005 ml/min and 0.007 ml/min were chosen for the $2^{nd}$ and $3^{rd}$ samples, respectively to adjust the sample collection time. The cumulative volume of the MSM-tryptone injected into the core during the experiment was 5.75 PV (760 ml). The pH of the effluent sample was measured using a pH meter (AB15, Accumet Engineering Corp.) integrated with an electrode (13-620-104A, Accumet Engineering Corp.). The pH measurement was performed within an hour after effluent transferred from PA to Tedlar bag and gasses separated from the effluent. The measured pH values of the effluent samples are listed in Table 4.3.

The gas phases generated during the core flooding experiment were comprised of $CH_4$ and $CO_2$. Other gases such as $H_2$ may have also been generated, but these were not measured with the available GC. The total volume of gases collected with each effluent sample, cumulative volume of $CH_4$ and $CO_2$ and molar ratios of $CH_4$ and $CO_2$ at each sampling time are listed in Table 4.3. Table 4.4 shows the percentage of $CH_4$ and $CO_2$ for each effluent sample produced during the core flooding experiment. The error associated with volume measurement of gases transferred from the Tedlar bag to GC was calculated based on the least count of syringe used for gas transfer. The calibration error

Table 4.3: Cumulative $CH_4$ and $CO_2$ generation and their molar ratio (without solubility correction)

| Sample No. | Time (days) | Effluent pH | Gas Volume Collected (ml) | Cum. $CH_4$ ($\mu$mol) | Cum. $CO_2$ ($\mu$mol) | Molar ratio $CO_2/CH_4$ |
|---|---|---|---|---|---|---|
| 1 | 10 | n/a | 4.0 | 4.6 | 30.2 | 6.5 |
| 2 | 24 | 6.05 | 5.5 | 8.4 | 60.4 | 7.8 |
| 3 | 34 | 6.08 | 10.0 | 29.0 | 285.8 | 10.9 |
| 4 | 45 | 6.04 | 16.0 | 85.1 | 591.6 | 5.4 |
| 5 | 58 | 6.01 | 17.0 | 169.5 | 918.3 | 3.8 |
| 6 | 69 | 6.02 | 15.0 | 252.6 | 1235.0 | 3.8 |
| 7 | 80 | 5.86 | 13.3 | 294.9 | 1473.3 | 5.6 |
| 8 | 90 | 5.93 | 22.4 | 371.2 | 1846.5 | 4.9 |

was the measurement error associated with preparation of calibration standard and it was calculated based on the least count of syringe used to prepare the measurement standard. The measurement variation was calculated based on the standard deviation of peak areas obtained when the volume of gas was injected three times into GC (details are available in Appendix). During the gas analysis, there is a possibility that the air inside the syringe needle could have been mixed with the gas inside the vial. Such mixing would results in negligible error in gas measurements reported here. Also, while transferring the produced gas from the vial to the GC, the possibility of partial gas displacement with air cannot be ruled out.

During the initial stages of the experiment, the rate of methanogenesis was slow and it can be defined as the lag phase of the methane production. Hence, the quantities of gases generated in the $1^{st}$ and the $2^{nd}$ samples were less than the subsequent samples. While comparing the $2^{nd}$ and $3^{rd}$ samples, almost three-fold and six-fold increase in the volume production of $CH_4$ and $CO_2$, respectively was observed (Tables 4.3 and 4.4). Also, from the $3^{rd}$ sample onwards, the total gas volume and percentage of $CH_4$ showed an increasing trend. Increased $CO_2$ generation in the $3^{rd}$ sample compared to the $2^{nd}$ sample indicated the initiation of enhanced metabolic rates.

Table 4.4: Percentage of $CH_4$ and $CO_2$ in the effluent gas sample analysed using GC.

| Sample No. | Time (days) | $CH_4$ (%) | $CO_2$ (%) |
|---|---|---|---|
| 1 | 10 | 2.80 | 18.4 |
| 2 | 24 | 1.70 | 13.38 |
| 3 | 34 | 5.02 | 54.93 |
| 4 | 45 | 8.54 | 46.58 |
| 5 | 58 | 12.10 | 46.83 |
| 6 | 69 | 13.51 | 51.44 |
| 7 | 80 | 7.75 | 43.68 |
| 8 | 90 | 8.3 | 40.6 |

Overall, more than a five-fold increase in the percentage of $CO_2$ compared to the $CH_4$ was observed. This higher rate of $CO_2$ production compared to the $CH_4$ was likely due to the accumulation of $CO_2$ from bacterial fermentation processes. Coal, a complex mix of large molecular weight aliphatic, aromatic and heterocyclic hydrocarbons is postulated to be transformed by primary and secondary fermenters to small molecular weight intermediates such as fatty acids, organic acids, alcohols, $H_2$ and $CO_2$ [Warwick et al., 2008; Strapoc et al., 2011; Flores et al., 2008]. $H_2$ producing acetogenic microbes can convert organic acids such as fatty acids into butyrate, propionate, acetate, formate, $H_2$ and $CO_2$ [Flores et al., 2008; Strapoc et al., 2011; Whiticar et al., 1986]. Acetoclastic methanogens produce equimolar concentrations of $CH_4$ and $CO_2$ from acetic acid [Ferry, 2011]. Note, $CO_2$ can also be produced from the fermentation of tryptone. These illustrates possible cause of generation of large amount of $CO_2$ in comparison to $CH_4$. However, $CO_2$ can also be converted to acetate by acetogens or utilized by hydrogenotrophic methanogens to produce $CH_4$ [Garcia et al., 2006]. The high concentration of $CO_2$ in the effluent gases suggests that such processes are not likely the dominant pathway of $CO_2$ utilization for the present coal microcosm.

Figure 4.3 shows the cumulative production of $CH_4$ and $CO_2$ in $\mu$mol per gram of subbituminous coal. The values were corrected to ambient room temperature and atmospheric pressure. The fraction of a gas volume that can still

be dissolved in the liquid effluent sample depends on the partial pressure and temperature. Therefore, the total quantity of analysed $CH_4$ and $CO_2$ was corrected further by considering their solubility. The gas solubility was calculated using Henry's law [Wilhelm et al., 1977; Wiesenburg and Guinasso Jr., 1979]. The error bar for each data point was calculated considering the measurement and calibration errors and the variability in the measurement (details available in Appendix A.7).

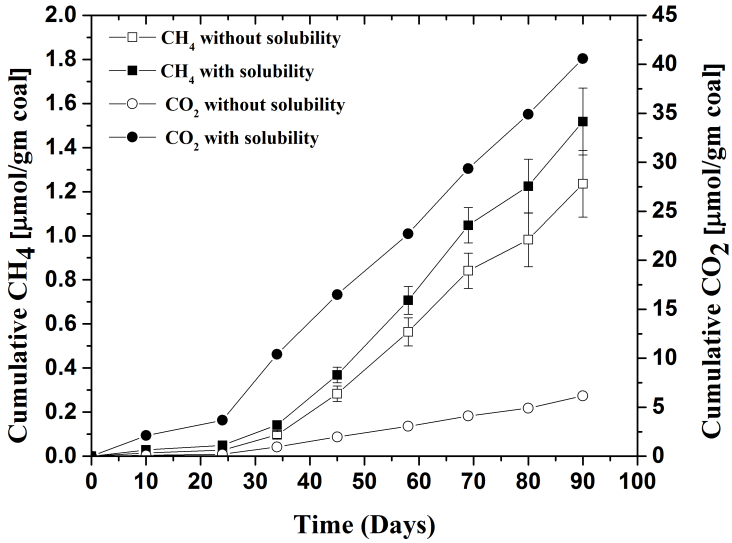


Figure 4.3: Effect of solubility on cumulative $CH_4$ and $CO_2$ generation. Each data point corresponds to the sample number in a sequential manner.

Table 4.3 and Figure 4.3 suggest that the ratio of $CO_2$ to $CH_4$ increase up to the $3^{rd}$ sample, followed by a decrease trend for the subsequent samples (except for last two samples). This indicates that microbial reactions favoured the production of $CO_2$ rather than $CH_4$ at the beginning of the methanogenesis. This lag period before methane production occurs was also has been observed in static methanogenic culture bottle experiments. With the progression of methanogenesis, more methane started to be produced from the precursors, such as acetate (and possibly, $CO_2$). Acetoclastic methanogenesis (acetate to $CH_4$) may have been dominant at the beginning of the core flood and as time progressed hydrogenotrophic methanogenesis ($CO_2$ to $CH_4$) may

Table 4.5: The quantity of adsorbed CH4, recovered during the degassing of coal core at the end of experiment.

| Cumulative $CH_4$ ($\mu$mol) | Cumulative $CO_2$ ($\mu$mol) | Molar ratio, $CO_2/CH_4$ | Cumulative $CH_4$ ($\mu$mol/g coal) Without solubility | Without solubility |
|---|---|---|---|---|
| 453.4 | 2188.4 | 4 | 1.509 | 1.813 |

have become responsible for some of the methane generation. Cumulative $CH_4$ and $CO_2$ generation varied linearly with the core flooding time beyond the $2^{nd}$ sample (Figure 4.3). The $CH_4$ and $CO_2$ were continuously produced until the experiment ceased. The data suggest that $CH_4$ production had not reached its peak, and fermentative bacteria and methanogens were actively involved in the bioconversion of coal throughout the experiment. When the final, $8^{th}$ sample, was collected on the $90^{th}$ day, the solubility-corrected cumulative $CH_4$ and $CO_2$ production values were 1.52 and 40.57 $\mu$mol/gm coal, respectively, compared to the uncorrected values of 1.24 and 6.14 $\mu$mol/gm coal, respectively. With the consideration of solubility, a 20% increase in $CH_4$ production was observed.

The degassing of the coal core at the end of experiment could recover some of the $CH_4$, which was adsorbed in the coal matrix during the core flooding experiment We collected the methane desorbed from the coal matrix, once the core flooding experiment was stopped (after 90 days), without the injection of MSM into the core. It was found that solubility corrected and uncorrected cumulative $CH_4$ became 1.81 and 1.51 $\mu$mol/gm of coal, respectively (Table 4.5). The molar ratio of $CH_4$ to $CO_2$ was 0.24, which was compared with values obtained from the core flooding experiment (See Table 4.3).

It was found that there was a slight decrease in pH from an average of 6.04 for $2^{nd}$ - $6^{th}$ samples to an average of 5.90 for $7^{th}$ - $8^{th}$ samples, which may be due to the accumulation of carboxylic acids. Observed reduction in $CH_4$ production for $7^{th}$ and $8^{th}$ samples also supports such correlation to the pH level. As the pH level decreases, the rate of methanogenesis also decreases [Taconi et al., 2008]. The decrease in pH may be affected the ability of methanogens

to convert simple molecules such as acetic acid into methane [Taconi et al., 2008].

## 4.4 Comparison to Bottle Experiments

Closed, static and low pressure culture bottle experiments reported in the literature demonstrated that the total methane production from the coal sample depends on the ratio of volume of inoculated medium to the mass of coal [Toledo et al., 2010; Harris et al., 2008; Ulrich and Bower, 2008; Jones et al., 2008, 2010; Wawrik et al., 2012; Gallagher et al., 2013]. Increases in this ratio resulted in substantial increase in the contact surface area between coal, medium, nutrients and microbes, which in turn resulted in more methane generation. Such bottle experiments can be distinguished from the current core flooding experiments in many aspects. The sample preparation, experimental methods and quantity of medium and nutrient and compounds such as $H_2/CO_2$, acetate, added during the bottle experiment were different from that carried out for the core flooding experiment. The commonly adopted method and the range of compounds used in several bottle experiments, available in the literature, are summarized here. In ′typical′ bottle experiments, the sample was prepared in such a way that, the quantity of coal (0.5-10 gm) was added to a serum bottle and the medium and inoculum were added with a specified ratio of volume of medium in ml to mass of coal in grams (1.5-12.5) [Harris et al., 2008; Ulrich and Bower, 2008; Jones et al., 2008; Wawrik et al., 2012; Gallagher et al., 2013]. The head space volume was flushed with $N_2/CO_2$ or $H_2/CO_2$ with this ratio generally equalling 4:1 and pressurized to a value between 106-138 kPa [Harris et al., 2008; Ulrich and Bower, 2008; Jones et al., 2008; Wawrik et al., 2012; Gallagher et al., 2013].

In contrast to the bottle experiments, the quantity of the coal sample used in this core flooding experiment was 300.4 gm. At any time, the coal pack was in contact with a single pore volume of microbial suspension, i.e., MSM-tryptone. In bottle experiments, the contact surface area of coal sam-

ple with nutrient rich inoculated medium was higher compared to the core flooding experiment. In contrast, coal packing was denser in the core flooding experiment and the operating pressure was higher than those in the bottle experiments. The gas generated in the bottle experiment could easily move to the headspace; while for the core flooding experiment, gas can be adsorbed by the coal matrix. The pressure reduction during the sampling process confirmed this hypothesis. Hence, the recovery of the analysable gas from the core flooding experiment was less due to the gas adsorption compared to that from the bottle experiment. In the core flooding experiment, achieving an even distribution of microbes inside the coal pack could be a challenge, which could limit the coal bioavailability. In the bottle experiment, the quantity of added carbon sources such as acetate, formate, bicarbonate and $CO_2$ could contribute to the overall methane yield [Green et al., 2008; Harris et al., 2008; Ulrich and Bower, 2008], which may cause an overestimation of the microbial degradation capability of coal. Due to these reasons, results from the core flooding experiment and those from the bottle studies available in literature could not be directly compared. The core flooding experiment can be characterized as a system having a more natural ′quantity′ of coal, with less direct surface contact of coal with microbes, and less contact with enriched nutrient solution, i.e., lower bioavailability. The maximum production of $CH_4$ in the present study was 13.51% observed on $69^{th}$ day (Table 4.4), as compared to 10.1% on $49^{th}$ day reported by Toledo et al. [Toledo et al., 2010] and around 8.7% on $155^{th}$ day reported by Luca Technologies Inc Luca Technologies Inc. [2004].

## 4.5 Changes in Coal Permeability

Permeability changes were observed for the coal pack after inoculation and during continuous flooding operations with-MSM-tryptone. Figure 4.4 shows the variation in absolute permeability of the coal pack corresponding to the time averaged pressure drop measured at each sampling cycle of the core flooding experiment. The permeability of the core calculated at the $1^{st}$ sampling

was 13.27 mD, which was comparable to the permeability estimated from the water injection, the Klinkenberg effect and the Kozeny-Carman equation. This suggests that no significant changes in permeability occurred during the initial inoculation of the coal pack. However, permeability decreased as the experiment progressed. The most significant decrease in permeability was observed during the $3^{rd}$ sampling period. This significant change in permeability may have been due to a combination of microbial growth [Taylor et al., 1990; Vandevivere and Baveye, 1992] and gas adsorption [Lin et al., 2008; Mazumder and Wolf, 2008; Mazumder et al., 2008], which might have facilitated the collapse of void space inside the core holder. Microbial growth on the surface of coal particles results in the formation of areas of biofilm and the adherence of an increased number of microbial cells on the coal surface [Taylor et al., 1990; Vandevivere and Baveye, 1992; Hazrin-Chong and Manefield, 2012]. Hence, the decrease in coal permeability over time may be due in part to the blocking of a coal pores by microbial biofilms on the coal surface [Taylor et al., 1990] or accumulation of discrete microcolonies in the pore spaces [Vandevivere and Baveye, 1992].

It is to be noted that the volume of total gas produced with the $3^{rd}$ sample was double compare to that of the $2^{nd}$ sample (Figure 4.3). When the coal pack is saturated with produced gases, the adsorption of these gases (depending on their partial pressure) results in the swelling of coal [Lin et al., 2008; Mazumder and Wolf, 2008; Mazumder et al., 2008]. This swelling effect of the coal core may lead to its decrease in the permeability over time. The swelling effect due to the $CO_2$ sorption is more pronounced than $CH_4$ or $N_2$ adsorption [Lin et al., 2008; Mazumder and Wolf, 2008; Mazumder et al., 2008]. The microbial growth and the gas generation in subsequent samples resulted in further decreases in the permeability, as shown in Figure 4.4. The rate of decrease in permeability from the $5^{th}$ sample onwards was less in comparison to the previous samples, since there was no significant increase in the volume of gas generated and the coal matrix may be saturated with gases generated

from the $4^{th}$ sample onward. Permeability was reduced to almost half of its initial value at the end of the $4^{th}$ sampling and further reduced to 5.75 mD at the end of the $8^{th}$ sample.

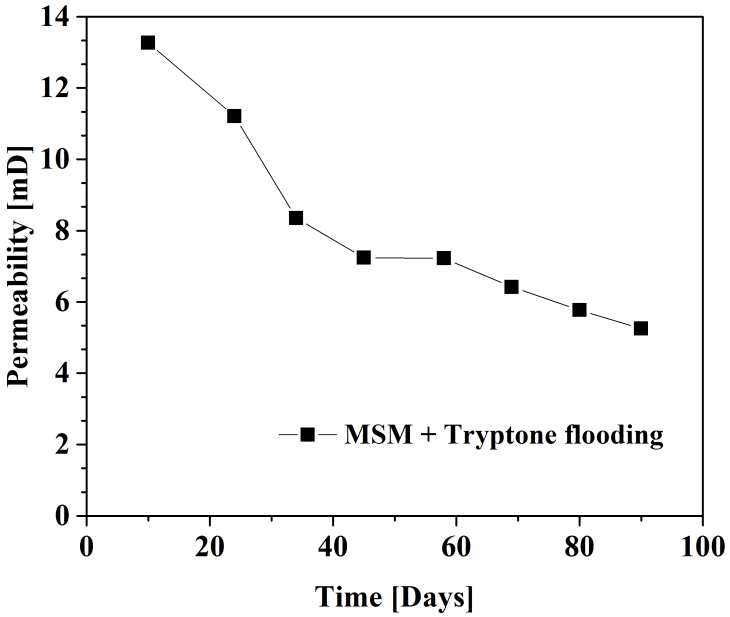


Figure 4.4: Permeability variation of the coal pack as a function of flooding time.

## 4.6 Signature Metabolites in the Effluent

Figure 4.5 shows the relative concentrations of different putative metabolites detected in MSM-tryptone (sample # 0) prior to injection and also for effluents collected at different intervals during the core flooding (sample # 1-8, corresponding to Table 4.3). The suite of analytes detected is presented as a heat map [Xia et al., 2012] for three replicates of each samples. A dendrogram at the top of heat map shows the clustering of metabolites based on the similarity of their occurrence in the samples. The relative concentration of each metabolite was graded (from -2 to 4) using color codes in the heat map. Low concentration values of metabolites tend towards light blue color while higher concentration values tend towards dark red color. The concentration of a compound in a sample is relative to its concentration in other samples. The

numbers (1-8) indicated on the left panel of the map corresponds to the effluent sample number represented in Table 4.3. These numbers are independent from those used for grading the metabolites concentration (located at the top of heat map).

GC-MS analysis of ethyl acetate extracts of the effluent samples (1-8) compared to the MSM-tryptone control (0) showed the appearance, disappearance or accumulation of various chemical compounds over time. Most of the compounds identified in the core flooding effluent samples have been reported to be signature metabolites of anaerobic and/or aerobic biotransformation of hydrocarbon compounds suggesting that microbial transformation of hydrocarbon constituents within coal took place. However, since control experiments of the inoculum grown on only MSM-tryptone were not conducted, it cannot be ruled out that some of the metabolites detected could be due to the transformation of the growth medium into signature compounds and not from the bulk coal itself. Mono-, di- or aromatic carboxylic acids of $C_2$-$C_{11}$ were the main hydrocarbon intermediates detected in the core flooding effluents, which may indicate the metabolism of larger molecular weight hydrocarbons.

Phenylacetate, benzoate and glutarate present in high concentration in MSM-tryptone (pre-injection phase) were likely utilized by microbes in the core, though could have potentially been produced over time. The appearance of alkylsuccinic acid, methyl succinate and p-tolylacetate in the in the lag phase (labelled as Sample # 1) effluent (within 10 days residence time in the coal pack) may have been as a result of the early transformation of simple coal constituents such as alkanes and mono aromatics or from tryptone itself. The appearance of metabolites, such as naphthoic acids, in subsequent samples was likely indicative of the relatively slower transformation of polycyclic aromatic hydrocarbons. The transient nature of most of the metabolites were observed in Figure 4.5, which is typical of the production and utilization of pathway intermediates by various species of microbes in a microbial consortium. The

majority of metabolites accumulated at a relatively higher concentrations in the later samples (late-phase, between 70-90 days), suggesting that microbial activity increased with the incubation period within the coal core. These compounds may be transient nature and if the core had been operated for a longer period of time, these metabolites may have been converted eventually to methane.

The range of compounds detected, identified and quantified in this work were limited. Nevertheless, the compounds detected were consistent with anaerobic degradation of coal constituents and have been shown to be present *in-situ* within coal seams [Duncan et al., 2009; Wawrik et al., 2012]. The presence of alkylsuccinic acid (methyl succinate) may indicate the transformation of alkane compounds via addition to fumarate [Gieg and Suflita, 2002; Parisi et al., 2009]. In addition, the detection of hexanoic and fatty acids may be indicative of alkane biodegradation. The aromatic constituents of coal may have been degraded based on the detection of toluic acids, phthalic acids and cresols. The presence of naphthoic acids may also be indicative of the biodegradation of the polycyclic aromatic hydrocarbon. The increased diversity of intermediates available for (resulting from) microbial metabolism over time may reflect the effect of increasing biomass causing a more rapid assimilation of easily utilisable components in tryptone, forcing thereby the utilisation of coal.

Note, as seen in the Figure 4.5, the inconsistent concentration of some metabolites (eg., benzoate in sample # 1, transcinnamate in sample # 4) in technical replicates, is likely due to the volatile nature of these compounds and depending on how fast the samples were acidified, they may be lost. In addition, it may be due to variations in the ability of the GC-MS machine to detect compounds in the samples or peak area integration. In such case, two similar concentrations were considered for the data interpretation.

Among the metabolites accumulated in the core flooding effluent, succinic

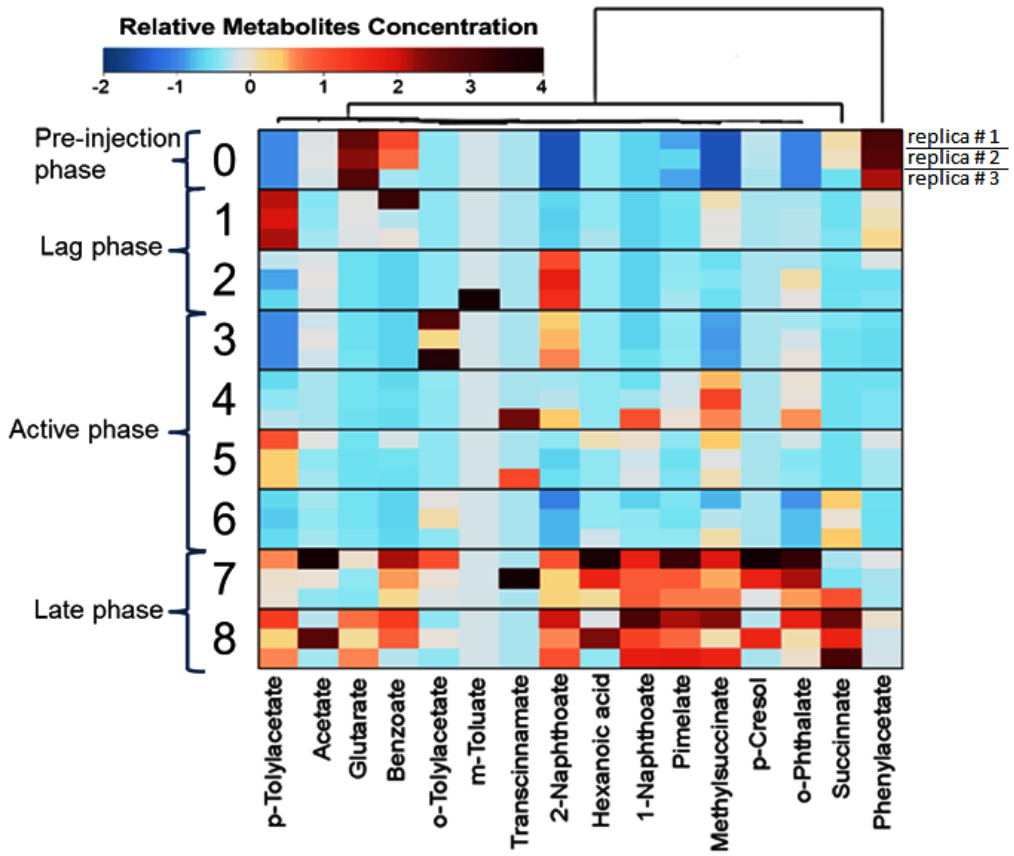


Figure 4.5: Heat map showing the relative concentration of compounds detected in MSM-tryptone (0) and core flooding effluent samples (1-8) and relationships between samples are described using hierarchical clustering. Concentration of compounds increase from blue to red and the concentration of each compound in a sample is relative to its concentration in other samples. Each sample block consists of three technical replicates of each sample.

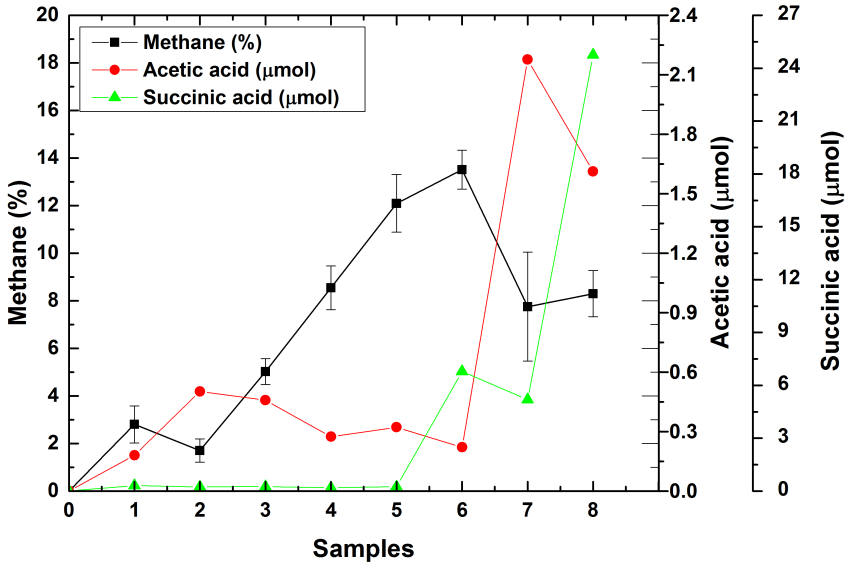


Figure 4.6: Percentage methane, acetic and succinic acid concentration in MSM-tryptone (0) and effluent samples (1-8).

acid is a value added product that can be used as a precursor in the production of polyesters, as a nutraceutical compound and in pharmaceutical preparations [Zeikus et al., 1999]. This suggests that, in addition to methane, other valuable products such as organic acids may be produced in the core flooding effluents. It was observed that the succinic acid production increased hundred-fold (from Sample # 5-8) as methanogenesis progressed (Figures 4.5 and 4.6). The plot of the percentage of methane presents in the effluent gases and concentrations of acetic acid (Figure 4.6) shows the inverse correlation between methane production and acetic acid concentration. Acetic acid, a methanogenic intermediate substrate, was inversely proportional to methane generation, i.e., it was present in high concentrations for the $2^{nd}$ sample and it's concentration decreased in the subsequent samples (3-6) while $CH_4$ production increased (Figures 4.5 and 4.6), indicating that it may have been used by acetoclastic methanogens for enhanced methane production. The concentration of acetic acid increased in the $7^{th}$ sample, which corresponds to the decline in the methane generation. For the $8^{th}$ sample, the decrease in the concentration of acetic acid again correlated to the increase in methane generation. These results indicated that acetic acid was utilized by methanogens as

a substrate for the methane generation, Hence, acetoclastic reaction was likely to be the dominant methanogenic pathway for the present bioconversion process observed during the core flooding experiments described here. However, 16S rRNA sequence data of the methanogens present in the microbial culture and stable isotopic data of the $CH_4$, $CO_2$ and effluent sample are required for the validation of the predominant methanogenic pathways involved in the present study. The formation of acetic acid from the tryptone fermentation cannot be ruled out, hence simultaneous running of the bottle experiment with and without (control) the addition of coal to the microbial culture containing MSM-tryptone can be used to justify the metabolites formation only from the coal bioconversion. However, there may be other inhibitory or stimulatory properties affecting the use of acetate (coal) as a substrate for methanogenesis.

## 4.7 Summary

Results obtained from the core flooding were presented in this chapter. For the characterization of the coal pack, porosity and permeability were estimated. Gas adsorption into the coal matrix and microbial growth were resulted into the decrease of coal permeability during the core flooding experiment. The progress in the methane generation until the experiment stopped, indicated that microbial action and biostimulation enhanced coal methanogenesis. Acetoclastic reaction was likely to be a predominant pathway of methanogenesis in the present experiment. The rate of methanogenesis was affected by the accumulation of metabolites. Results from the present work were compared with those from the bottle experiment available in the literature. Bioavailability of the coal and bio-solubilisation of coal organic molecules controlled the overall methane generation. Key metabolites detected in the core flooding effluent sample showed the presence of alkane, aromatic and fatty acid metabolism in the coal biodegradation process. The detailed summary of the present coal bioconversion process was discussed in chapter 5.

# Chapter 5

# Conclusion and Future Prospects

## 5.1 Summary and Concluding Remarks

The objective of the present work was to conduct laboratory core flooding experiments for the bioconversion of coal into methane by stimulating microbes involved in coal conversion. In order to simulate the bioconversion process at *in-situ* coal bed conditions, core flooding experiment was carried out in a core holder packed with crushed coal (150-250 $\mu$m), operated at elevated pressure and with a continuous flow of nutrient rich MSM along the coal pack. Varying permeable reservoir was replicated as a packed column of two layers with different permeability.

Since methanogens are strictly anaerobes, the experimental system was maintained at anaerobic conditions. An anoxic mineral salts medium, (WR-86) with tryptone amendment, was continuously supplied to the coal pack as a growth medium for methanogenesis during the core flooding experiment. The anaerobic methanogenic culture, QSAF, enriched from coal cuttings was used to inoculate the coal pack. The detailed description of the developed experimental setup was provided in chapter 3. The procedure for the execution of the core flooding experiment, sample and microbial culture preparation, gas desorption from the effluent, gas and effluent analysis were described in detail.

For the characterization of porous medium, the porosity and permeability of the coal core was estimated. It was observed that the coal permeability changes as methanogenesis progresses due to the formation of biofilm and extracellular polymeric substance on the surface of coal particles and gas adsorption into the coal matrix. At the end of experiment (90 d) the permeability was changed to more than a half of the initial permeability.

Results indicated that bio-augmented microorganisms can generate methane more rapidly. Molar ratio of the $CH_4$ and $CO_2$ indicated that acetoclastic reaction was likely to be the dominant pathway at the beginning of methanogenesis and later $CO_2$ reduction pathway was also likely to be responsible for the methanogenesis. The degassing of the coal core at the end of the experiment could recover some of the $CH_4$, which was adsorbed in the coal matrix during the core flooding experiment. With the consideration of solubility, a 20% increase in production of $CH_4$ in the effluent samples was observed. Methanogenesis was continuously progressing until the experiment was stopped on the $90^{th}$ day of a continuous flooding cycle.

The percentages of $CH_4$ obtained in the present work were in comparison with the results from the bottle experiments reported in the literature. More quantity of coal, less surface contact of coal with microbes and enriched nutrient solution and lower bioavailability in the core flooding experiment led to the lower generation of $CH_4$/ gram of coal compared to the bottle experiment. Moreover, methane generation is mass transfer limited, which in turn depends on the dissolution rate of coal organic macromolecules such as hydroxyl, methoxy, carboxylic groups etc. Running core flooding experiment for longer time might have resulted in the enhanced microbial transformation of a substantial amount of these functional groups (depend on the quantity of coal) into $CH_4$.

The rate of methanogenesis was affected by the accumulation of metabo-

lites or waste by-products. Higher rate of $CO_2$ production compared to the $CH_4$ was due to the cumulative $CO_2$ from the bacteria fermentation process and its inefficient utilization by the methanogens. The decrease in the molar ratio of $CO_2$ to $CH_4$ indicated that methanogenic reaction favoured into the production of $CH_4$ in the subsequent samples. Running experiment for further extended period of time might result in the $CH_4$ production surpassing the $CO_2$ production. Quantity of $CO_2$ produced in the present experiment can be mitigated by optimizing $CO_2$ reduction pathway of methanogenesis.

Metabolites analyses were performed on the effluent sample collected at different stages of the experiments. Several key signature metabolites were detected in the effluent samples. Transient accumulation of these metabolites indicated their production and consumption over time. Metabolites such as succinic acid, methylsuccinate, pimelic acid, acetic acid, hexanoic acid o-phthalate and benzoate detected in the effluent samples, signifies the n-alkane, fatty acid and aromatic metabolism. Metabolites analysis showed the early transformation of the alkane and mono aromatic compounds and slower transformation of the polycyclic aromatic hydrocarbons. It was observed that some metabolites, such as phenylacetate, benzoate and glutarate ,were utilized by microbes and also produced over time. Presence of succinic acid in the effluent, suggests that the coal bioconversion process can be used for extraction of other biotechnologically relevant value-added products apart from $CH_4$ generation. Increase in the production of $CH_4$ with utilization of acetic acid indicated that acetoclastic methanogens utilized acetate as a substrate for $CH_4$ production

Finally, based on the laboratory scale investigation of the coal bioconversion process, we made the following major conclusions.
Microbial culture introduced into the coal pack was actively involved in the coal methanogenesis. Methanogenesis process was progressed at elevated pressure. Methane generation was expedited continuously until the experiment stopped and it indicated that methanogenesis will continue further for long

time. By supplying nutrients, keeping endemic microbes growing and removing metabolites or waste by-products that inhibit the methanogenesis, biogenic $CH_4$ production can be accelerated. Hence, the life of the CBM reservoirs can be extended. Stimulating the growth of methanogens known for $CO_2$ reduction, such as *Methanomicrobiales* and *Methanobacteria*, $CO_2$ production can be mitigated. Promising results for *in-situ* methane production obtained from the core flooding experiment will aid in the design and deployment of enhanced coal bed methane strategies in the field.

## 5.2 Future Work

Although the results presented in this work indicated that methanogens can produce methane from the coal, significant room for the development of optimum engineering method to accelerate the methanogenesis process and understanding of the whole biodegradation process at laboratory and field scale is still there. Some of the notable future recommendations are highlighted below:

- Coal bioconversion into methane occurs through multiple reactions. Most of the hydrolytic reactions and methanogenic reactions involved in the coal bioconversion can release energy. These exothermic reactions might result in the increases of temperature within the coal bed. Most of the methanogens and other anaerobic bacteria take part in the coal bioconversion process favour a certain temperature range for their metabolism. Catabolic reactions in the coal biodegradation are also temperature dependant. The future core flooding experiments can focus on the measurement of *in-situ* temperature at discrete positions along the core holder and also identification of the favourable temperature for optimum methanogenesis.

- Nutrients such as tryptone are appropriate for laboratory scale experiment. However, it would likely be inappropriate for field trials because of its expense. Selection of nutrient is important for the stimulation of

methanogenesis. Suitable, cost effective nutrient for field trial can be identified.

- Coal methanogenesis is mass transfer limited (dissolution rate of coal functional groups), which depend on the available surface area of the coal. In the actual reservoir, addition of selected solvent can increase the pore volume. This will increase the surface area and make the pore network more easily accessable to the microbes. Investigation can be carried out to understand the effect of solvent addition on pore and fracture volumes and thereby rate of methanogenesis.

- Since the rate of methanogenesis is controlled by substrates utilization of microbes, further research can be focussed on the investigation of microbial interaction with intact and fractured coal.

- More research works are to be done to obtain a thorough understanding of the coal biodegradation, identification of the chemical species that limit biodegradation and to develop methods to overcome the impediments.

- Availability of nutrients come into contact with microbes affect the rate of methanogenesis. Rate of transport of nutrients into microbial cells is to be investigated more.

- Reaction kinetics model for the estimation of conversion efficiency of coal into valuable fuel products, such as $CH_4$ and metabolic value added by-products, and rate of methanogenic reaction are to be developed.

- Since the coal core is more representative of *in-situ* conditions, the core flooding experiment can be extended by replacing crushed coal with intact coal.

# References

Budwill, K. (1996). Anaerobic microbial degradation of poly(3-hydroxyalkanoates) with various terminal electron acceptors. *Journal of Environmental Polymer Degradation*, 4(2):91–102.

Budwill, K., Koziel, S., and Vidmar, J. (2011). Advancements in understanding and enhancing biogenic methane production from coals. volume 2, pages 1621–1629.

Carman, P. C. (1939). Permeability of saturated sands, soils and clays. *The Journal of Agricultural Science*, 29:262–273.

Catcheside, D. and Ralph, J. (1999). Biological processing of coal. *Applied Microbiology and Biotechnology*, 52(1):16–24.

Center for Climate and Energy Solutions, U.S.A ((October 15, 2013)).

Chaudhari, L., Hadia, N., Mitra, S., and Vinjamur, M. (2011). Flow visualization of two-phase flow through layered porous media. *Energy Sources, Part A: Recovery, Utilization and Environmental Effects*, 33(10):948–958.

Cheung, K., Klassen, P., Mayer, B., Goodarzi, F., and Aravena, R. (2010). Major ion and isotope geochemistry of fluids and gases from coalbed methane and shallow groundwater wells in Alberta, Canada. *Applied Geochemistry*, 25(9):1307–1329.

Clayton, J. (1998). Geochemistry of coalbed gas - a review. *International Journal of Coal Geology*, 35(1-4):159–173.

Duncan, K., Gieg, L., Parisi, V., Tanner, R., Tringe, S., Bristow, J., and Suflita, J. (2009). Biocorrosive thermophilic microbial communities in Alaskan North Slope oil facilities. *Environmental Science and Technology*, 43(20):7977–7984.

Faison, B. (1991). Microbial conversions of low rank coals. *Nature Biotechnology*, 9(10):951–956.

Faiz, M. and Hendry, P. (2006). Significance of microbial activity in australian coal bed methane reservoirs - a review. *Bulletin of Canadian Petroleum Geology*, 54(3):261–272.

Fakoussa, R. and Hofrichter, M. (1999). Biotechnology and microbiology of coal degradation. *Applied Microbiology and Biotechnology*, 52(1):25–40.

Fedorak, P. and Hrudey, S. (1984). The effects of phenol and some alkyl phenolics on batch anaerobic methanogenesis. *Water Research*, 18(3):361–367.

Ferry, J. (2011). Fundamentals of methanogenic pathways that are key to the biomethanation of complex biomass. *Current Opinion in Biotechnology*, 22(3):351–357.

Flores, R. M., Rice, C. a., Stricker, G. D., Warden, A., and Ellis, M. S. (2008). Methanogenic pathways of coal-bed gas in the Powder River Basin, United States: The geologic factor. *International Journal of Coal Geology*, 76(1-2):52–75.

Formolo, M., Martini, A., and Petsch, S. (2008). Biodegradation of sedimentary organic matter associated with coalbed methane in the powder river and san juan basins, u.s.a. *International Journal of Coal Geology*, 76(1-2):86–97.

Gallagher, L., Glossner, A., Landkamer, L., Figueroa, L., Mandernack, K., and Munakata-Marr, J. (2013). The effect of coal oxidation on methane production and microbial community structure in powder river basin coal. *International Journal of Coal Geology*, 115:71–78.

Gamson, P., Beamish, B., and Johnson, D. (1993). Coal microstructure and micropermeability and their effects on natural gas recovery. *Fuel*, 72(1):87–99.

Garcia, J.-L., Ollivier, B., and Whitman, W. (2006). The order methanomicrobiales. In Dworkin, M., Falkow, S., Rosenberg, E., Schleifer, K.-H., and Stackebrandt, E., editors, *The Prokaryotes*, pages 208–230. Springer New York.

Gieg, L. and Suflita, J. (2002). Detection of anaerobic metabolites of saturated and aromatic hydrocarbons in petroleum-contaminated aquifers. *Environmental Science and Technology*, 36(17):3755–3762.

Global Carbon Project (2013). Carbon budget and trends 2013. (released on 19 november 2013) along with any other original peer-reviewed papers and data sources as appropriate.

Green, M., Flanegan, K., and Gilcrease, P. (2008). Characterization of a methanogenic consortium enriched from a coalbed methane well in the powder river basin, u.s.a. *International Journal of Coal Geology*, 76(1-2):34–45.

Hadia, N., Chaudhari, L., Mitra, S., Vinjamur, M., and Singh, R. (2007). Experimental investigation of use of horizontal wells in waterflooding. *Journal of Petroleum Science and Engineering*, 56(4):303–310.

Hadia, N., Chaudhari, L., Mitra, S., Vinjamur, M., and Singh, R. (2008a). Effect of scaling parameters on waterflood performance with horizontal and vertical wells. *Energy and Fuels*, 22(1):402–409.

Hadia, N., Chaudhari, L., Mitra, S., Vinjamur, M., and Singh, R. (2008b). Waterflood profiles and oil recovery with vertical and horizontal wells. *Energy Sources, Part A: Recovery, Utilization and Environmental Effects*, 30(17):1604–1618.

Hadia, N., Mitra, S., and Vinjamur, M. (2012). Estimation of permeability heterogeneity in limestone outcrop by pressure measurements: Experiments

and numerical simulation. *Experimental Thermal and Fluid Science*, 40:177–184.

Harris, S. H., Smith, R. L., and Barker, C. E. (2008). Microbial and chemical factors influencing methane production in laboratory incubations of low-rank subsurface coals. *International Journal of Coal Geology*, 76(1-2):46–51.

Hazrin-Chong, N. and Manefield, M. (2012). An alternative sem drying method using hexamethyldisilazane (hmds) for microbial cell attachment studies on sub-bituminous coal. *Journal of Microbiological Methods*, 90(2):96–99.

International Energy Agency (2012). $Co_2$ emissions from fuel combustion highlights.

J. H. Ward, J. (1963). Hierarchical grouping to optimize an objective function. *Journal of the American Statistical Association*, 58:236–244.

Jin, S., Bland, A. E., and Price, H. S. (2009). Biogenic methane production enhancement systems.

Jones, E. J. P., Voytek, M. A., Corum, M. D., and Orem, W. H. (2010). Stimulation of methane generation from nonproductive coal by addition of nutrients or a microbial consortium. *Applied and Environmental Microbiology*, 76(21):7013–7022.

Jones, E. J. P., Voytek, M. A., Warwick, P. D., Corum, M. D., Cohn, A., Bunnell, J. E., Clark, A. C., and Orem, W. H. (2008). Bioassay for estimating the biogenic methane-generating potential of coal samples. *International Journal of Coal Geology*, 76(1-2):138–150.

Kinnon, E., Golding, S., Boreham, C., Baublys, K., and Esterle, J. (2010). Stable isotope and water quality analysis of coal bed methane production waters and gases from the bowen basin, australia. *International Journal of Coal Geology*, 82(3-4):219–231.

Klinkenbeg, L. (1941). The permeability of porous media to liquids and gases, drilling and production practice. *American Petroleum Institution*, pages 200–213.

Kotarba, M. (2001). Composition and origin of coalbed gases in the upper silesian and lublin basins, poland. *Organic Geochemistry*, 32(1):163–180.

Kotelnikova, S. (2002). Microbial production and oxidation of methane in deep subsurface. *Earth-Science Reviews*, 58(3-4):367–395.

Krumbein, W. C. and Sloss, L. L. (1963). *Stratigraphy and sedimentation*. W. H. Freeman and Co., San Francisco, CA, second edition.

Lin, W., Tang, G.-Q., and Kovscek, A. (2008). Sorption-induced permeability change of coal during gas-injection processes. *SPE Reservoir Evaluation and Engineering*, 11(4):792–802.

Luca Technologies Inc. (2004). Active biogenesis of methane in wyoming′s powder river basin. Technical report.

Mazumder, S. and Wolf, K. (2008). Differential swelling and permeability change of coal in response to CO2 injection for ECBM. *International Journal of Coal Geology*, 74(2):123–138.

Mazumder, S., Wolf, K., Hemert, P., and Busch, A. (2008). Laboratory experiments on environmental friendly means to improve coalbed methane production by carbon dioxide/flue gas injection. *Transport in Porous Media*, 75(1):63–92.

McInerney, M. and Bryant, M. (1981). Anaerobic degradation of lactate by syntrophic associations of methanosarcina barkeri and desulfovibrio species and effect of h2 on acetate degradation. *Applied and Environmental Microbiology*, 41(2):346–354.

Nobakht, M., Moghadam, S., and Gu, Y. (2007). Effects of viscous and capillary forces on co2 enhanced oil recovery under reservoir conditions. *Energy & Fuels*, 21(6):3469–3476.

Orem, W., Tatu, C., Lerch, H., Rice, C., Bartos, T., Bates, A., Tewalt, S., and Corum, M. (2007). Organic compounds in produced waters from coalbed natural gas wells in the powder river basin, wyoming, usa. *Applied Geochemistry*, 22(10):2240–2256.

Orem, W., Voytek, M., Jones, E., Lerch, H., Bates, A., Corum, M., Warwick, P., and Clark, A. (2010). Organic intermediates in the anaerobic biodegradation of coal to methane under laboratory conditions. *Organic Geochemistry*, 41(9):997–1000.

Papendick, S. L., Downs, K. R., Vo, K. D., Hamilton, S. K., Dawson, G. K., Golding, S. D., and Gilcrease, P. C. (2011). Biogenic methane potential for Surat Basin, Queensland coal seams. *International Journal of Coal Geology*, 88(2-3):123–134.

Parisi, V., Brubaker, G., Zenker, M., Prince, R., Gieg, L., Da Silva, M., Alvarez, P., and Suflita, J. (2009). Field metabolomics and laboratory assessments of anaerobic intrinsic bioremediation of hydrocarbons at a petroleum-contaminated site. *Microbial Biotechnology*, 2(2 SPEC. ISS.):202–212.

Pashin, J. (2007). Hydrodynamics of coalbed methane reservoirs in the black warrior basin: Key to understanding reservoir performance and environmental issues. *Applied Geochemistry*, 22(10):2257–2272.

Penner, T. J., Foght, J., and Budwill, K. (2010). Microbial diversity of western canadian subsurface coal beds and methanogenic coal enrichment cultures. *International Journal of Coal Geology*, 82(1-2):81–93.

Pfeiffer, R. S., Ulrich, G. A., and Finkelstein, M. (2010). Chemical amendments for the stimulation of biogenic gas generation in deposits of carbonaceous material.

Potter, M. (1908). Bacteria as agents in the oxidation of amorphous carbon. *Proceedings of the Royal Society of London. Series B*, 80(539):239–259.

Rice, C., Flores, R., Stricker, G., and Ellis, M. (2008). Chemical and stable isotopic evidence for water/rock interaction and biogenic origin of coalbed methane, fort union formation, powder river basin, wyoming and montana u.s.a. *International Journal of Coal Geology*, 76(1-2):76–85.

Rice, D. (1993). Composition and origins of coalbed gas. in: Law, b.e., rice, d.d. (eds), hydrocarbons from coal. *American Association of Petroleum Geologists Studies in Geology*, 38:159–184.

Rice, D. and Claypool, G. (1981). Generation, accumulation, and resource potential of biogenic gas. *American Association of Petroleum Geologists Bulletin*, 65(1):5–25.

Santosh, V., Mitra, S., Vinjamur, M., and Singh, R. (2007). Experimental and numerical investigations of waterflood profiles with different well configurations. *Energy and Fuels*, 21(6):3353–3359.

Scheidegger, A. E. (1974). *The physics of flow through porous media*. University of Toronto Press, Toronto, third edition.

Schlegel, M., McIntosh, J., Bates, B., Kirk, M., and Martini, A. (2011). Comparison of fluid geochemistry and microbiology of multiple organic-rich reservoirs in the illinois basin, usa: Evidence for controls on methanogenesis and microbial transport. *Geochimica et Cosmochimica Acta*, 75(7):1903–1919.

Scott, A. (2002). Hydrogeologic factors affecting gas content distribution in coal beds. *International Journal of Coal Geology*, 50(1-4):363–387.

Scott, A., Kaiser, W., and Ayers Jr, W. (1994). Thermogenic and secondary biogenic gases, san juan basin, colorado and new mexico - implications for coalbed gas producibility. *American Association of Petroleum Geologists Bulletin*, 78(8):1186–1209.

Shen, P., Wang, J., Yuan, S., Zhong, T., and Jia, X. (2009). Study of enhanced-oil-recovery mechanism of alkali/surfactant/polymer flooding in porous media from experiments. *SPE Journal*, 14(2):237–244.

Smith, J. and Pallasser, R. (1996). Microbial origin of australian coalbed methane. *AAPG Bulletin*, 80(6):891–897.

Smith, J. W., Gould, K. W., Hart, G. H., and Rigby, D. (1985). Isotopic studies of australian natural and coal seam gases. *AIMM bulletin*, 290(6):43–51.

Smith, M. and Mah, R. (1980). Acetate as sole carbon and energy source for growth of methanosarcina strain 227. *Applied and Environmental Microbiology*, 39(5):993–999.

Speight, J. G. (2013). *Coal-fired power generation handbook*. Scrivener Publishing and Jhn Wiley & Sons, Inc.

Strapo, D., Mastalerz, M., Eble, C., and Schimmelmann, A. (2007). Characterization of the origin of coalbed gases in southeastern illinois basin by compound-specific carbon and hydrogen stable isotope ratios. *Organic Geochemistry*, 38(2):267–287.

Strapo, D., Picardal, F., Turich, C., Schaperdoth, I., Macalady, J., Lipp, J., Lin, Y.-S., Ertefai, T., Schubotz, F., Hinrichs, K.-U., Mastalerz, M., and Schimmelmann, A. (2008). Methane-producing microbial community in a coal bed of the illinois basin. *Applied and Environmental Microbiology*, 74(8):2424–2432.

Strapoc, D., Mastalerz, M., Dawson, K., MacAlady, J., Callaghan, A., Wawrik, B., Turich, C., and Ashby, M. (2011). Biogeochemistry of microbial coal-bed methane. *Annual Review of Earth and Planetary Sciences*, 39:617–656.

Taconi, K. A., Zappi, M. E., French, W. T., and Brown, L. R. (2008). Methanogenesis under acidic ph conditions in a semi-continuous reactor system. *Bioresource Technology*, 99(17):8075 – 8081.

Taylor, S., Milly, P., and Jaffe, P. (1990). Biofilm growth and the related changes in the physical properties of a porous medium. 2. permeability. *Water Resources Research*, 26(9):2161–2169.

Thauer, R., Jungermann, K., and Decker, K. (1977). Energy conservation in chemotrophic anaerobic bacteria. *Bacteriological Reviews*, 41(1):100–180.

Toledo, G. V., Richardson, T. H., Stingl, U., Mathur, E. J., and Venter, G. (2010). Methods to stimulate biogenic methane production fromhydrocarbon-bearingearing formations.

Ulrich, G. and Bower, S. (2008). Active methanogenesis and acetate utilization in powder river basin coals, united states. *International Journal of Coal Geology*, 76(1-2):25–33.

Unal, B., Perry, V. R., Sheth, M., Gomez-Alvarez, V., Chin, K.-J., and Nüsslein, K. (2012). Trace elements affect methanogenic activity and diversity in enrichments from subsurface coal bed produced water. *Frontiers in microbiology*, 3(May):175.

Vandevivere, P. and Baveye, P. (1992). Effect of bacterial extracellular polymers on the saturated hydraulic conductivity of sand columns. *Applied and Environmental Microbiology*, 58(5):1690–1698.

Warwick, P., Breland Jr., F., and Hackley, P. (2008). Biogenic origin of coalbed gas in the northern gulf of mexico coastal plain, u.s.a. *International Journal of Coal Geology*, 76(1-2):119–137.

Wawrik, B., Mendivelso, M., Parisi, V., Suflita, J., Davidova, I., Marks, C., Van Nostrand, J., Liang, Y., Zhou, J., Huizinga, B., Strapo, D., and Callaghan, A. (2012). Field and laboratory studies on the bioconversion of coal to methane in the san juan basin. *FEMS Microbiology Ecology*, 81(1):26–42.

Weniger, P., Franc, J., Krooss, B., Bzek, F., Hemza, P., and Littke, R. (2012). Geochemical and stable carbon isotopic composition of coal-related gases from the sw upper silesian coal basin, czech republic. *Organic Geochemistry*, 53:153–165.

Whiticar, M., Faber, E., and Schoell, M. (1986). Biogenic methane formation in marine and freshwater environments: $Co_2$ reduction vs. acetate fermentationisotope evidence. *Geochimica et Cosmochimica Acta*, 50(5):693 – 709.

Wiesenburg, D. and Guinasso Jr., N. (1979). Equilibrium solubilities of methane, carbon monoxide, and hydrogen in water and sea water. *Journal of Chemical and Engineering Data*, 24(4):356–360.

Wilhelm, E., Battino, R., and Wilcock, R. (1977). Low-pressure solubility of gases in liquid water. *Chemical Reviews*, 77(2):219–262.

Xia, J., Mandal, R., Sinelnikov, I., Broadhurst, D., and Wishart, D. (2012). Metaboanalyst 2.0-a comprehensive server for metabolomic data analysis. *Nucleic Acids Research*, 40(W1):W127–W133.

Zeikus, J., Jain, M., and Elankovan, P. (1999). Biotechnology of succinic acid production and markets for derived industrial products. *Applied Microbiology and Biotechnology*, 51(5):545–552.

Zhou, Z., Ballentine, C., Kipfer, R., Schoell, M., and Thibodeaux, S. (2005). Noble gas tracing of groundwater/coalbed methane interaction in the san juan basin, usa. *Geochimica et Cosmochimica Acta*, 69(23):5413–5428.

# Appendix A

# Appendix

## A.1 Calibration of Differential Pressure Transducer

A differential pressure transducer, C-DP-1, (DP15, Validyne Engineering Corp.) was used to measure the differential pressure across the core holder as described in Chapter 3. It can be used for measuring any pressure, ranges from 0.08 psi(d) to 3200 psi(d) by replacing pressure sensing diaphragm. The pressure sensing diaphragms are available for different ranges of the measurable full scale differential pressure between 0.08 psi(d) and 3200 psi(d). A diaphragm (range dash no. 44) with pressure ranges between 0-32 psi(d) was used for measuring differential pressure across the core holder. The output voltage from the DP15 transducer was 35mV/V full scale. The carrier demodulator was used to convert the output signal from the transducer to 10V DC output, which is required for the DAQ unit. The pressure automated calibration equipment (Druck PACE5000, General Electric Company) was used to calibrate the DP15 differential pressure transducer.

### A.1.1 Equipment and Connections

Following equipments were used and connections were established for the pressure calibration purpose. IEC power connector was used to connect the power supply and rear of the Druck PACE5000. RS232 cable was used to connect the Druck PACE5000 calibration equipment to the computer. Nitrogen pres-

sure supply line was connected to the SUPPLY + connection port of the DP15 transducer and SUPPLY − connection port of the DP15 transducer was vented to the atmosphere. The power cable from the conditioning box of the CD15 demodulator was connected to the power supply. The DP15 transducer was connected to the conditioning box using a PTA02A-10-6P connector on the rear panel of the conditioning box. The red output binding post on the front panel of the conditioning box was connected to the positive connection terminal, AIX+, (X can be 1, 2, 3...) on the DAQ card (NI USB-6009) using a red electric wire. Similarly, the black output binding post of the conditioning box was connected to the negative connection terminal, AIX−, of the DAQ card using a black electric wire. The DAQ card was connected to the computer CPU using a USB cable.

### A.1.2 Calibration

The software used for the pressure calibration were (1) the commercial software, NI Measurement and Automation Explorer (National Instruments Corp.) and (2) the custom build Pressure Calibration Project (PCP) software, (programmed by Vidhya Subramanian with the instruction from Dr. David Nobes at Optical Diagnostic Group, Mechanical Engineering, University of Alberta). The set voltages corresponding to minimum pressure (zero psi) and maximum pressure (32 psi) were zero and 10V, respectively. "Zero set" of the DP15 transducer was performed by adjusting the "Zero" knob on the Validyne conditioning box until the voltage reading on the PCP software reached as close as possible to zero. Similarly, the span was set by adjusting the "Span" knob until the voltage reading reached as close as possible to 10V. The voltage corresponding to each set pressure (0-32 psi(d) with intervals of 4 psi(d)) was recorded after both pressure and voltage readings reached steady values. The voltages correspondig to minimum and maximum set pressures were ensured to be as close as possible to zero and 10V, respectively. The calibration plot was obtained by plotting differential pressure and voltage readings, as shown in Figure A.1. The obtained calibration plot was linear, with Pearson′s corre-

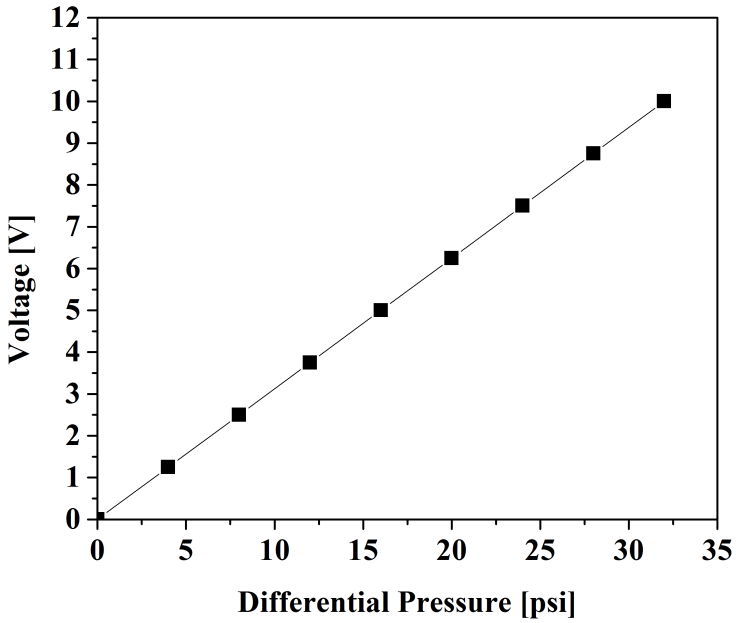


Figure A.1: Calibration curve of the differential pressure transducer, C-DP-1.

lation factor of $R^2 = 1$.

## A.2 Calibration of Inline Pressure Transducers

The upstream and downstream inline pressure transducers (FP2000 series, Honeywell International Inc), C-PT-1 and C-PT-2 (see Figure 3.1 of Chapter 3), were pre-calibrated at Honeywell International Inc. The minimum pressure (zero psi(g)) and maximum pressure (750 psi(g)) were set corresponding to the minimum voltage (0V) and maximum voltage (10V), respectively. A linear calibration plots were obtained for both transducers, C-PT-1 and C-PT-2, which are shown in Figure A.2. The obtained correlation factors for both plots were equal to unity, as shown in Figure A.2. The gauge pressure can be calculated from the produced signal voltage, using the following correlation equation:

$$P_{gauge} = 75.02 \times v - 0.843 \tag{A.1}$$

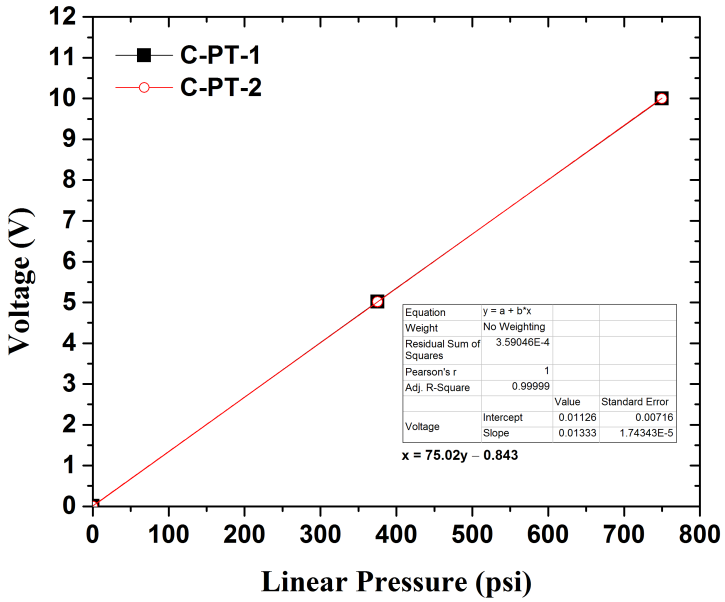


Figure A.2: Calibration curve of the inline pressure transducer, C-PT-1 and C-PT-2.

where,$P_{gauge}$ is the inline gauge pressure, (Pa); and $v$ is the signal voltage produced, (V).

## A.3 Operating Pressure for the Experiment

The operating (pore) pressure chosen for the experiment was in accordance with the hydrostatic pressure of the reservoir. The reservoir pressure increases as depth increases, as shown in Figure A.3. The normal hydrostatic pressure gradient in coalbed methane wells is about 0.097 MPa/m (0.43 psi/ft.) [Pashin, 2007; Scott, 2002]. This hydrostatic pressure gradient varies slightly from one reservoir to another. Also, at some locations, this hydrostatic pressure gradient may ranges from normal to extremely underpressured. Figure A.3 shows the pressure-depth plot of the coal reservoir with hydrostatic pressure gradient is 0.01 MPa/m (0.44 psi/ft.). Most coalbed methane is recoverable from depth between 150 m and 1000 m [Pashin, 2007]. The operating pressure chosen for the experiment were 500 psi which is corresponding to the depth 346 m.

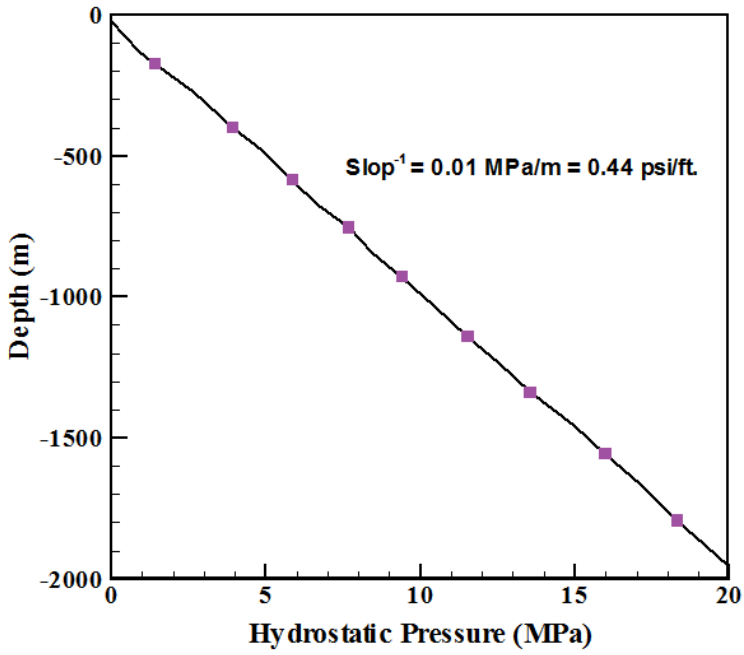


Figure A.3: Variation of hydrostatic pressure of the reservoir with depth.

## A.4 Formation Fluid Preparation

A mineral salts medium, MSM, (WR-86) with added tryptone (nutrient), defined as a simulated formation fluid was used as a growth medium for methanogenesis during the core flooding experiment as described in Chapter 3. The preparation and composition of MSM were adopted from protocols available in the literature [Fedorak and Hrudey, 1984]. The concentration of each constituents of MSM are shown in Table A.1. The composition of mineral I, mineral II, and vitamin B, and their concentration are shown in Table A.2. The $KH_2PO_4$, the resazurin (oxygen indicator) and the $Na_2S$. $9H_2O$ were added to the growth medium. The media (3 litre) prepared in carboy was autoclaved for 45 minutes, and cooled under an oxygen free nitrogen atmosphere to remove dissolved oxygen. The carboy lid was fit with a pressure gauge and valve for introducing nitrogen. Valve on the carboy lid can be used to remove dissolved oxygen. Carboy was kept under nitrogen atmosphere (4 psi(g)) to stop air entrainment. The carboy was cooled under nitrogen atmosphere. After the media was autoclaved, sodium sulphite was introduced as a reducing agent,

Table A.1: Composition of the growth medium

| Solution | Volume added (ml)/100.2 ml |
|---|---|
| Distilled water | 97 |
| Mineral I | 1 |
| Mineral II | 0.1 |
| Vitamin B | 0.1 |
| Phosphate | 1 |
| Resazurin | 1 |

followed by tryptone addition with 5 g/L concentration. The media in carboy was transferred to a glove bag, which was previously flushed with nitrogen (4 psig(g)) to prevent air entrainment.

## A.5 $CH_4$ and $CO_2$ Calibration Standards

We report here the detailed procedures for the preparation of $CH_4$ and $CO_2$ calibration standards used for the gas analysis, which described in Chapter 3. The custom calibration standard was prepared for the measurement of both $CH_4$ and $CO_2$, which were produced in the core flooding experiment. Pure $CH_4$ and $CO_2$ were used for the preparation of the calibration standard. The procedure explained in Budwill et al. [Budwill, 1996] was used to prepare the calibration standards of both $CH_4$ and $CO_2$.

### A.5.1 $CH_4$ Calibration Standard

The calibration standards of $CH_4$ were prepared for 0.16%, 4%, 8%, 15% and 25% of $CH_4$. For each standard, a known amount of $CH_4$ was added to air-containing sealed 158-ml serum bottles. The volume of $CH_4$ (ml) added to each serum bottle was calculated using the following equation:

$$CH_4\ (\%) = \frac{\text{volume of } CH_4\ (\text{ml})}{\text{volume of } CH_4\ (\text{ml}) + 158\ (\text{ml})} \times 100 \qquad (A.2)$$

A gas sample from each standard was injected into the 5700A model GC in order to obtain peak area. Average peak area was calculated from the peak areas obtained during three trials. The volume of $CH_4$ added into the serum bottle, its percentage, the peak areas of the three trials, and the average peak

Table A.2: Stock solutions used in the growth medium

| Solution | Component | Concentration in distilled water (g/l) |
|---|---|---|
| Mineral I | NaCl | 50 |
| | $CaC4l_2$. $2H_2O$ | 10 |
| | $NH_4Cl$ | 50 |
| | $MgCl_2$. $6H_2O$ | 10 |
| Mineral II | $(NH_4)Mo7O_{24}$. $4H_2O$ | 10 |
| | $ZnSO_4$. $7H_2O$ | 0.1 |
| | $H_3BO_3$ | 0.3 |
| | $FeCl_2$. $4H_2O$ | 1.5 |
| | $CoCl_2$. $6H_2O$ | 10 |
| | $MnCl_2$. $4H_2O$ | 0.03 |
| | $NiCl_2$. $6H_2O$ | 0.03 |
| | $AlK(SO_4)_2$. $12H_2O$ | 0.1 |
| Vitamin B | Nicotinic Acid | 0.1 |
| | Cyanocobalamine | 0.1 |
| | Thiamine | 0.05 |
| | p-Aminobenzoic acid | 0.05 |
| | Pyridoxine | 0.25 |
| | Pantothenic acid | 0.025 |
| Phosphate | $KH_2PO_4$ | 50 |
| Resazurin | Resazurin | 0.1 |
| Sulfide | $Na_2S$. $9H_2O$ | 25 |

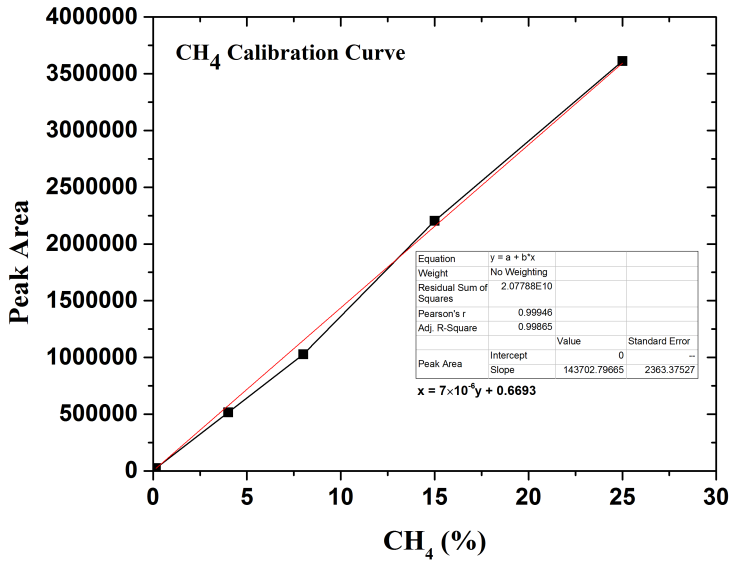


Figure A.4: Calibration curve for $CH_4$ measurement.

area are listed in Table A.3. The calibration plot was obtained by plotting each percentage of $CH_4$ and the corresponding average peak area, as shown in Figure A.4. The obtained calibration plot was linear with Pearson′s correlation factor of $R^2 \sim 1$.

Table A.3: The volume of $CH_4$ (ml) added into serum bottle, its percentage and the peak areas of gas injection for the preparation of $CH_4$ calibration standard

| $CH_4$ added (ml) | | 0.25 | 6.58 | 13.74 | 27.88 | 52.67 |
|---|---|---|---|---|---|---|
| $CH_4$(%) | | 0.16 | 4 | 8 | 15 | 25 |
| Peak Area | Trial i | 24194 | 513920 | 1024300 | 2193300 | 3591000 |
| | Trial ii | 24243 | 520520 | 1036800 | 2210300 | 3606500 |
| | Trial iii | 23682 | 516010 | 1023400 | 2206400 | 3638600 |
| | Average | 24039.6 | 516816.6 | 1028166.6 | 2203333.3 | 3612033.3 |

The percentage of $CH_4$ can be calculated from the known peak area using the following calibration equation:

$$CH_4\ (\%) = 7\ \times 10^{-6} \times \text{ peak area} + 0.6693 \qquad \text{(A.3)}$$

### A.5.2 $CO_2$ Calibration Standard

Five calibration standards of $CO_2$ were prepared for 5.2%, 10.5%, 20.9%, 31.4%, and 52.4% of $CO_2$. Initally, the serum bottle was evacuated to avoid the gas compression that occurs when a large volume of gas is added to an air-containing bottle. For each standard, a known amount of $CO_2$ was added to each evacuatd, sealed 158-ml serum bottle, and the remaining volume was occupied by air. The volume of $CO_2$ (ml) added into the serum bottle was calculated from the following equation:

$$CO_2\ (\%) = \frac{\text{volume of } CO_2\ (\text{ml})}{158\ (\text{ml})} \times 100 \tag{A.4}$$

Peak areas were obtained for three trials of $CO_2$ injection, as shown in Table A.4. The volume of $CO_2$ added to the serum bottle, its percentage, the peak areas of the three trials, and the average peak area are listed in Table A.4. A linear calibration plot was produced by plotting each percentage of $CO_2$ and the corresponding average peak area, as shown in Figure A.5. The obtained Pearson$'$s correlation factor, $R^2 \sim 1$.

Table A.4: The volume of $CO_2$ added into serum bottle, and the percentage of $CO_2$ for the preparation of calibration standard and the peak areas of gas injection

| $CO_2$ added (ml) | | 8.27 | 16.54 | 33.09 | 49.63 | 82.72 |
|---|---|---|---|---|---|---|
| $CO_2$(%) | | 5.2 | 10.5 | 20.9 | 31.4 | 52.4 |
| Peak Area | Trial i | 753299 | 1395930 | 2933382 | 3971982 | 7339437 |
| | Trial ii | 720016 | 1439228 | 2869994 | 4287133 | 7508979 |
| | Trial iii | 735186 | 1440456 | 2981680 | 4241754 | 7572077 |
| | Average | 736167 | 1439842 | 2928352 | 4287133 | 7473498 |

The percentage of $CO_2$ can be calculated from the known peak area using the following calibration equation:

$$CO_2\ (\%) = 7\ \times 10^{-6} \times \text{ peak area} + 0.4564 \tag{A.5}$$

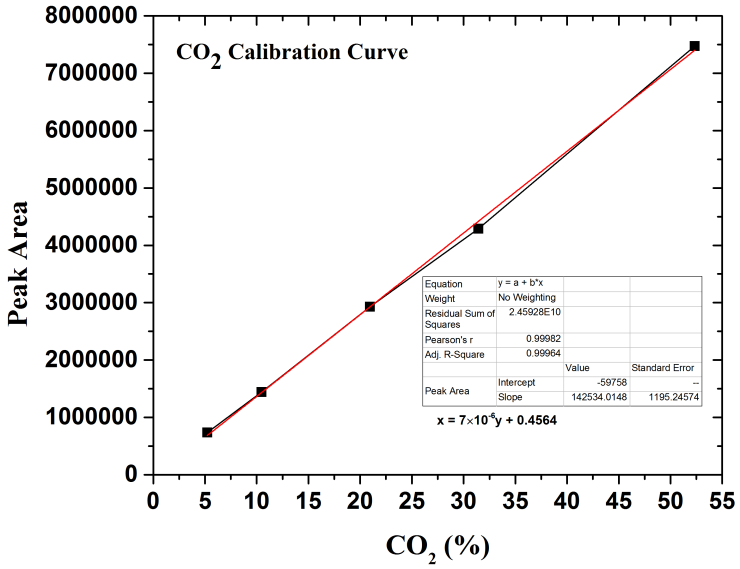


Figure A.5: Calibration curve for $CO_2$ measurement.

## A.6 Gas Measurement

We report here the detailed procedures for the $CH_4$ and $CO_2$ measurements, which described in Chapter 3. Results of these gas measurements have been presented in Table 4.3 and Figures 4.3, and 4.6 of Chapter 4.

The volume of gas, $V_G$, produced in the core flooding experiment was collected in the tedlar bag. Three different methods were employed for the quantification of gas.

**Method 1**: Gas was transferred from the tedlar bag to the sealed vial using a syringe. The total volume of gas inside the vial, $V_{g,vial}$, was calculated as the sum of the volume of gas transferred from the tedlar bag, $V_{1,g,tedlar}$, and the volume of air present inside the vial, $V_{air}$ as:

$$V_{g,vial}\ (\text{ml}) = V_{1,g,tedlar}\ (\text{ml}) + V_{air}\ (\text{ml}) \tag{A.6}$$

To prevent the compression effect and consequent gas leaks inside the air-containing vial, the quantity of gas transferred into each vial was less than its volume. Headspace gas of 0.1 ml from this vial was injected into the GC (three trials of gas injection) using a 0.5 ml syringe. The average peak area

was calculated from the peak areas obtained for these three trials. Percentages of $CH_4$ and $CO_2$ were calculated from the average peak area using calibration equations, Eqs. A.3 and A.5, respectively. The volume of each gas, $V_{1,CH_4}$ or $V_{1,CO_2}$, was calculated from the obtained percentage of each gas and the total volume of the gas inside the vial, $V_{g,vial}$, as:

$$V_{1,CH_4}\ (\text{ml}) = \frac{CH_4\ (\%) \times V_{g,vial}\ (\text{ml})}{100} \tag{A.7}$$

$$V_{1,CO_2}\ (\text{ml}) = \frac{CO_2\ (\%) \times V_{g,vial}\ (\text{ml})}{100} \tag{A.8}$$

**Method 2**: Gas from the tedlar bag was transferred to the evacuated vial, $V_{2,g,tedlar}$. Vacuum percentage was calculated corresponding to the vacuum pressure. The volume of the air inside the vial, $V_{air}$, was calculated from the known percentage of the vacuum and the volume of vial, $V_{vial}$, as:

$$V_{air}\ (\text{ml}) = \frac{(100 - \%\ \text{Vacuum}) \times V_{vial}(\text{ml})}{100} \tag{A.9}$$

The total volume of gas inside the vial, $V_{g,vial}$ was calculated as:

$$V_{g,vial}\ (\text{ml}) = V_{2,g,tedlar}\ (\text{ml}) + V_{air}\ (\text{ml}) \tag{A.10}$$

Similar to method 1, headspace gas of 0.1 ml was removed from the vial was injected into the GC (three trials of injection) using a 0.5 ml syringe. The average peak area was calculated from the peak areas obtained for three trials. Percentages of $CH_4$ and $CO_2$ were calculated from the average peak area using calibration equations, Eqs. A.3 and A.5, respectively. The volume of each gas, $V_{2,CH_4}$ or $V_{2,CO_2}$, was calculated using Eqs. A.7 and A.8, respectively.

The total percentage of each gas produced in the experiment was calculated by combining the volume of each gas from method 1 and method 2 and the known volume of total gas transferred to the vial, $V_{g,tedlar}$, as:

$$V_{CH_4}\ (\%) = \frac{V_{1,CH_4}\ (\text{ml}) + V_{2,CH_4}\ (\text{ml})}{V_{1,g,tedlar} + V_{2,g,tedlar}} \times 100 \tag{A.11}$$

$$V_{CO_2}\ (\%) = \frac{V_{1,CO_2}\ (\text{ml}) + V_{2,CO_2}\ (\text{ml})}{V_{1,g,tedlar} + V_{2,g,tedlar}} \times 100 \tag{A.12}$$

The total volume of each gas produced in the experiment was calculated from the percentage of each gas (from Eqs. A.11 or A.12) and the cumulative volume of the gas sample produced in the experiment, $V_G$:

$$V_{CH_4}\ (\text{ml}) = \frac{V_{CH_4}\ (\%) \times V_G\ (\text{ml})}{100} \tag{A.13}$$

$$V_{CO_2}\ (\text{ml}) = \frac{V_{CO_2}\ (\%) \times V_G\ (\text{ml})}{100} \tag{A.14}$$

**Method 3**: Volume of gas (0.1 ml) from the tedlar bag was directly injected into the GC. The average peak area was calculated from the peak areas obtained for three trials. Total percentages of $CH_4$ and $CO_2$ produced in the experiment were calculated from the average peak area using the calibration equations, Eqs. A.3 and A.5, respectively. The total volume of each gas produced in the experiment was calculated using Eqs. A.13 and A.14.

Methods used for analyzing the each experimental gas sample are shown in Tables A.5, A.6, A.7 and A.8 were as follows:

**Sample 1**: (Method 1) 4 ml of gas (i.e., $V_{1,g,tedlar} = 4$ ml) from the tedlar bag was transferred to a vial of 8 ml volume, where $V_{g,vial} = 12$ ml.

**Sample 2**: (Method 1) 5.5 ml of gas (i.e., $V_{1,g,tedlar} = 5.5$ ml) from the tedlar bag was transferred to a vial of 8 ml volume, where $V_{g,vial} = 13.5$ ml.

**Sample 3**: (Method 1) 10 ml of gas (i.e., $V_{1,g,tedlar} = 10$) from the tedlar bag was transferred to a vial of 12.5 ml volume, where $V_{g,vial} = 22.5$ ml.

**Sample 4**: (Method 1) 6 ml of gas (i.e., $V_{1,g,tedlar} = 6$ ml) from the tedlar bag was transferred to a vial of 12.5 ml volume, where $V_{g,vial} = 18.5$ ml. (Method 2) 10 ml of gas (i.e., $V_{2,g,tedlar} = 10$ ml) from the tedlar bag was transferred to a 12.5 ml evacuated vial, where vacuum level = 72%.

**Sample 5**: (Method 1) 3 ml of gas (i.e., $V_{1,g,tedlar} = 3$ ml) from the tedlar bag was transferred to a vial of 12.5 ml volume, where $V_{g,vial} = 15.5$ ml.

(Method 2) 4 ml of gas (i.e., $V_{2,g,tedlar} = 4$ ml) from the tedlar bag was transferred to a 12.5 ml evacuated vial, where vacuum level = 72%. (Method 2) 10 ml of gas (i.e., $V_{2,g,tedlar} = 10$ ml) from the tedlar bag was transferred to a 12.5 ml evacuated vial, where vacuum level = 72%.

**Sample 6**: (Method 1) 12.5 ml of gas (i.e., $V_{1,g,tedlar} = 12.5$ ml) from the tedlar bag was transferred to a vial of 12.5 ml volume, where $V_{g,vial} = 25$ ml. (Method 2) 2.5 ml of gas (i.e., $V_{2,g,tedlar} = 2.5$ ml) from the tedlar bag was transferred to a 12.5 ml evacuated vial, where vacuum level = 72%. (Method 3) 0.1 ml of gas from the tedlar bag was directly injected into both 5700A model GC and 5890 series ii model GC for $CH_4$ and $CO_2$, respectively.

**Sample 7**: (Method 2) 12.9 ml of gas (i.e., $V_{2,g,tedlar} = 12.9$ ml) from the tedlar bag was transferred to a 12.5 ml evacuated vial, where vacuum level = 92%. (Method 3) 0.1 ml of gas from the tedlar bag was directly injected into 5700A model GC for $CH_4$.

**Sample 8**: (Method 2) 12.5 ml of gas (i.e., $V_{2,g,tedlar} = 12.5$ ml) from the tedlar bag was transferred to a 12.5 ml evacuated vial, where vacuum level = 92 %. (Method 2) 9.2 ml of gas (i.e., $V_{2,g,tedlar} = 9.2$ ml) from the tedlar bag was transferred to a 12.5 ml evacuated vial, where vacuum level = 92%. (Method 3) 0.1 ml of gas from the tedlar bag was directly injected into both 5700A model GC and 5890 series ii model GC for $CH_4$ and $CO_2$, respectively.

The combined gas volume or percentage obtained from method 1 and method 2 were comparable with that obtained from method 3. Different methods followed for the analysis of each gas sample, the peak area, volume and percentage of $CH_4$ for each method and total/actual volume and percentage of $CH_4$ are listed in Tables A.5 and A.6. Similarly, those for the $CO_2$ are listed in Tables A.7 and A.8.

## A.7 Error Analysis of Gas Measurements

We report here the error estimates associated with the experimental calculations performed in Chapter 4. The total error associated with gas measurements consists of errors due to standard deviation of the peak areas obtained during the gas injection into GC, errors on the total gas volume measurements using the syringe, and measurement errors on the preparation of calibration standards. The total error was calculated by considering all these three errors. This total error has been manifested in Figures 4.3, and 4.6 of Chapter 4.

### A.7.1 Standard Deviation and Percentage Error

The three peak areas obtained corresponding to the three trials of gas injections were averaged. The measurements of gas (percentage of both $CH_4$ and $CO_2$) were calculated from the average peak area, as discussed earlier. The uncertainty in the measurement was calculated in the form of standard deviation. The standard deviation (S.D.) of the peak areas is given by:

$$\sigma = \sqrt{\frac{\sum (x - \bar{x})^2}{N - 1}} \tag{A.15}$$

where, $\sigma$ is the standard deviation; $x$ is the peak area and $\bar{x}$ is the average peak area.

Initially, the standard deviation in the peak area was added (for the upper limit of the measurement) or subtracted (for the lower limit of the measurement) to the average peak area in Eqs. A.3 and A.5 to find the percentage of $CH_4$ and $CO_2$, respectively. Equations A.6 to A.14, were used for further calculations. The percentage error due to standard deviation was calculated as the difference in net percentage of gas obtained (Eqs. A.11 and A.12) with or without considering the standard deviation. The standard deviation in peak area, percentage, volume (ml) and the net percentage error for $CH_4$ measurements are depicted in Table A.9 and A.10, and for $CO_2$ measurements are listed in Tables A.7 and A.8.

### A.7.2 Measurement Error

Error in the measurement was due to the systematic error in the volume measurement of the gas. This measurement error was calculated by taking account of the least count of the syringe used to measure the gas volume. The least count of the syringe was 1.0 ml. The uncertainty of the measuring syringe is considered to be 50% of the least count. This uncertainty was taken into account in Eq. A.6 to modify the volume of gas transferred to the vial as:

$$\mathrm{V}_{g,vial}(\pm ml) = \mathrm{V}_{1,g,tedlar}\,(ml) \pm 0.5(ml) + \mathrm{V}_{air}(ml) \tag{A.16}$$

The total volume (ml) and percentage of gas were calculated by considering the least count in the modified Eq. A.16 and using Eqs. A.7 to A.14. The measurement error (± % or ml) is due to the difference in the percentage or volume of gas (Eqs. A.11 and A.14) with and without considering the least count.

### A.7.3 Calibration Error

The calibration error was the measurement error in the preparation of the calibration standard and it was due to the bias on the part of the experimenter in the volume measurement of gas using the syringe. Least count of the measuring syringe was taken into account for the calculation of gas percentage of the calibration standard. The modified calibration equation was obtained by plotting the corrected gas percentage and peak areas. This modified calibration equation was used to calculate the percentage of each experimental sample gas. Equations A.6 to A.14) were used for the further calculations. The calibration error was calculated as the difference in the net percentage or volume (ml) of the gas obtained, with or without considering the modified calibration equation. The measurement and calibration errors in the $CH_4$ measurement are listed in Tables A.13 and A.14.

### A.7.4 Total Error

The total error (E) associated with each sample was calculated as the root mean square (RMS) of the uncertainties due to standard deviation in the measurement ($E_{Std.Dev.}$), measurement error ($E_{meas}$) and calibration error ($E_{calib}$), which is given by:

$$E = \sqrt{E_{meas} + E_{calib} + E_{Std.Dev.}} \tag{A.17}$$

The net error due to standard deviation, the measurement error, the calibration error and the total error associated with each sample for $CH_4$ and $CO_2$ are listed in Tables A.15 and A.16, respectively.

## A.8 Solubility of $CH_4$ and $CO_2$ in the Effluent

The fraction of a gas volume can still be dissolved in liquid effluent sample at atmospheric conditions. The solubility of gas in the effluent was also considered to find the net production of $CH_4$ and $CO_2$ in the core flooding experiment. These results have been manifested in the Figure 4.3 of Chapter 4. The quantity of gas dissolved in the effluent is related to its partial pressure. Henry's law was used to find gas solubility in effluent, which is equivalent to the available solubility data (www.chemicalbook.com), which is given as:
The solubility of $CH_4$ in water ($S_{CH_4}$) = 22.7 mg/L
The solubility of $CO_2$ in water ($S_{CO_2}$) = 1450 mg/L
Density of $CH_4$ at room temperature ($24^0$C) and pressure [1 atm] ($\rho_{CH_4}$)= 0.656 g/L
Density of $CO_2$ at room temperature ($24^0$C) and pressure [1 atm] ($\rho_{CO_2}$) = 1.817 g/L
Quantity of $CH_4$ and $CO_2$ dissolved in 100 ml of the effluent, which was collected each time during the core flooding experiment was calculated using the following equation:

$$\mathrm{CH}_{4_{(soluble)}}\ (\mathrm{ml}) = \frac{\mathrm{V}_{CH_4}\ (\%) \times S_{CH_4}}{\rho_{CH_4} \times 1000} \tag{A.18}$$

$$\mathrm{CO_2}_{(soluble)}\ (\mathrm{ml}) = \frac{\mathrm{V}_{CO_2}\ (\%) \times S_{CO_2}}{\rho_{CO_2} \times 1000} \tag{A.19}$$

Calculated quantities of both $CH_4$ and $CO_2$ dissolved in the effluent are shown in Table A.17.

## A.9 Metabolic Compounds

All metabolites detected in the effluent samples are shown in Table A.18. Relative concentration of the primary metabolites (depend on the concentration) are shown in Figure 4.5 of Chapter 4, in the form of a heat map. Not all of these metabolites are detected in every effluent samples, which are analysed. The number of metabolites, which can be detected by the method used in this present work are limited. There can be many other metabolites formed during the coal methanogenesis, which are not detected.

## A.10 Design of Piston Accumulator

The custom build downstream side piston accumulators (PA) were used for the collection of effluent. The volume capacity of the PA = 125 ml. The main components of the PA assembly are cylindrical body, piston, end plug and end cover. The PA designed for working pressure (hydraulic pressure) of 6894.75 kPa (1000 psi). Using Lamme$'$s equation (Eq. A.20) the maximum hoop (circumferential) stress ($f_{h_{max}}$) is calculated to be 129469.75 kPa (18778 psi) which is less than yield strength and maximum allowable stress of stainless steel 316. Maximum working pressure ($P_{max}$), the PA can withstand, was calculated using Barlow$'$s equation (Eq. A.21) = 51710.6 kPa (7500 psi). Hence, the safety factor is given for the PA = 7.5.

$$f_{h_{max}} = \frac{P(D^2 + d^2)}{(D^2 - d^2)} \tag{A.20}$$

$P$ is the working pressure (kPa); $D$ is the outer diameter (mm) and $d$ is the inner diameter (mm).

$$P_{max} = \frac{2 \times S \times t}{D} \tag{A.21}$$

where $S$ is the allowable stress $\sim$ 137895.14 kPa (20000 psi) and $t$ is the thickness = 9.52 mm (0.375 inch).

Following pages shows the exploded view of the piston accumulator (PA) assembly, sectioned view of the PA assembly, the cylindrical main body, the piston, the end plug and the end cover. Required dimensions and details are provided for each component.

| PART NUMBER | DESCRIPTION | QTY. |
|---|---|---|
| Body | MecE machine shop | 1 |
| Piston | MecE machine shop | 1 |
| End Plug | MecE machine shop | 2 |
| End Cap | MecE machine shop | 2 |
| Dynamic O-Ring AS 568 -121 | Parker | 2 |
| Static O-Ring AS 568 -121 | Parker | 2 |
| Backup Ring (Parback Elastomer) | Parker | 2 |

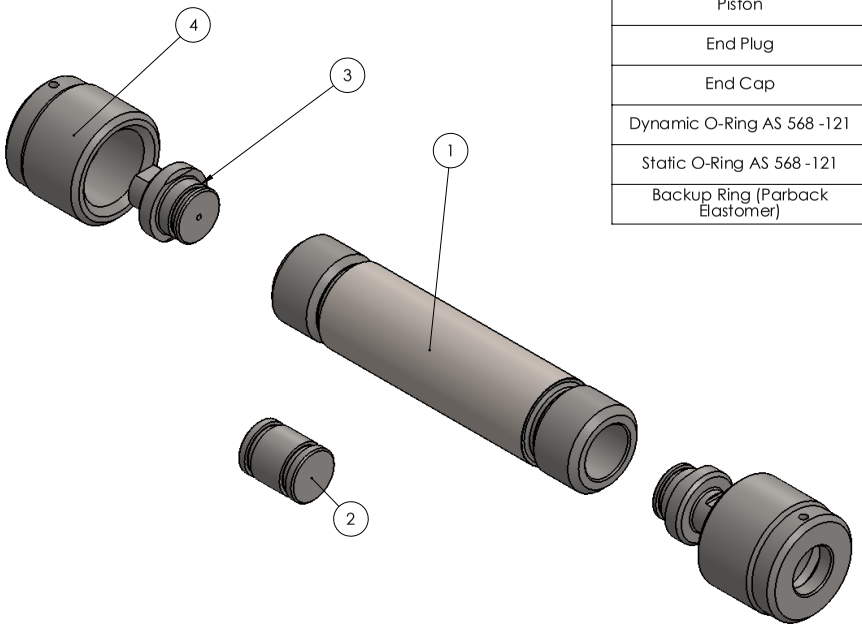


**SolidWorks Student Edition.**
**For Academic Use Only.**

| | | | |
|---|---|---|---|
| **Nobes Lab** | UNLESS OTHERWISE SPECIFIED: | | The Department of Mechanical Engineering<br>UNIVERSITY OF ALBERTA |
| Contact: Anil Stephen | DIMENSIONS ARE IN MM<br>TOLERANCES:<br>ANGULAR: ± 0.5°<br>.X = ± 0.25<br>.XX = ± 0.05 | DRAWN BY: Anil Stephen | TITLE: Piston Accumulator |
| Email:anil3@ualberta.ca | | SMB | |
| Phone:587-709-3456 | | CHECKED BY | |
| Comments: | SURFACE FINISH µm 0.6 | **Speed Code** | |
| | MATERIAL: | **MecE Job #** | |
| | | File Name: Piston Accumulator Exploaded | SIZE: B; Project: CMC Project; REV |
| | Lab Location: NINT 6-93 | Anil Stephen<br>Friday, November 23, 2012 10:55:36 AM | |
| | DO NOT SCALE DRAWING | Monday, October 29, 2012 12:50:16 PM | SCALE: 1:5; Mass: ; SHEET 1 OF 1 |

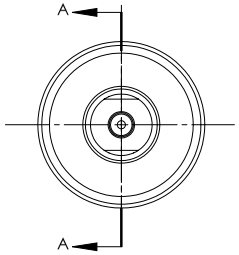


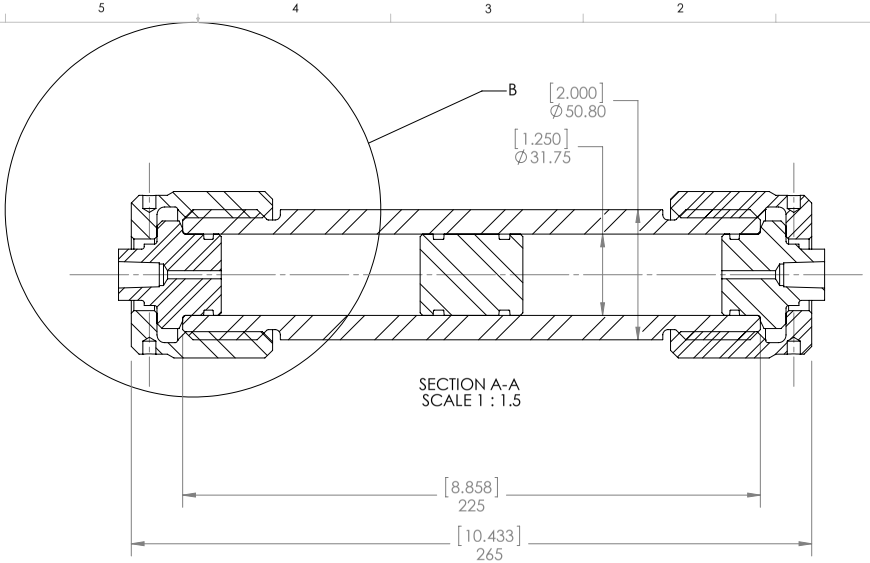


SECTION A-A
SCALE 1 : 1.5

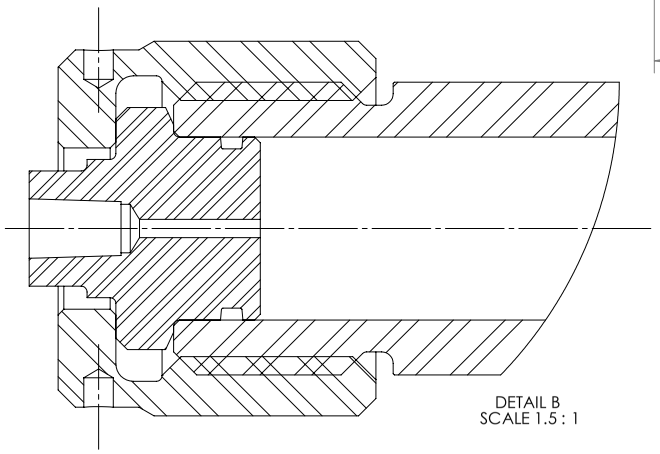

DETAIL B
SCALE 1.5 : 1

**SolidWorks Student Edition.**
**For Academic Use Only.**

| | | | | | |
|---|---|---|---|---|---|
| **Nobes Lab** | UNLESS OTHERWISE SPECIFIED: | | | The Department of Mechanical Engineering UNIVERSITY OF ALBERTA | |
| Contact: Anil Stephen | DIMENSIONS ARE IN MM<br>TOLERANCES:<br>ANGULAR: ± 0.5°<br>.X = ± 0.25<br>.XX = ± 0.05 | DRAWN BY | Anil Stephen | TITLE: Piston Accumulator | |
| Email:anil3@ualberta.ca | | SMB | | | |
| Phone:587-709-3456 | | CHECKED BY | | | |
| Comments: | SURFACE FINISH 0.6 µm | **Speed Code** | | | |
| | MATERIAL: | **MecE Job #** | | | |
| | | File Name: Piston Accumulator | | SIZE: B | Project: CMC Project |
| | Lab Location: NINT 6-93 | Anil Stephen<br>Friday, November 23, 2012 10:54:09 AM | | | REV |
| | DO NOT SCALE DRAWING | Monday, October 29, 2012 12:50:16 PM | | SCALE: 1:2 | Mass: SHEET 2 OF 1 |

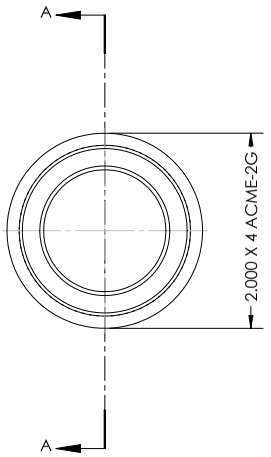


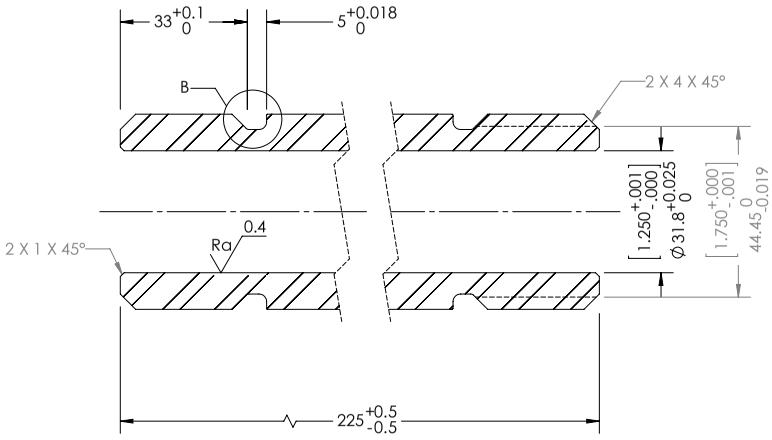


SECTION A-A

SCALE 1 : 1

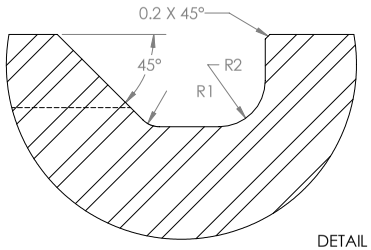


DETAIL B
SCALE 6 : 1

**SolidWorks Student Edition.**
**For Academic Use Only.**

| | | | | |
|---|---|---|---|---|
| **Nobes Lab** | UNLESS OTHERWISE SPECIFIED: | | NAME | The Department of Mechanical Engineering<br>UNIVERSITY OF ALBERTA |
| Contact: Anil Stephen | DIMENSIONS ARE IN MM<br>TOLERANCES:<br>ANGULAR: ± 0.5°<br>.X = ± 0.25<br>.XX = ± 0.05 | DRAWN BY | Anil Stephen | TITLE: Body |
| Email:anil3@ualberta.ca | | SMB | | |
| Phone:587-709-3456 | | CHECKED BY | | |
| Comments: | SURFACE FINISH 1.6 µm | **Speed Code** | ME 283 | |
| | MATERIAL: | **MecE Job #** | | |
| | | File Name: Body | | SIZE B / Project: CMC Project / REV |
| | Lab Location: NINT 6-93 | anil3 | | SCALE: 1:5 / Mass: / SHEET 3 OF 7 |
| | DO NOT SCALE DRAWING | Friday, November 23, 2012 10:51:06 AM<br>Friday, August 31, 2012 10:40:23 AM | | |

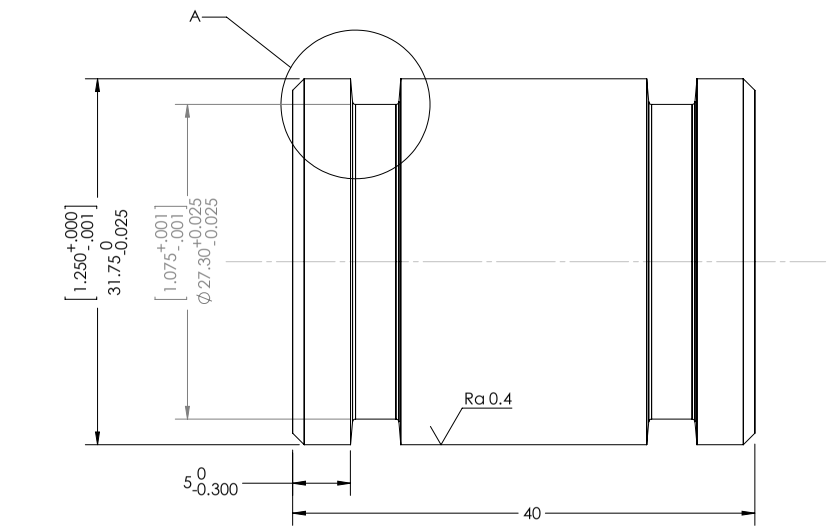


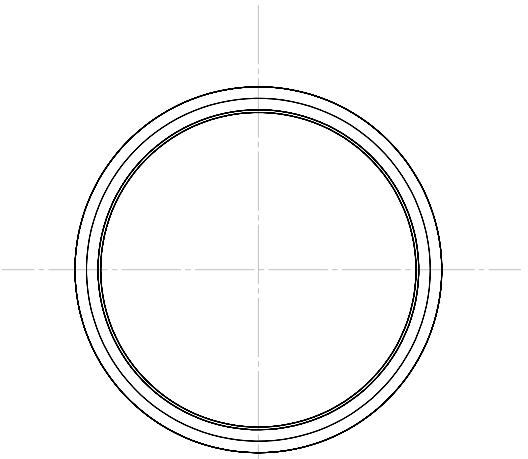

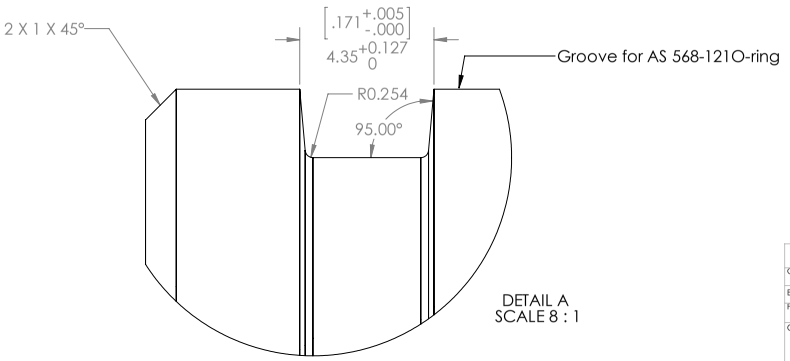


DETAIL A
SCALE 8 : 1

**SolidWorks Student Edition.**
**For Academic Use Only.**

| | | | | | |
|---|---|---|---|---|---|
| **Nobes Lab** | UNLESS OTHERWISE SPECIFIED: | | NAME | The Department of Mechanical Engineering UNIVERSITY OF ALBERTA | |
| Contact: Anil Stephen | DIMENSIONS ARE IN MM | DRAWN BY | Anil Stephen | | |
| Email:anil3@ualberta.ca | TOLERANCES: ANGULAR: ± 0.5° .X = ± 0.25 .XX = ± 0.05 | SMB | | TITLE: Piston | |
| Phone:587-709-3456 | | CHECKED BY | | | |
| Comments: | SURFACE FINISH µm 0.4 | **Speed Code** | | | |
| | MATERIAL: | **MecE Job #** | | | |
| | | File Name: Piston | | SIZE B | Project: CMC Project |
| | Lab Location: NINT 6-93 | anil3 | Wednesday, January 02, 2013 3:21:19 PM | | REV |
| | DO NOT SCALE DRAWING | | Friday, August 31, 2012 1:30:43 AM | SCALE: 1:1 | Mass: SHEET 4 OF 7 |

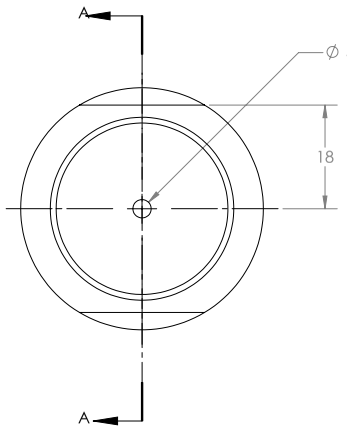


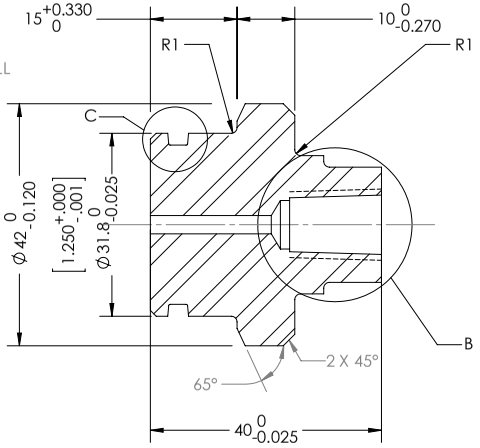


SECTION A-A
SCALE 1.5 : 1

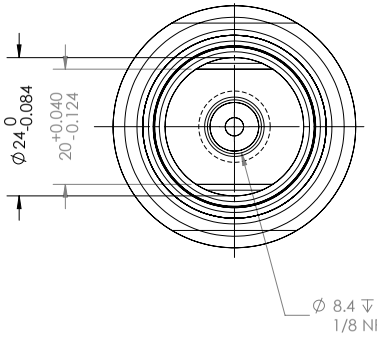


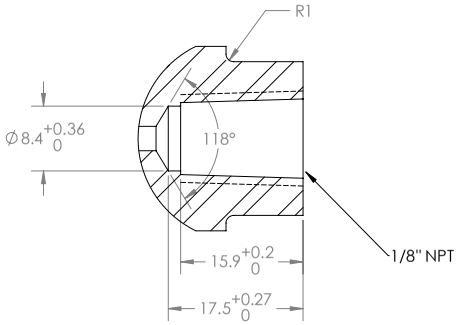


DETAIL B
SCALE 2 : 1

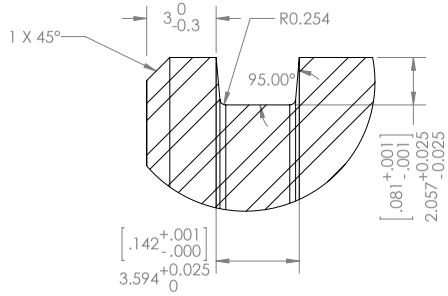


DETAIL C
SCALE 6 : 1

**SolidWorks Student Edition.**
**For Academic Use Only.**

| | | | | |
|---|---|---|---|---|
| **Nobes Lab** | UNLESS OTHERWISE SPECIFIED: | | NAME | The Department of Mechanical Engineering, UNIVERSITY OF ALBERTA |
| Contact: Anil Stephen | DIMENSIONS ARE IN MM<br>TOLERANCES:<br>ANGULAR: ± 0.5°<br>.X = ± 0.25<br>.XX = ± 0.05 | DRAWN BY | Anil Stephen | TITLE: End Plug |
| Email:anil3@ualberta.ca | | SMB | | |
| Phone:587-709-3456 | | CHECKED BY | | |
| Comments: | SURFACE FINISH 0.6 µm | **Speed Code** | | |
| | MATERIAL: | **MecE Job #** | | |
| | | File Name: End Plug | | SIZE: B; Project: CMC Project; REV |
| | Lab Location: NINT 6-93 | anil3 | | |
| | DO NOT SCALE DRAWING | Wednesday, December 19, 2012 1:11:23 PM<br>Thursday, September 06, 2012 2:07:02 PM | | SCALE: 1:1; Mass: ; SHEET 6 OF 7 |

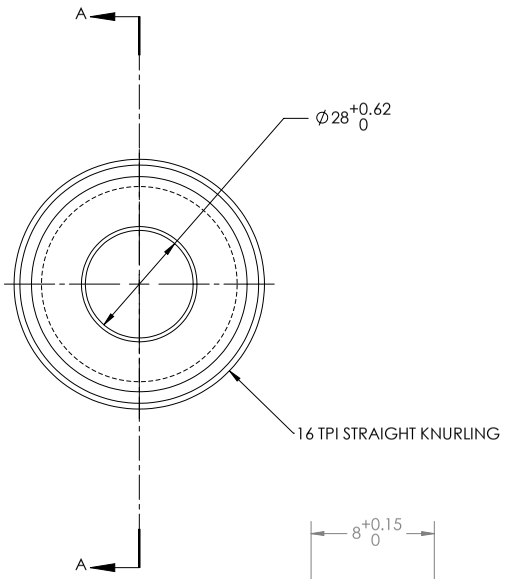


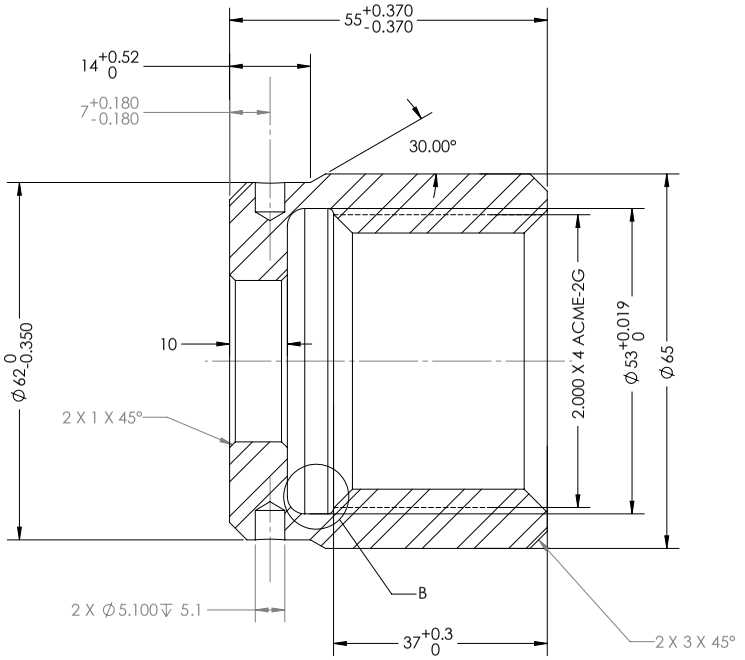


SECTION A-A

SCALE 1.5 : 1

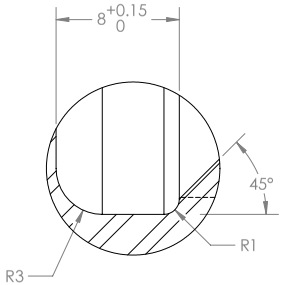


DETAIL B
SCALE 4 : 1

**SolidWorks Student Edition.**
**For Academic Use Only.**

| | | | | |
|---|---|---|---|---|
| **Nobes Lab** | UNLESS OTHERWISE SPECIFIED: | | NAME | The Department of Mechanical Engineering, UNIVERSITY OF ALBERTA |
| Contact: Anil Stephen | DIMENSIONS ARE IN MM<br>TOLERANCES:<br>ANGULAR: ± 0.5°<br>.X = ± 0.25<br>.XX = ± 0.05 | DRAWN BY | Anil Stephen | TITLE: End Cap |
| Email:anil3@ualberta.ca | | SMB | | |
| Phone:587-709-3456 | | CHECKED BY | | |
| Comments: | SURFACE FINISH µm 1.6 | **Speed Code** | | |
| | MATERIAL: | **MecE Job #** | | |
| | | File Name: End Cap | SIZE: B | Project: CMC Project; REV |
| | Lab Location: NINT 6-93 | Anil Stephen<br>Thursday, November 22, 2012 7:14:56 PM<br>Thursday, September 06, 2012 5:26:37 PM | SCALE: 1:2 | Mass: SHEET 7 OF 7 |
| | DO NOT SCALE DRAWING | | | |

Table A.5: $CH_4$ measurement for the $1^{st}$ - $5^{th}$ samples. The methods adopted, the average peak area, the percentage and volume of $CH_4$ for each methods are listed. The total percentage and volume of $CH_4$ for each sample are estimated.

| | Sample #1 | Sample #2 | Sample #3 | Sample #4 | | Sample #5 | | |
|---|---|---|---|---|---|---|---|---|
| | Method 1 | Method 1 | Method 1 | Method 1 | Method 2 | Method 1 | Method 2 | Method 2 |
| Gas Collected (ml) | 4 | 5.5 | 10 | 16 | | 17 | | |
| Gas in vial (ml) | 12 | 13.5 | 22.5 | 18.5 | 13.5 | 15.5 | 7.5 | 13.5 |
| Avg. Peak Area | 142980 | 44636 | 226516.6 | 391225 | 682263.3 | 354520 | 731110 | 1104300 |
| $CH_4$ (%) | 0.93 | 0.7 | 2.2 | 3.4 | 5.4 | 3.2 | 5.8 | 8.4 |
| $CH_4$ (ml) | 0.112 | 0.094 | 0.502 | 0.63 | 0.74 | 0.49 | 0.43 | 1.13 |
| Total $CH_4$ (ml) | 0.112 | 0.094 | 0.502 | 1.37 | | 2.06 | | |
| Total $CH_4$ (%) | 2.8 | 1.7 | 5.02 | 8.54 | | 12.10 | | |



Table A.6: $CH_4$ measurement for the $6^{th}$ - $8^{th}$ samples. The methods adopted, the average peak area, the percentage and volume of $CH_4$ for each methods are listed. The total percentage and volume of $CH_4$ for each sample are estimated.

| | Sample #6 | | | Sample #7 | | Sample #8 | | |
|---|---|---|---|---|---|---|---|---|
| | Method 1 | Method 2 | Method 3 | Method 2 | Method 3 | Method 2 | Method 2 | Method 3 |
| Gas Collected (ml) | 15 | | | 13.3 | | 22.4 | | |
| Gas in vial (ml) | 25 | 6 | – | 13.9 | – | 13.5 | 10.2 | – |
| Avg. Peak Area | 1045266.6 | 83664.5 | 1809900 | 964180 | 955540 | 1067500 | 736096.6 | 1138050 |
| $CH_4$ (%) | 8.0 | 1.3 | 13.3 | 7.91 | 7.42 | 7.36 | 5.8 | 8.64 |
| $CH_4$ (ml) | 2.0 | 0.075 | 2 | 1.03 | 0.99 | 1.1 | .0.59 | 1.93 |
| Total $CH_4$ (ml) | 2.075 | | 2.0 | 1.15 | 0.92 | 1.75 | | 1.93 |
| Total $CH_4$ (%) | 13.8 | | 13.3 | 8.12 | 7.36 | 7.8 | | 8.6 |

Table A.7: $CO_2$ measurement for the $1^{st}$ - $5^{th}$ samples. The methods adopted, the average peak area, the percentage and volume of $CO_2$ for each methods are listed. The total percentage and volume of $CO_2$ for each sample are estimated.

| | Sample #1 | Sample #2 | Sample #3 | Sample #4 | | Sample #5 | | |
|---|---|---|---|---|---|---|---|---|
| | Method 1 | Method 1 | Method 1 | Method 1 | Method 2 | Method 1 | Method 2 | Method 2 |
| Gas Collected (ml) | 4 | 5.5 | 10 | 16 | | 17 | | |
| Gas in vial (ml) | 12 | 13.5 | 22.5 | 18.5 | 13.5 | 15.5 | 7.5 | 13.5 |
| Avg. Peak Area | 811140.6 | 713672.6 | 3422314 | 3487581.3 | 3611550 | 1297468 | 3196257 | 4983199 |
| $CO_2$ (%) | 6.1 | 5.5 | 24.4 | 24.9 | 25.7 | 9.5 | 22.8 | 35.3 |
| $CO_2$ (ml) | 0.74 | 0.74 | 5.49 | 4.6 | 3.47 | 1.48 | 1.71 | 4.77 |
| Total $CO_2$ (ml) | 0.74 | 0.74 | 5.49 | 8.08 | | 7.96 | | |
| Total $CO_2$ (%) | 18.4 | 13.38 | 54.9 | 50.47 | | 46.8 | | |



Table A.8: $CO_2$ measurement for the $6^{th}$ - $8^{th}$ samples. The methods adopted, the average peak area, the percentage and volume of $CO_2$ for each methods are listed. The total percentage and volume of $CO_2$ for each sample are estimated.

| | Sample #6 | | Sample #7 | Sample #8 | | |
|---|---|---|---|---|---|---|
| | Method 1 | Method 2 | Method 2 | Method 2 | Method 2 | Method 3 |
| Gas Collected (ml) | 15 | | 13.3 | 22.4 | | |
| Gas in vial (ml) | 25 | 6 | 12.9 | 13.5 | 10.2 | – |
| Avg. Peak Area | 4220220.6 | 452636 | 6368573 | 5585637.3 | 3990318.3 | 6072369 |
| $CO_2$ (%) | 30.0 | 3.6 | 45 | 39.6 | 28.4 | 43 |
| $CO_2$ (ml) | 7.5 | 0.22 | 5.81 | 5.34 | 2.9 | 9.62 |
| Total $CO_2$ (ml) | 7.72 | | 6 | 9.1 | | |
| Total $CO_2$ (%) | 51.4 | | 43.7 | 40.6 | | |

Table A.9: Uncertainty due to standard deviation (S.D.) in $CH_4$ measurement for the $1^{st}$ - $5^{th}$ samples. S.D. in peak area, S. D. in % and volume of $CH_4$, total percentage of uncertainty due to S.D. in $CH_4$ generation are listed.

| | Sample #1 | Sample #2 | Sample #3 | Sample #4 | | Sample #5 | | |
|---|---|---|---|---|---|---|---|---|
| | Method 1 | Method 1 | Method 1 | Method 1 | Method 2 | Method 1 | Method 2 | Method 2 |
| Std. Dev. Peak Area (±) | 8461.4 | 338.5 | 3610.2 | 21276.8 | 8230.4 | 4186 | 4572.1 | 15092 |
| S.D. in $CH_4$ (±, %) | 0.05 | 0.002 | 0.025 | 0.15 | 0.06 | 0.0057 | .03 | 0.11 |
| S.D. in $CH_4$ (±, ml) | 0.117 | 0.0003 | 0.006 | 0.035 | | 0.02 | | |
| Total S.D. in $CH_4$ (±, %) | 0.15 | 0.005 | 0.06 | 0.22 | | 0.12 | | |



Table A.10: Uncertainty due to standard deviation (S.D.) in $CH_4$ measurement for the $6^{th}$ - $8^{th}$ samples. S.D. in peak area, S. D. in % and volume of $CH_4$, total percentage of uncertainty due to S.D. in $CH_4$ generation are listed

| | Sample #6 | | | Sample #7 | | Sample #8 | | |
|---|---|---|---|---|---|---|---|---|
| | Method 1 | Method 2 | Method 3 | Method 2 | Method 3 | Method 2 | Method 2 | Method 3 |
| S.D. Peak Area (±) | 10066.9 | 6939.7 | – | 141528.5 | 65390.9 | 707.1 | 5569.2 | 35850.3 |
| S. D. in $CH_4$ (±, %) | 0.07 | 0.05 | – | 7.91 | 7.42 | 0.005 | 0.04 | 0.3 |
| S.D. in $CH_4$ (±, ml) | | 0.021 | | 0.22 | | | 0.067 | |
| Total S.D. in $CH_4$ (± %) | | 0.14 | | 1.66 | | | 0.3 | |

Table A.11: Uncertainty due to standard deviation (S.D.) in $CO_2$ measurement for the $1^{st}$ - $5^{th}$ samples. S.D. in peak area, S. D. in % and volume of $CO_2$, total percentage of uncertainty due to S.D. in $CO_2$ generation are listed.

| | Sample #1 | Sample #2 | Sample #3 | Sample #4 | | Sample #5 | | |
|---|---|---|---|---|---|---|---|---|
| | Method 1 | Method 1 | Method 1 | Method 1 | Method 2 | Method 1 | Method 2 | Method 2 |
| S.D. Peak Area (±) | 22249.3 | 7742.0 | 64686.1 | 161363.1 | 55869.8 | 62869 | 174477.8 | 277468.9 |
| S.D. in $CO_2$ (±, %) | 0.156 | 0.05 | 0.45 | 1.13 | 0.4 | 0.4 | 1.2 | 1.94 |
| S.D. $CO_2$ (±, ml) | 0.02 | 0.007 | 0.1 | 0.23 | | 0.42 | | |
| Total S.D. in $CO_2$ (± %) | 0.467 | 0.133 | 1.02 | 1.46 | | 2.48 | | |



Table A.12: Uncertainty due to standard deviation (S.D.) in $CO_2$ measurement for the $6^{th}$ - $8^{th}$ samples. S.D. in peak area, S. D. in % and volume of $CO_2$, total percentage of uncertainty due to S.D. in $CO_2$ generation are listed.

| | Sample #6 | | Sample #7 | Sample #8 | | |
|---|---|---|---|---|---|---|
| | Method 1 | Method 2 | Method 2 | Method 2 | Method 2 | Method 3 |
| S.D. Avg. Peak Area (±) | 100276.8 | 6604.3 | – | 66346.2 | 127947.1 | 198803.4 |
| S.D. in $CO_2$ (±, %) | 0.7 | 0.046 | – | 0.46 | 0.9 | 1.4 |
| S.D. in $CO_2$ (±, ml) | 0.178 | | – | 0.16 | | |
| Total S.D. in $CO_2$ (± %) | 1.18 | | – | 0.71 | | |

Table A.13: Measurement and calibration error for $CH_4$ samples, $1^{st}$ - $5^{th}$

| | Sample #1 | Sample #2 | Sample #3 | Sample #4 | | Sample #5 | | |
|---|---|---|---|---|---|---|---|---|
| | Method 1 | Method 1 | Method 1 | Method 1 | Method 2 | Method 1 | Method 2 | Method 2 |
| **Measurement error** (±, ml) | 0.005 | 0.003 | 0.011 | 0.017 | 0.027 | 0.02 | 0.043 | 0.063 |
| Total meas. error (±, ml) | 0.005 | 0.003 | 0.0.011 | 0.044 | | | 0.12 | |
| Total meas. error (±, %) | 0.12 | 0.063 | 0.11 | 0.28 | | | 0.72 | |
| **Calibration** | | | | | | | | |
| error (±, ml) | 0.015 | 0.022 | 0.037 | 0.031 | 0.023 | 0.025 | 0.01 | 0.022 |
| Total calib. error (±, ml) | 0.0.015 | 0.022 | 0.037 | 0.054 | | | 0.06 | |
| Total calib. error (±, %) | 0.38 | 0.4 | 0.37 | 0.34 | | | 0.35 | |

Table A.14: Measurement and calibration error for $CH_4$ samples, $6^{th}$ - $8^{th}$

| | Sample #6 | | | Sample #7 | | Sample #8 | | |
|---|---|---|---|---|---|---|---|---|
| | Method 1 | Method 2 | Method 3 | Method 2 | Method 3 | Method 2 | Method 2 | Method 3 |
| **Measurement error** (±, ml) | 0.04 | 0.006 | 0.06 | 0.051 | 0.037 | 0.043 | 0.03 | 0.043 |
| Total meas. error (±, ml) | | 0.05 | | 0.043 | | | 0.073 | |
| Total meas. error (±, %) | | 0.33 | | 0.33 | | | 0.33 | |
| **Calibration** | | | | | | | | |
| error (±, ml) | 0.04 | 0.01 | 0.024 | 0.023 | 0.023 | 0.038 | 0.038 | 0.038 |
| Total calib. error (±, ml) | | 0.05 | | 0.0.023 | | | 0.038 | |
| Total calib. error (±, %) | | 0.33 | | 0.17 | | | 0.17 | |

Table A.15: Uncertainty in the measurements of $CH_4$.

| sample | Gas Volume Collected (ml) | Standard Deviation ± % | Measurement Error ± % | Calibration Error ± % | Total Error ± % |
|---|---|---|---|---|---|
| 1 | 4.00 | 0.15 | 0.12 | 0.38 | 0.43 |
| 2 | 5.50 | 0.01 | 0.06 | 0.42 | 0.42 |
| 3 | 10.00 | 0.06 | 0.11 | 0.37 | 0.39 |
| 4 | 16.00 | 0.22 | 0.28 | 0.33 | 0.49 |
| 5 | 17.00 | 0.12 | 0.72 | 0.37 | 0.82 |
| 6 | 15.00 | 0.14 | 0.33 | 0.33 | 0.49 |
| 7 | 13.30 | 1.66 | 0.33 | 0.17 | 1.70 |
| 8 | 22.40 | 0.3 | 0.33 | 0.17 | 0.48 |

Table A.16: Uncertainty in the measurements of $CO_2$.

| sample | Gas Volume Collected (ml) | Standard Deviation ± % | Measurement Error ± % | Calibration Error ± % | Total Error ± % |
|---|---|---|---|---|---|
| 1 | 4.00 | 0.47 | 0.77 | 1.03 | 1.37 |
| 2 | 5.50 | 0.133 | 0.50 | 0.84 | 0.99 |
| 3 | 10.00 | 1.02 | 1.22 | 0.77 | 1.77 |
| 4 | 16.00 | 1.46 | 1.98 | 0.63 | 2.54 |
| 5 | 17.00 | 2.48 | 2.85 | 0.74 | 3.85 |
| 6 | 15.00 | 1.18 | 1.18 | 0.71 | 1.81 |
| 7 | 13.30 | 0.00 | 1.69 | 0.33 | 1.72 |
| 8 | 22.40 | 0.71 | 2.14 | 0.36 | 2.29 |

Table A.17: Dissolved quantity of $CH_4$ and $CO_2$ in the effluent samples.

| sample | Dissolved $CH_4$ (ml) | Dissolved $CO_2$ (ml) |
|---|---|---|
| 1 | 0.10 | 14.68 |
| 2 | 0.06 | 10.68 |
| 3 | 0.17 | 43.84 |
| 4 | 0.30 | 37.17 |
| 5 | 0.42 | 37.37 |
| 6 | 0.47 | 41.05 |
| 7 | 0.27 | 34.86 |
| 8 | 0.29 | 32.40 |

Table A.18: List of metabolites detected in the core flooding effluent sample.

| Key-metabolites | |
|---|---|
| Acetic Acid | 1-Naphthoate |
| Butanoic Acid-3-methyl | 2-Naphthoate |
| Benzoate | 1,2,3, 4 - tetrahydro-2-naphthoate |
| Salicylic Acid | o-Tolylacetic Acid |
| Benzylsuccinate | p-Tolylacetic Acid |
| o-Toluate | 1-phenylethanol |
| m-Toluate | Phenylacetic Acid |
| p - Toluate | Transcinnamic acid |
| 2-Pyrrolidone Carboxylic Acid | o-phthalate |
| Octanedioic Acid | Methylsuccinate |
| Hydrocinnamic Acid | Octylsuccinate |
| Benzoic Acid-3-methoxy | Glutaric Acid |
| Benzoic Acid-3, 4-bis trymethylsilyl oxy | Succinic Acid |
| 1H-Indole-3-acetic acid | 1-methylcyclohexane carbox |
| p-methylbenzylsuccinate | Pimelic Acid |
| Hexadecanoic Acid | Hexanoic Acid |
| Octadecanoic Acid | p-Cresol |